This is to certify that the

thesis entitled

Use of Injection Island Genetic Algorithms in the

Optimization of Composite Flywheels

presented by

David James Eby

has been accepted towards fulfillment
of the requirements for

Master's degree in Mechanics

Ronald C. Averill

Major professor

Date 10/3/97

USE OF INJECTION ISLAND GENETIC ALGORITHMS IN THE OPTIMIZATION OF COMPOSITE FLYWHEELS

By

David J. Eby

A THESIS

Submitted to

Michigan State University

in the partial fullfillment of the requirements

for the degree of

MASTERS OF SCIENCE

Department of Materials Science and Mechanics

1997

ABSTRACT

USE OF ISLAND INJECTION GENETIC ALGORITHMS IN THE OPTIMIZATION OF COMPOSITE FLYWHEELS

By

David J. Eby

This thesis presents an approach to optimal design of elastic flywheels using an Island Injection Genetic Algorithm (iiGA). An iiGA in combination with a structural finite element code is used to search for shape variations to optimize the Specific Energy Density (SED) of elastic flywheels while controlling angular velocity and penalizing designs that are deemed unsafe. SED is defined as the amount of rotational energy stored per unit mass. iiGAs seek solutions simultaneously at different levels of refinement of the problem representation (and correspondingly different definitions of the fitness function) in separate subpopulations (islands). Solutions are sought first at low levels of refinement with an axi-symmetric plane stress finite element code for high speed exploration of the coarse design space. Next, individuals are injected into populations with a higher level of resolution that use an axi-symmetric three dimensional finite element code to "fine-tune" the structures. Discretizing the fitness function into "sub-fitness" functions while using a computationally inexpensive axi-symmetric plane stress finite element code allows efficient and robust exploration. The problem at hand is a combinatorial and parametric search. Since Genetic Algorithms (GAs) are particularly efficient at combinatorial optimization but lack in the area of hill climbing, hybrid iiGAs that combine Threshold Accepting (TA) and various local optimization procedures are developed to increase the robustness of the GA.

ACKNOWLEDGMENTS

I wish to express my gratitude to Dr. Erik Goodman and Dr. William F. Punch III for all the support, insight guidance and expertise extended throughout my research. I would like also thank the Genetic Algorithms Research Group for their patience and advice. Particularly Owen Mathews, Boris Gelfand and Victor Miagkikh for their hard work and assistance during this research.

Also, I would like to thank the Computational Mechanics Research Group for their support and assistance. Finally, I would like to thank my advisor Dr. Ronald Averill for his incredible amount of guidance, understanding and foresight throughout the duration of my thesis.

Table of Contents

List of Tables

List of Figures

Chapter 1

Introduction

1.1 Introduction

Everyday a new optimization problem is encountered. For instance, what is the quickest path to work? Where and how congested is the road construction? Am I better off just riding my bike? If so, what is the shortest distance? This simple problem is easily solved, while many engineering optimization problems cannot be as cleanly approached. Engineering involves a wide class of problems and optimization techniques. Many engineering design approaches such as the "make-it-and-break-it" mentality are simple, out-of-date concepts that have been revolutionized with computer simulations that exploit various mathematical concepts such as the finite element method to avoid costly design iterations. Even with the aid of high speed supercomputers, this design process can be hindersome, producing designs that evolve extremely slowly over a long period of time. The next step in the engineering of systems is the automation of optimization through computer simulation. After all, optimization is simply engineering on a grander scale.

Optimization approaches include analytical hill climbing, random search, directed random search and hybrid methods. Hill climbing or gradient-based methods are single point search methods that are severely restricted in their application due their numerous limitations. Random search methods are limited to a class of practical problems that have small search spaces. A directed random search method such as a Genetic Algorithm (GA) is a multiple point search method that can be an effective optimization approach to a broad class of problems. Injection Island Genetic Algorithms (iiGAs) can help reduce the computational intensity associated with typical GAs by searching at various levels of resolution within the search space. iiGAs can also incorporate various optimization schemes to create hybrid methods.

An optimization problem can have single or multiple goals. Multi-objective optimization first arose in a natural fashion in economics. Typically, most engineering optimization problems contain multiple objectives such as: minimizing cost while maximizing safety, manufacturability and or performance. Of all the applications of optimization in engineering, structural optimization using GAs is the focus of this study.

1.2 Problem Definition

1.2.1 Flywheels

Shape optimization of flywheels for the maximization of SED is an appealing thought that has received its fair attention by researchers. The concept of a flywheel is as old as the axe grinder's wheel, but could very well hold the key to tomorrow's problems of efficient energy storage. The flywheel has a bright outlook because of the recent achievement of high specific energy densities with composite materials. Composite materials have high specific strength, which can be seen to govern the threshold of specific energy density in the equation:

$$SED_{max} = K_s \frac{\sigma_{ult}}{\rho} \tag{1}$$

σ_{ult} is the ultimate strength of the material and ρ is the density of the material. K_s is a non-dimensional shape factor with minimum value of zero and a maximum value of unity that occurs as the radius tends to infinity.

The overall objective in the current study was to maximize specific energy density (SED) of flywheels, which is defined as:

$$SED = \frac{1}{2}\frac{I\omega^2}{m} \tag{1.2}$$

where ω is angular velocity, m is the total mass and I is the mass moment of inertia of the flywheel defined by:

$$I = \int_V \rho r^2 dV \tag{1.3}$$

where ρ is the density of the material.

A simple example of a flywheel is a solid, flat rotating disk. The SED of a flat solid disk can be increased by varying the shape of the disk to redistribute the inertial forces induced from rotation. This thesis presents an approach to optimal design of elastic flywheels using Genetic Algorithms (GAs). A GA in combination with a structural finite element analysis code is used to search for shape variations in the optimization of composite flywheels. The variables to be optimized include: Specific Energy Density (SED) and "air gap" growth. Failure at this angular velocity would be catastrophic. Excessive "air gap" growth occurs when the inner most ring of an annular flywheel expands beyond acceptable tolerances of flywheel bearings due to forces induced from rotations. It would be ideal to maximize SED, and to reduce "air gap" growth while maintaining a reasonable angular velocity of a flywheel, by means of shape optimization. A GA represents a robust, efficient optimization technique used to solve this problem.

A flywheel stores kinetic energy by rotating a mass about a constant axis, which makes it easy to integrate flywheels into energy conservation systems. Systems such as vehicles currently use flywheels during braking for regenerating energy lost during deceleration. Another practical application is energy storage in low satellite orbits where photoelectric cells are exposed to 60 minutes of light to charge, followed by 30 minutes of darkness where stored energy must be used. Electrochemical energy storage (e.g., in batteries) is limited by low cyclic lifetimes, low longtime reliability and low specific energies, all major concerns in satellite applications. The flywheel is well-suited for this application due to high cyclic lifetimes, longtime reliability and high specific energies. Also, large scale flywheels could be used in energy plants to store huge amounts of energy. Finding practical applications for flywheels is not the problem, but optimizing the SED of flywheels, given a problem specific set of parameters and constraints, provides a challenge.

1.2.2 Optimization Approach

This thesis presents and compares a set of various optimization approaches applied to flywheels. This set includes simple Genetic Algorithms (sGA), GAs with topological "ring" structure, Island Injection Genetic Algorithms (iiGAs), Threshold Accepting (TA) algorithms and hybrid GAs. Hybrid GAs contain local improvement methods and/or TA algorithms to help improve the performance of a typical GA.

Unlike traditional optimization techniques, GAs do not require the gradient of the objective function to exist. GAs only need the definition of the objective, or fitness. This makes GAs applicable to a large set of problems. A GA is a multi-point search procedure modeled specifically on the mechanics of natural selection. A sGA is multi-point search procedure that occurs within isolated surroundings, interacting with nothing else. Parallel GAs that use for an example, a topological “ring’ structure constitute a set of multi-point searches. Structured migration allows the exchange of search points among the set. An iiGA also uses structured migration of search points among a set, but allows exploration of various levels of resolution of the search space. iiGAs search various levels of resolution to quickly find building blocks to inject into higher levels of resolution. iiGAs can also use various fitness evaluation tools and fitness definitions. TA algorithms are a single point hill climbing search procedure with a mechanism for climbing out of local optima (based on statistical mechanics of annealing). A local improvement method is also sometimes incorporated into the GA, allowing more rapid search of local areas to be explored. Hybrid GAs combine a mixture of any of the GA approaches with local and/or TA algorithms.

1.3 Literature Review

The following is a summary of literature reviewed for the current research. The articles are reviewed in categories. The first is structural optimization in general, the second is GA optimization applications and the last is the optimization of flywheels.

1.3.1 Structural Optimization

According to Jenkins [25] the process of structural optimization is an attractive goal to a designer because there is a satisfaction in producing the “best” design for a stated objective. This is, of course, only a fraction of the motivation behind structural optimization. Olhoff and Taylor [34] state that considerations such as limited energy resources, shortage of economic and some material resources, strong technological competition, and environmental problems are the motivations behind structural optimization. Structural optimization often contains multiple objectives such as minimizing cost while maximizing quality. Stadler and Dauler [49] present a broad overview and history of multicriterion optimization. Horn [24] argues that most, if not all optimization problems have multiple objectives. Both Horn [24] and Olhoff and Taylor [49] claim that the entire "trade off" set, or Pareto front, should be sought, but they vary drastically in their approach to this Pareto front. Olhoff and Taylor [49] make multicriterion decisions first with multiple runs using the classical variations of calculus approach while Horn [24] claims that the Pareto front should be found simultaneously with a Pareto "Niched" GA. Belegundu et al. [1], Sundaresan, et al. [50], and Khot, et al. [26] present an alternate point of view for optimization, that is robust design through minimum sensitivity. The goal of the optimization is to design engineering systems so that they are desensitized to variations in uncertainty variables, such as manufacturing errors. Osyczka, Kuchta and Czula [35] present an approach to optimization of multicriterion systems with computationally expensive evaluations. Jenkins [25] presents a general paper on structural optimization using GAs while Haslinger and Jedelsky [22] concentrate on shape optimization via GAs.

Stadler and Dauler [49] state that multicriterion optimization is rooted in economics, and was first treated in the book The Wealth of Nations (1776) by Smith. The first reference to multicriterion optimization was given by Edgeworth's book Mathematical Physics [24]. Horn [24] states Vilfred Pareto (1896) noted that a partial ordering of solutions exists before any multicriterion decisions are drawn defined by the Pareto criterion. The Pareto criterion states that a solution is superior if it is at least as good as other solutions in some criteria and better than other solutions in at least one criterion. More rigidly, Horn

[24] states that, given k attributes, all of which are to maximized, a solution A, with attributes $(a_0,a_1,a_2,...,a_{k-1})$, and a solution B with attributes $(b_0,b_1,b_2,...,b_{k-1})$, we say that A dominates B if and only if for all i: $a_i \geq b_i$, and there exists a j such that $a_j>b_j$. Some of the pairs of the solution set are not comparable in the sense that neither solution dominates the other and are termed incompatible. But conversely there are solutions that are dominated and can be discarded before any multicriterion decisions are made. The set of solutions that are not dominated by any other solution constitutes the Pareto front. This is demonstrated in the two dimensional (k=2) graph in Figure 1.1, where the objectives are to minimize cost and maximize quality. This simple example can be extended to include more complex multicriterion objective functions (k>2) by simply increasing the dimension of the plot. Figure 1.3 also demonstrates why the Pareto front could be sought. At points E and F in Figure 1.3, the "knees" of the front exist, which represent points at which small sacrifices in one objective causes large sacrifices in the other. In this case a rational decision maker needs to be presented with this information for analysis.

Olhoff and Taylor [34] discuss the fundamentals of structural optimization based on the mathematical properties of the governing equations for optimal design. They started by reviewing the basic concepts and well defined areas of optimization. This includes the conventional design method in which changes in the design are followed by an analysis of the design. Typically, this procedure is continued until a satisfactory design in cost and/or response is developed. This procedure is largely based on educated guess work by the designer.

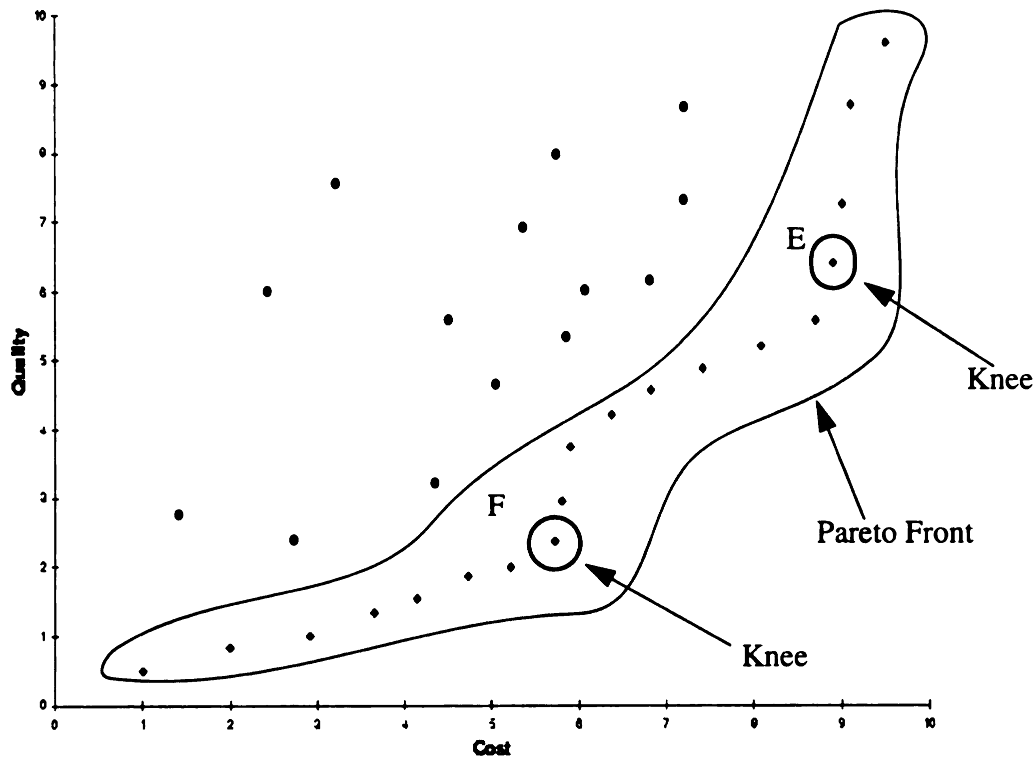

Figure 1.1. The "knees" of a typical Pareto front.

Olhoff and Taylor [34] labeled structural optimization as a design problem in which preassigned parameters and design variables are subdivided with an objective function to be maximized or minimized with respect to the design variables. Typical design variables were categorized, such as: cross-sectional, layout, material, and loading. These design variables are roughly continuous or discrete according to the manner in which they are related to the spatial variables. Cross-sectional design variables such as area and moments of area can be viewed as discrete or continuous, depending on what cross-sectional properties are manufacturable or available. Layout of a structure can be divided into topological and configurational design variables. Topological design variables account for the defining connectivity of the members in the structure and are integer variables, while configurational design variables describe surfaces and or centerlines of bars and are usually considered continuous variables. Material design variables are usually discrete, representing choices among alternate material properties. Loading design variables can be continuous or discrete, representing conditions placed on a structure.

Olhoff and Taylor [34] state that constraints are any set of design variables that can be represented by a point in the design space, which help reduce the total number of possible designs. Geometrical constraints such as maximum and minimum thickness are imposed explicitly on the design variables. Behavioral constraints are broken down into equality and inequality constraints. Equality constraints are stated as the equations governing structural response. Inequality constraints are imposed locally, such as local allowable stress, or globally, such as compliance. Both equality and inequality constraints are often nonlinear and implicit with respect to design variables.

The objective function must be expressed in terms of the design variables such that its value is definable anywhere in the design space. This objective function is to be maximized or minimized with respect to the set of design variables within the design space. A problem with a single objective function defines a single criterion optimization problem. Olhoff and Taylor [34] present the classical calculus of variations for single criterion optimization problems. A single criteria optimization problem can be rigorously stated as:

Determine D_i, $i=1,\ldots,n$ which

minimize $F(D_1,\ldots,D_n) = 0$,

subject to $h_j(D_1,\ldots,Dn) = 0$, $j=1,\ldots,p$

and $g_k(D_1,\ldots,D_n) \leq 0$, $k=1,\ldots,q$.

Where D_i is a vector of design variables, F is the objective function which is to be minimized with respect to the design vector under p equality and q inequality constraints. Assuming that the function F is differentiable with respect to the design variables, a calculus of variations approach can be defined. There are numerous well established single criterion optimization problems in the area of static loading, including design against plastic collapse, elastic response, optimal layout of trusses and dynamic loading under frequency constraints using calculus of variations, Olhoff and Taylor [34].

Granhi [21] presents an overview of optimization of structures using sensitivity derivatives calculation for repeated eigenvalues for frequency constraint approximations. Various optimization algorithms and applications are also reviewed.

Horn [24] argues that most, if not all, optimization problems have multiple objectives. Horn [24], Olhoff and Taylor [34] present approaches to multiple objective optimization problems in different ways. Both papers agree that the Pareto front should be sought, but they approach it differently.

Horn [24] classifies three approaches according to how they handle the problems of searching for the Pareto front and when the multicriterion decision is made. The first approach makes a multicriterion decision first and then performs a search. The second searches first, and then makes a multicriterion decision using a rational decision maker. The third integrates search and multicriterion decision making.

When a multicriterion decision is to be made before searching, the objective function is aggregated into a single objective function. A scalar-aggregate or an order-aggregate can define a multicriterion objective function. The simplest scalar aggregate is a weighted sum of the single objective functions. The decision maker tries weighting the objectives according to their merit. One drawback of such an approach is that it only accounts for linear variations among the criteria. This weighted sum can be generalized into any non-linear relationship, but weights are still at best guided by intuitional guesswork. This approach can be, in general, applied to any type of optimization algorithm to find the Pareto front by running multiple optimization runs, varying each weight from 0 to a maximum value while holding the other weights constant; but a weighted sum cannot capture concave portions of the Pareto optimal surface. This due to the fact that linear aggregative methods are biased towards convex portions of the Pareto front [24]. A lexicographic approach is a non-scalar aggregate approach to multicriterion objective problems, Horn [24]. This approach requires the decision maker to order the criteria and rank the solutions best to worst without assigning any scalar values. The approach can be tackled with evolutionary computation such as GAs by using rank-based and tournament-style selection methods.

An aggregated approach is, at best, an overly simplistic view of multicriterion optimization problems. Is it possible to combine objectives that contrast each other into a single objective? Horn [24] recognizes this difficulty, if not impossibility, of making multicriterion decisions before searching. Many dominated solutions can be eliminated by searching first and isolating the Pareto solutions in the current set defined by the Pareto criterion. Horn [24] obviously limits this application to a multi-point search algorithm such as GAs. Integrated search and decision making requires a preliminary multicriterion search that is given to a rational decision maker to narrow the search. Additional multicriterion search is conducted in the reduced search area. Again the decision maker narrows the search. This process is repeated until satisfactory results are found. Of course, any reduction of search space also reduces diversity and eliminates a full exploration of the search space for a multi-point search such as a GA. Pareto ranking plus niching tries to overcome this downfall by maintaining diversity along the Pareto front to deter middling of the Pareto front. Middling is a phenomenon that causes multi-point searches such as GAs (that are searching for the Pareto front) to have a population converge to the middle or center of the Pareto front. Even with controlled middling of the front, the search space is limited and not fully explored.

Olhoff, Taylor [25] and Bendsoe et al. [2] present three approaches to multicriterion optimization problems using the calculus of variations: weighted sum, goal attainment (bound method) and constraint method. All three are explained in the following paragraphs.

The weighted sum method is stated as:

$$\min_{D}\left(\sum_{i} w_i g_i\right) \tag{1.4.1}$$

The design D is to be minimized, where g_i is a single optimization criterion that defines the multicriterion optimization problem and w_i is the weight assigned to each criterion. Each weight is to represent the worth of each criteria based on the designer's preference.

The constraint method is given as:

$$\min_{D}(c_k) \text{ subject to } c_i - b_i \le 0 \quad (i=1,2,\ldots,n \ i \ne k) \tag{1.42}$$

where the constraint bounds $b_i \ge 0$ are specified by the designer.

The goal or bound method is given as:

$$\min_{D}(\beta) \text{ subject to } w_i g_i - \beta \le 0 \quad (i=1,\ldots,n) \tag{1.4.3}$$

The object is to minimize D with prescribed g_i over β.

Osyczka, Kuchta and Czula [35] present an approach to multicriterion optimization with expensive function evaluations. They maintain the most efficient approach to optimization of multicriterion systems with computationally expensive evaluations can be approximated by replacing the expensive evaluation with an alternate evaluation function that reflects the overall behavior of the system and is computationally cheaper while easier to optimize. The search for an alternate cheap accurate evaluation function can be viewed as another complex problem.

Belegundu et al. [1], Sundaresan et al. [50], and Khot et al. [36] present the idea of robust optimization through desensitizing engineering systems to uncertainties, such as manufacturing errors and operational variances. Traditionally, the sensitivity of optimal designs are recorded after the product is manufactured. G. Taguchi [50] developed a method to measure sensitivity of a system during the inital design process. The method had three stages: 1.) System design, where inital design varibles are chosen, 2.) Parameter design, where design parameters are optimized to desensitize the system to external influences, 3.) Tolerance design, where designers decide on allowable tolerances to represent an optimal deign. The method was first developed at a time when little computer simulation was available, so most data was gathered from actual experiments. The method was also developed to be efficient with respect to the number of evaluations needed. Due to the lack of computer simulation, Taguchi used orthogonal arrays for approximating expected sensitivity design values. The approximations made in the statistcal model are presented along with examples of robust design of gears and beverage cans. The optimization of robust design of gears was achieved by desensitizing gear profile to manufacturing errors while minimizing transmission error. The robust design of the beverage can was to minimize weight by desensitizing beverage can geometry while lessening the sensitivity to manufacturing error.

1.4.2 Application of Genetic Algorithms to Engineering Systems

This next section describes applications of GAs to engineering systems. A wide array of subjects is covered to demonstrate the diversity of GAs in engineering applications. Engineering systems included are: general engineering, structural, composite and aerodynamic systems.

To begin the general engineering applications, a paper by Crossely and Laananen [8] on the conceptual design of helicopters to reduce weight for specified helicopter missions using GAs will be reviewed. The GA was combined with an industrial sizing code specifically developed for helicopter design. Tournament selection was used with uniform crossover and bitwise mutation. A G-bit improvement scheme was also applied, which is analogous to a hill climbing approach, but was considered to be more like a gradient-like bitwise improvement approach. This scheme is applied to an individual if no improvement has been made in three generations. The G-bit improvement scheme varies one bit at a time and places the most fit individual found back into the population, replacing the poorest individual. This approach requires more computational effort, but previous studies found it to improve results. The GA run was terminated if no improvement was found for five generations. The design parameters the GA searched included integer, discrete and continuous variables. Variables that were integer include the number of engines and rotor blades. Variables that were continuous were rotor tip speed, disk loading, wing loading, wing aspect ratio and maximum blade loading. Various turboshafts were represented with discrete variables. The observation was made that the binary coding can cause bias in the initial generation if a design variable is not a power of two. The authors claim this bias is easily overcome if poor fitness is associated with the biased design variable.

Homaifar et al. [23] used a simple GA in the optimization of an engineering system consisting of turbofan engines. The criterion to be optimized were thrust per unit mass flow rate and overall efficiency. The key parameters were Mach number, compressor pressure ratio, fan pressure ratio and bypass ratio. Single criterion runs were first found for both objectives (thrust per unit mass flow rate and overall efficiency). The multicriterion optimization approach was based on the scalar aggregated weighted sum as noted previously by Horn [24]. Simple approximations were introduced to predict the field flow equations.

The final two general engineering papers reviewed are applications of GAs in heat transfer. Fabbri [10] used a GA to search for two-dimensional fin surfaces that have optimal thermal characteristics. The thickness of a symmetric two-dimensional fin was modeled with a polynomial and the distribution of temperature was obtained by solving Laplace's equation using the finite element method. The fin was considered to be immersed in a fluid with a constant bulk temperature with an applied temperature at one end. The fitness was based on compared effectiveness. Compared effectiveness is the ratio of the heat flux removed by the fin of variable shape to a rectangular fin of same volume and length. The polynomial was varied from first to fifth order in separate runs. The results seem to be affected by the polynomial order. As the order of the profile increased the oscillation of fin shape also increased. The results seem to be an artifact of the modeling of fin thickness as a polynomial. In fact, the number of local maximum and minimum thicknesses are identical to the order of the polynomial and none are similar with respect to fin profile.

The last general engineering paper reviewed is an application of simple GAs in the optimization of cooling of electronic components by Queipo et al. [41]. First, the combinatorial problem of searching for the optimal or near optimal combination of various rectangular cross sections placed at equally spaced locations along a ventilated two-dimensional channel was approached using a GA. The objective was to minimize the total thermal failure rate of a set of in-line convectively cooled electronic components. A transient finite difference flow code was used in the thermofluids-optimized packing of electronic components. The failure rate is considered to vary according to the Arrhenius equation, which is an exponential function. It was found that the heat transfer from electronic components is very sensitive to variations in geometry when convection is the dominant heat transfer mechanism. Due to excessive computational effort (30 minutes per evaluation) in solving the transient analysis, a population size of seven that was run for seven generations yielded at best a partial solution. A good first approach to any problem is to consider a linear static approximation, which was not considered by Queipo et al. [41]. A second problem presented extends the first problem with additional constraints of minimizing total interconectivity wire length. The effects of buoyancy were neglected in the balance of momentum equation. The last example reviews the effects of buoyancy-induced flow on the previous examples. Buoyancy is essentially flow induced from the tendency of heated fluids to rise. The effect of neglecting buoyancy caused slight errors in the simplified two-dimensional study.

There are many papers concerning applications of GAs in the optimization of structures. The first reviewed is by Nakanishi and Nakagiri [32], which used a GA with a boundary cycle and the finite element method to search for planar and three-dimensional topological frames that have a minimal deformation at the applied loads. The weight was constrained to be constant. The boundary cycle is used to represent the topology of a frame in which there are no members that have a free tip. The authors assume that a frame structure that has members that are not connected to at least one other member cannot be an optimal design. This is because members with a free tip do not transmit any forces or contribute any stiffness to the structure while wasting mass. Two and three-dimensional example problems demonstrate that the boundary cycle increases efficiency by exploring only reasonable portions of the search space, reducing the size of search space significantly.

Jenkins [25] first gives motivations to use GAs in structural optimization. This includes efficient exploration of large search spaces and robustness with respect to global optimization. An introduction to binary coding of chromosome structure for discrete and continuous variables is given. A simple GA is introduced with definitions of genetic operations such as crossover and mutation. A simple example of the minimization of a simple algebraic function is presented. Penalty functions are introduced in order to satisfy constraints in the optimal design of a trussed-beam roof structure.

Haslinger and Jedelsky [22] concentrate on shape optimization using GAs. The main point of this paper is that when using the finite element method, if a portion of the structure is always constant, i.e. never changing, the stiffness matrix associated with the finite element method for this portion of the structure is also constant. Instead of continuously recomputing the stiffness matrix, it should be stored and reused in order to decrease computational expense. It should be noted that Haslinger and Jedelsky [23] do not mention that the primary variables do not need to be computed when they are not of practical value for certain locations in the structure. This also will reduce computational intensity associated with computing gradients.

Furuya and Haftka [14] determined optimum placement of actuators on large scale space structures using simple GAs and effective indices. Actuators are used to help control the vibrational response of the structure. Effective indicies represent the vibration-suppression characteristics of the structure. An approximate solution to predict the effective indicies was used in the analysis by ignoring the fractions of elastic energy contributed by the actuators. This reduced the computational time required to compute the modal characteristics by an order of magnitude. This approximation was justified by assuming the actuators are small, not affecting the energy distribution of the structure.

Parmee and Vekeria [36] used island injection GAs to perform shape optimization of concrete plates to minimize weight while maintaining an allowable stress level. The finite element method was used in the evaluation of the stresses in the variable thickness plate. An island injection Genetic Algorithm (iiGA) approach was applied to help reduce the computational intensity associated with a refined finite element mesh. Each island evaluated individuals with a refined finite element mesh to accurately predict the response of the plate. The iiGA searched at various levels of resolution by representing the plate by various levels of geometric resolution. An iiGA has structured migration of individuals amongst islands, which injects good solutions into islands with an increased level of resolution. As an example, an island with a coarse geometric resolution represented a plate by dividing it into four rectangular areas, allowing each rectangle to have a thickness that varied linearly. A refined geometric resolution simply subdivided each rectangular, increasing the number of thickness design variables. The process of injecting solutions from low levels of resolution was continued until a satisfactory level of geometric resolution was obtained. Islands with a low level of resolution converged much quicker compared to islands with a higher level of resolution due to the reduced search space. This motivated the authors to consider a dynamic island injection GA, where the islands at a low level of resolution were terminated and reseeded after convergence. The iiGA helped decrease computational time with little or no decrease in the fitness of the best individual found. The dynamic island injection GA showed a further decrease in computational effort with little or no effect on the final result.

The first application of GAs in composite structures reviewed is by Todoroki and Watanabe [51]. They used a simple GA to optimize the placement and fiber orientation of stiffeners on a laminated composite plate that had a bolt at the center. A uniform displacement across one edge of a rectangular plate caused a stress concentration near the bolt. Only a quarter of the rectangular plate was modeled due to symmetry. The objective of the problem was to reduce the strain energy near the stress concentration by redistributing stresses throughout the plate with composite stiffeners. The stiffeners were to be applied after the curing of the laminated composite plate. Evaluation of fitness was performed with a finite element code that used three-noded triangular plate elements. A location consisted of a square composed of two triangular finite elements with a similar face. Three different fiber orientations were used for each location: $[0]_2$, [45/-45] and $[90]_2$. Also, there was a possibility that the location lacked a stiffener. Several simple GA runs were performed to find good GA parameters with a similar simplified problem. For this particular problem, the authors found that a low crossover rate (20%) with a high mutation (10%) performed the best.

Haftka et al. [13, 14] used a simple GA to optimize the stacking sequence of a laminated composite plate for buckling load maximization. First, GA parameters such as population size, and genetic operator probabilities were tuned by numerical experiments.

Often GAs require a large number of analyses, sometimes in the millions. A serious problem with GAs occurs when a single analysis is computationally demanding. In light of this, the objective of the work was to reduce the computational intensity associated with GAs. One step made in this direction was the use of a binary tree. A binary tree was used to store all previous analyses performed in the optimization and retrieved later if an exact duplicate analysis was reiterated, avoiding costly repeat analyses. A binary tree can reduce computational costs when a high computational price is paid for each evaluation (compared to the time used to search the binary tree). A drawback of the binary tree is the need for a large amount of available memory to store previous design information. A second step made in the direction of reducing the computational intensity of GAs was the approximation of certain buckling loads. Buckling loads were computed exactly for each design string created by genetic operators. The set of all possible combinations of design strings is approximated by a linear least square fit based on bending lamination parameters. The best of these combinations replaces the nominal design in the population. This technique searches a small neighborhood of designs for a local optimum. This particular local search caused difficulties with singular optima by interfering with crossover operations. This problem was alleviated by seeding the initial population with certain designs.

Flynn and Sherman [12] outlined a two-step procedure to locate various GA configurations for multicriterion optimization of flat aircraft panels. The panels were composed of 13 materials (3 isotropic and 10 composite). A GA that searched for the Pareto front was used in the multicriterion optimization based on four object functions: panel buckling, bay buckling, weight and the total number of frames and stiffeners. Just as Haftka et al. [14] performed pre-trial runs to tune GA parameters, so did Flynn and Sherman

[12] in the first phase of their two-step procedure. 'Rule of thumb' values were gathered from related GA publications. The GA parameters were then tested on a simplified aircraft panel design. The second phase identified successful configurations and placed them into a "preferred" set. Comparing results to other optimization techniques, the "preferred" set of GA configurations produced designs that were lighter and at least as good in all other criteria.

The next application of GAs in composite structures is by Punch et al. [27, 38]. They searched for optimal laminated composite beams with a coarse grained island injection Genetic Algorithm (iiGA). The objective was to find stacking sequences for laminated composites beam that maximized the amount of mechanical energy absorbed by the beam before fracture. A goal of approaching the problem with an iiGA was to reduce computational effort. This was accomplished with an iiGA by searching at various levels of spatial resolution on separate computational nodes. Structured migration amongst islands allowed good individuals at low spatial resolution to be injected into islands of higher spatial resolution. The fitness of the beam was evaluated with a new finite element model developed for composite laminate analysis. The new finite element model accounted for layerwise variations of displacements and stresses by assuming a piecewise linear continuous through-the-thickness in-plane displacement distribution. A clamped-clamped graphite-epoxy composite layered beam had a point load applied at its midspan. The GA was allowed to place either a 0 or 90 degree ply in each element in the discretized beam. The concept of thin compliant layers to modify the load path characteristics of the structure to increase the amount of mechanical energy absorbed was modeled by allowing the GA to choose either an identical material or a material with a significantly reduced stiffness above each composite layer. First, a symmetric beam with a small search space (approximately 10^6 designs) was explored with the island injection GA. The final results from the island injection GA were confirmed to be the global optimal solution by enumerating (exhausting) the search space. Next, larger search spaces that did not assume beam symmetry were explored with the island injection GA with promising results.

Mallot, et al. [28] used an island injection GA to optimize an idealized airfoil. The object of the problem was to find composite stacking sequences of sandwich plates that maintain an appropriate opposite twist to compensate for in-flight aerodynamic loads that cause adverse airfoil twisting, while minimizing weight under stiffness and ply clustering constraints. Displacements and stresses were predicted with a finite element model based on first order shear deformation plate theory. A single "optimal" finite element mesh was employed that balanced accuracy and computational efficiency. Three different runs obtained from different GA topologies were presented. A single node, a "ring" topology GA containing seven islands and an island injection Genetic Algorithm topology containing seven islands. Each GA topology contained a total of 1400 individuals. In this study, both GA single node and ring topology converge within 50 generations. Using the island injection GA, the behavior sought from the islands exploring smaller search spaces (lower levels of resolutions) should initially make more progress, providing "building blocks" to be injected into islands with a larger search space (higher level of resolution). The islands with a higher resolution should receive the migrating individuals, then outperform islands with lower levels of resolution due to the expansion of search space. The iiGA approach was able to find designs which reduce weight by 66%, increase minimum in-plane stiffness values by 33% and increased the twist by a magnitude of 77 times the baseline design, but in opposite direction. The iiGA approach was the most efficient in terms of computational time.

Quagliarella [40], Obayah [33] and Foster [11] apply GAs to design shockless transonic airfoils. Quagliarella computed aerodynamic coefficients (drag and lift) of airfoils using a potential flowfield solver. A potential flowfield solver is a static linearized form of the Navier flow equations. This study began by using a GA to for wave drag minimization though shape optimization of a baseline airfoil. The results obtained were characterized by good behavior for the minimization of wave drag but presented poor results for lift coefficients. A new objective was formulated to simultaneously optimize drag and lift coefficients.

Obayah [33] approached the same problem for shockless plus non-shockless wave constraints with a GA by an inverse design method. A direct optimization method couples analysis methods to maximize (minimize) an object function by iterating directly on the geometry. The inverse design method in this paper deals with pressure distributions rather than geometry, to minimize, for example, drag under given lift and pitching moment. Once optimized target distributions are found, a corresponding geometry can be determined through the inverse method. A direct approach requires computational fluid dynamic evaluations of each individual in a population. This is not feasible when a single computational fluid dynamic evaluation could require an incredible amount of computational time. This makes inverse design methods attractive for any optimization approach in computational fluid dynamics because it does not require any computational fluid dynamic evaluation. This helps transform fluid flow optimization into a computationally tractable problem, which is vitally important for GAs.

Foster [11] compares two hybrid optimization techniques, gradient and GA optimization methods in aerodynamic shape optimization in hypersonic flow. This flow region was chosen because computational costs were not extremely high using an inexpensive Newtonian flow analysis. The first flow analysis method was based on the modified Newtonian impact theory, a simplified technique that is computationally cheaper, but can not capture all the physical behavior associated with complex fluid flow phenomena. The second flow analysis method is based on a parabolized Navier-Stokes solver, which can capture complex fluid flow phenomena at a slightly higher computational cost. The hybrid gradient technique combined hill climbing, the method of feasible directions and Rosen's projection method. The method of feasible directions is particularly effective for determining a search direction when inequality constraints are present. If an equality constraint is present then it is advisable to follow the constraint, which is performed with Rosen's projection method. The hybrid GA applied the hybrid gradient technique if the entire set of newly generated designs had been analyzed with no improvement. Examples included optimization of a half-sphere-cone to minimize wave drag and maximize lift, using both hybrid techniques. It was found that the hybrid GA convergence rates were comparable to standard gradient techniques. Also, the hybrid GA had the ability to search design spaces that gradient techniques could not.

1.3.3 Design Optimization Applications Via Other Methods

Chen et al. [5] used simulated annealing to place active and passively damped members in the optimization of truss structures. Actuators were used to help control the vibrational response of the structure. Unlike Furuya and Haftka [14], the elastic energy contributed by the actuators was not ignored.

Chu et al. [7] have been researching structural optimization problems with stiffness constraints. The paper presents a simple procedure with finite element analysis to minimize weight while satisfying stiffness requirements that are placed on structures such as bridges. At the end of each finite element analysis a sensitivity number indicating the change in stiffness for each member of the structure is calculated. Members that have little contribution to global stiffness of the structure are slowly removed in a step by step process. The sensitivity number for problems that have stiffness constraints is the inverse of the strain energy of the structure, or the overall stiffness of the structure. Maximizing the overall stiffness of the structure is equivalent to minimizing the strain energy. By removing one of the structure members the global stiffness will be decreased and the change in the strain energy can be defined (if the higher order terms are neglected). This change in strain energy was the sensitivity number for stiffness constrained problems. The process for calculating the sensitivity number for problems with displacement constraints can be defined by first applying a unit force at each of the nodes. Next, the displacements of the nodes under the displacement constraints are calculated. A relationship between elements and the displacement of the constrained nodes is defined as the sensitivity. The process is performed on a short cantilever beam, Mitchell truss and a plate in bending.

1.3.4 Optimization of Flywheels

The optimization of flywheels has been attempted by many researchers [3,6,15-17,46,48]. All of these optimization techniques, expect for Bhavikatti [3], make a plane stress assumption.

Bhavikatti [3] represented the shape of the annular flywheel as a polynomial and used a single point sequential linear programming method with various objective functions to optimize an annular isotropic flywheel using the finite element method with quadratic elements. The first objective function was the minimization of the differences between the maximum and minimum tangential stresses measured at 16 points along the radius of the flywheel. This resulted in an awkward bulging near the inner radius of the flywheel. This can be attributed to the fact that the highest stress will be in the tangential direction near the inner radius of the flywheel. The second objective was to level the stress along the center of the flywheel. This resulted in a flywheel that formed a shape that mainly concentrated on increasing stress in areas of low stress, instead of reducing stress in areas of high stress. The last objective function involved an aggregated weighted sum that tried to minimize volume and level stresses. This resulted in a flywheel with less volume yet the same maximum stress as the results from the second objective function.

Often, optimization problems require simplifications to make the problem computationally feasible and numerically tractable. The results are often artifacts of these simplifications. Seireg [48], Sandgren [46], Christensen [6], and Georgian [17] all researched shape optimization of flywheels in a day when the speed of computers was still relatively slow. Assuming a plane stress approximation was the only possible approach to form the problem that was computationally feasible.

Recently, Genta [16] used a simple GA to help design flywheels using a plane stress finite difference model in search of the constant stress profile. Genta acknowledged the shortcoming of the plane stress analysis by using various constraints on the fitness function to reduce the complex three-dimensional stresses that will occur, for example, at the inner most portion of an annular flywheel that has steep gradients in ring thickness. To avoid flywheel ring oscillation that affected generations of flywheels, the initial population was seeded with flywheels with thicknesses that only varied linearly in height.

4.4.5 Paper Review for Improvement

The iiGA has the powerful ability to search at various levels of resolution with different evaluation tools and fitness objectives. This approach by the iiGA can be applied to any problem that the fitness of an individual can be first approximated with an efficient, simplified analysis. For instance, Osyyczka et al. [35] attempt an approach on a lower level by simply approximating expensive objective evaluations with less expensive evaluations that can hopefully reflect the overall response of a system accurately. A flaw in this approach lies in the fact that approximations in objective evaluations often give rise to solutions that are artifacts of the approximation. An iiGA approach can use approximate fitness evaluations to quickly search for low level building blocks to inject into islands with a refined analysis. The island with the refined analysis can recombine good parts of existing solutions (building blocks) to discover better solutions while discarding portions of the solution that violate the approximate fitness evaluation.

Queipo [41] used GAs to optimize the cooling of electronic components, evaluating fitness with a transient finite difference evaluation. Due to excessive evaluation time per individual (30 minutes), a small population size was allowed to generate a few generations. This approach could be improved by making computationally efficient approximations in the analysis. An iiGA topology can be designed that could slowly decrease the level of approximation until satisfactory evaluations occur. The approach could be improved further using an iiGA to search at various levels of resolution with the simplified analysis to discover building blocks that can be injected into a refined analysis.

Furuya and Haftka [8] approximate the modal response of large scale space structures by ignoring the elastic energy contributed from small actuators. A possible downfall in the approximation occurs if many acutators are all placed in a small area, contributing a large portion of elastic energy locally in the structure, changing the global response of the structure. This optimization approach could be improved with an iiGA by injecting solutions found with the approximations to an island that evaluates the objective function considering the elastic energy contributed from the actuators.

Crosseley and Laananen [8] used a G-bit improvement scheme to help improve the search efficiency of the GAs in the conceptual design of helicopters. This improvement scheme mimics Threshold Accepting by perturbing a solution to find a better solution on a bitwise basis. However, while the G-bit improvement scheme performs a local enumerative search on an individual, a Threshold Accepting algorithm climbs a hill in a dynamic fashion. A search that has direction should be more efficient than an exhaustive local search.

Many GA optimization approaches [11-13, 27, 33 43, 49, 51] can benefit through the use of an iiGA to search at various levels of resolution to help improve computational efficiency.

Typical examples of optimization approaches that result in solutions which are artifacts of an approximation of the objective evaluation are shown in [6, 7, 15-17, 46, 48]. The approximations of a plane stress objective function for flywheels in [6, 7, 15-17, 46, 48] resulted in the optimization tool exploiting the conditions of plane stress with flywheels that have thick gradients in ring thickness. It is completely reasonable to first attempt to approximate the response of a flywheel with a plane stress condition, but any optimization technique that finds better solutions by violating the assumption will only boast solutions that are artifacts of that assumption. Understanding approximations and their potential pitfalls can be crucial when analyzing any structure.

1.4 Present Study

An overall objective of this thesis was to develop tools for optimization of large scale three-dimensional composite structures. Combining a GA with the finite element method is by now a familiar approach in the optimization of structures. Using an iiGA with multiple evaluation tools with different fitness functions is a new approach aimed at decreasing computational time while increasing the robustness of a typical GA. New hybrid GAs were also developed to help increase computational efficiency and robustness of a typical GA. Hybrid techniques developed include GAs and iiGAs that incorporate a combination of local search methods and TA algorithms.

For reader familiarization, the mechanics of GAs and hybrid GA techniques will be reviewed. Mathematical development of two axi-symmetric finite element models will be presented. Results from the developed finite element codes will be verified with an industrial finite element code. An enumerable search space will be designed in order to compare and contrast optimization approaches. Next, optimum solid and annular multi-material flywheels will be sought. Finally, optimization of multi-material composite flywheels will be presented while constraining angular velocity and penalizing flywheels with large "air gap" growths.

Chapter 2

Algorithm Design and Comparison

2.1 Introduction

According to Carlson et al. [4], a good optimization scheme should not require full exploration of the search space, yet should progressively find better solutions without excessive computation. Unfortunately, no single approach is best for all classes of problems. Fortunately, certain optimization approaches work better for a specific class of problems. Calculus-based hill climbing search methods work well for an explicit class of problems that have a smooth convex objective function with a unimodal search space. Hill climbing methods assume the solution space is somewhat well behaved, which is only true for a relatively small class of problems. In fact, most search spaces are non-convex and multi-modal. Furthermore, a gradient-based approach requires that the problem have continuous design variables, which is inadequate for discrete problems. Dynamic programming is a hill climbing technique that can overcome some discrete problems but is limited to problems that have a relatively small search space. Enumerative search methods typically just exhaust the search space by exploring all possibilities, which is not efficient for problems with a large search space and or a problem associated with high evaluation times. A GA is a directed search procedure based on abstractions of the mechanics of natural selection and natural genetics [12].

Traditional methods can be limited in multicriteria optimization applications while GAs tend to excel with increased problem difficulty due to the increased search space complexity. Typically, a GA can converge to a global optimum, or a nearly globally optimal local optimum, by searching only a fraction of the search space. A possible downfall of GAs is their computational intensity. A GA is an evolutionary, combinatorial technique that is partial to problems with discrete solution spaces.

First an extensive background on the mechanics of Parallel GAs will be presented. GAs that use ring topologies will also be reviewed. Next, the mechanics of Island Injection GAs will be reviewed. Simulated Annealing and Threshold Accepting methods of optimization will also be presented.

2.2 Genetic Algorithms

Genetic Algorithms (GAs) are a powerful technique for search and optimization problems, and are particularly useful in the optimization of composite structures. The search space for a composite structure is generally discontinuous and strongly multimodal, with the possibility for many local sub-optimal solutions or even singular extrema. These facts severely limit gradient-type approaches to optimization, bringing this broad class of problems under scrutiny for application of GAs.

A GA is a search procedure modeled on the mechanics of natural selection rather than simulated reasoning processes. Specific knowledge is embedded in a representation called an organism, or in our case, a flywheel. A single chromosome will represent an organism (flywheel). Each chromosome will consist of a set of values of a certain length. Each chromosome of length n will be represented in the form of a vector, $<x_1, x_2, \cdots\cdots\cdots\cdots x_n>$. Each x_i is an allele, or a gene. Often, an allele is expressed through binary numbers, although many now use GAs with real numbers represented as floating point variables directly on the chromosome, together with 0-mean Guassian random mutation operators. Each allele depicts a characteristic of a certain flywheel. Evolution takes place specifically on chromosomes, not the "living creature" (flywheel) itself. Living creatures are created and destroyed by a process of decoding chromosomes. Natural selection is the connection between chromosomes and the performance of the chromosome structure and is a process that causes superior performing chromosomes to have a higher probability of reproduction, while inducing poorly performing chromosomes to have lower probability for reproduction. During reproduction, three things are commonly modeled which can cause children to differ from their parents: crossover, mutation and inversion. This in turn produces flywheel "children" with decoded chromosomes that can be quite different from the "parents' " coded structures. The amount of crossover is controlled by the user. A high crossover rate will produce new organisms quickly, but will have more probability to discard higher performing organisms, as well. A low crossover rate can stagnate the population, thus producing no new organisms. A large genetic pool increases diversity in a population, which in turn improves the ultimate results of the GA. A set of co-existing organisms (flywheels) defines a population, while successive populations are termed generations. Incorporating these processes in a computer algorithm will produce an algorithm that solves problems in a manner reminiscent of natural evolution.

GA's have search methods that are different than other search methods. GA's have the property of implicit parallelism. Implicit parallelism for a GA means that each evaluation searches (incompletely) in multiple hyperplanes of a given space. A GA does this efficiently by optimizing the trade-off between exploring new space and exploiting the information gained simultaneously. A hyperplane is a plane in hyperspace that corresponds to a plane in ordinary space. A hyperspace is any space of dimension higher than euclidean space (three dimensions). Large diverse populations increase the number of hyperspaces in which the GA searches for answers in hyperplanes. This improves the GA performance and computational intensity because the GA explore a larger search space. GA's explore many solutions simultaneously, and information gathered is shared concurrently among multiple searches. All of the searches have possible access to the information from other searches simultaneously. This is almost like a pair of hands that work separately, while knowing what the other hand is doing and having a common goal, only the GA can have more than 2 hands.

Figure 2.1 displays the structure of a simple GA. The simple GA begins by creating a single initial population, wherein flywheels of different shapes are randomly created. At this point a finite element program evaluates the "goodness" of each flywheel based on specific design parameters. Biased by the evaluations obtained, the GA uses unary and binary operators on these designs to create another population. This population maintains the previously "good" flywheels while discarding poorly performing flywheels. The program evaluates the new population members and continues with additional rounds of generation and selection. This is repeated until satisfactory solution(s) are obtained [12].

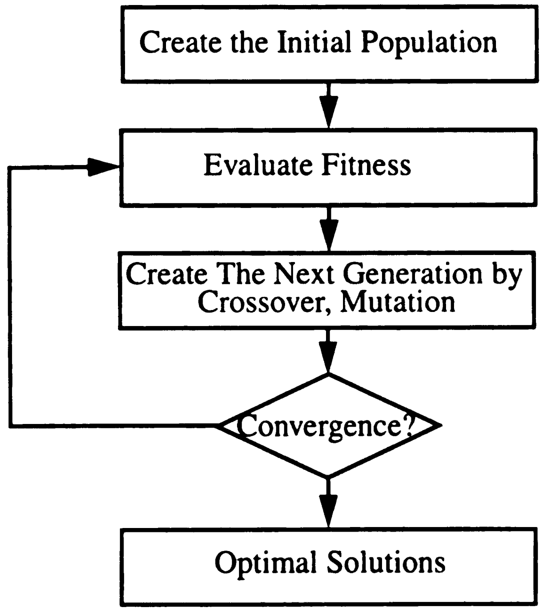

Figure 2.1. Simple GA structure.

2.2.1 Genetic Algorithm Coding and Structure

2.2.1.1 Design Coding and Search Space Dimensions

This section will define the design codings used to represent flywheels in this study. The design space and constraints must first be identified. The design space and constraints are identified by defining a maximum and minimum thickness, inner and outer radii, and a specified number of material choices. The fidelity of each design space is prescribed by the number of bits in the string defining each locus, or position on the chromosome. Each locus will represent a design variable in the flywheel. A group of loci in vector form represents a chromosome. For instance in a very simple case, the first two strings (composed of two bits) in the chromosome might represent the inner and outer radii of the flywheel. The third and fifth loci (three bits each) of the chromosome represent the inner and outer thickness of the first ring. The third loci (one bit) is the material property associated with the first ring.

This is demonstrated in the simple single-ringed flywheel chromosome shown below:

[0 1 , 1 0 , 1 1 1, 1, 0 1 1]

The locus that represent continuous design variables such as ring thickness are translated from binary to base ten quite easily. In binary mode, three bits convert into 2^3 or 8 equally spaced choices of heights ranging between the maximum and minimum thicknesses. For this chromosome there are 2^1 material property choices and 2^2 maximum and minimum radii. Binary decoding schemes have a slight drawback due to the fact that the number of choices (alleles) at loci that represent material properties must be a power of two or a biased solution will be achieved (this was also recognized by Furura and Haftka [13]). The total design space dimension is $2^2 \cdot 2^2 \cdot 2^3 \cdot 2^1 \cdot 2^3 = 2,048$. This design space could be quickly enumerated. The design space quickly grows: a six ringed flywheel with constant inner and outer radii with a single material property allowing three bits to define the search space for the ring thickness contains over 2 million search points. A GA can search a fraction of this design space and find the optimal solution. Increase the fidelity of the ring thickness representation to five bits and the search space grows to over 343 billion search points. This search space and much larger ones can also be explored efficiently with a GA.

2.2.1.2 Initial Population Generation

First, the GA must perform initiation and evaluation of the initial population. Following the above coding design, the GA creates a population of flywheels of various shapes composed of various materials, stochastically. Often, populations are initialized by the user, as in the case of Genta [16]. A measure of "goodness" or fitness is assigned to each individual by the fitness function.

2.2.1.3 Reproduction/Selection

The next process the GA must perform is selection. The selection mechanism for GAs is simply the process that favors the selection of fit individuals to be placed in a mating pool. Selection pressure is the degree to which the better individuals are favored: a higher selection pressure corresponds to an increase in favoring of highly fit individuals. The fitness function provides a means of comparing individuals and the selection process determines how the individual fitness values are compared. Selection mechanisms determine which chromosomes will be placed in the mating pool. The mating pool is comprised of the individuals that will reproduce to create new individuals through crossover and mutation. Roulette wheel, stochastic remainder, rank-based and tournament are all selection mechanisms. Tournament selection was used exclusively in this study due to its low selection pressure. Tournament selection allows for a group of individuals that are chosen stochastically to gather and compete in a tournament, the individual with the highest fitness is placed in a mating pool. Individuals from the mating pool are used to generate new offspring, with the resulting offspring forming the basis of the next generation. According to Miller and Goldberg [23], a smaller group size lessens pressure to converge by disallowing any "super" individual in initial populations to dominate the reproduction cycle, promoting diversity. Reproduction is the GA search catalyst that works by mimicking natural selection.

2.2.1.4 Crossover

The next genetic process performed by the GA is crossover. Pairs chromosomes that were placed in the mating pool through the selection process are combined through crossover. Uniform order-based, cycle, partially matched, one-point, two-point and uniform crossover are commonly used procedures. One-point crossover was used in this study and is explained in detail. Consider the two chromosomes shown below:

[0 1 , 1 0 , 1 1 1, 1, 0 1 1]

[1 1 , 0 0 , 0 0 1, 0, 0 1 0]

One-point crossover only occurs between loci. One-point crossover occurring between the second and third loci would result in the following new individuals:

[0 1 , 1 0 , 0 0 1, 0, 0 1 0]

[1 1 , 0 0 , 1 1 1, 1, 0 1 1]

In this particular case, the GA would create new individuals that have swapped their associated radii.

2.2.1.5 Mutation

Mutation is another process that aids GAs in the search procedure. The mutation operator is applied at a low rate to chromosomes in order to help introduce new genetic data into the population. This helps maintain diversity and reduces the probability of premature convergence. A single-bit mutation operator was used in this study. A single-bit mutation operator is demonstrated in the following chromosome at the third bit:

[1 1 , 1 0 , 1 1 1, 1, 0 1 1]

The new chromosome would be:

[1 1 , 0 0 , 1 1 1, 1, 0 1 1]

This single-point mutation would cause a change in the outer radius of the flywheel. When real numbers are represents as floating point numbers on the chromosome, it is common to use an alternative form of mutation, typically an additive Guassian operator with 0 mean and variance determined by the feasible range of the variable or the current diversity of the values at that locus in the current population.

2.3.1.6 Penalty Method

GAs cannot directly satisfy all constraints in many optimization problems. A GA can indirectly satisfy constraints through the use of the penalty method. Typically, the fitness of an individual will be punished for violations of constraints. Often, the global optimal solution lies near or at a constraint, so the penalty method can help the GA maintain solutions that nearly or just slightly violate the constraint.

2.2.2 Parallel Genetic Algorithms

Two problems associated with GAs are their computational intensity and their propensity to converge prematurely. An approach that ameliorates both of these problems is parallelization of GAs (PGAs), which also produces a more realistic model of nature than a single large population. PGAs both decrease processing time and better explore the search space.

Unlike some specialized sequential GAs which pay a high computational cost for maintaining subpopulations based on similarity comparisons (niching techniques, etc.), PGAs maintain multiple, separate subpopulations which may be allowed to evolve nearly independently. This allows each subpopulation to explore different parts of the search space, each maintaining its own high-fitness individuals and each controlling how mixing occurs with other subpopulations, if at all.

2.2.3 Island Injection Genetic Algorithms

Island injection Genetic Algorithms (iiGAs) represent an approach to search at various levels of resolution within a given space. This includes first searching at low levels of resolution on different nodes (islands) and then injecting the high-performance individuals into an island of higher resolution to "fine-tune" them. Islands with a low resolution can evaluate fitness with a simplified analysis that is computationally cheaper, while islands with a high resolution can use a refined, computationally expensive analysis. Also, different GA parameters can be used for each population. The rate of crossover, mutation, and the island interaction can all vary from island to island. For example, islands at low resolution can have a larger population size to take advantage of a computationally cheap fitness evaluation. Also, islands with a computationally cheap fitness evaluation and a low resolution can be further exploited by increasing the number of generations evaluated before injecting the information to other islands. Figure 2.2 shows a typical iiGA that can first search at a low level of geometric resolution and inject individuals into islands with a higher level of geometric resolution. iiGAs can use multiple evaluation tools, various fitness functions and performs multiple refinements in the geometric representation by increasing the number of rings in the flywheel. For composite analysis, material properties can vary from ring to ring.

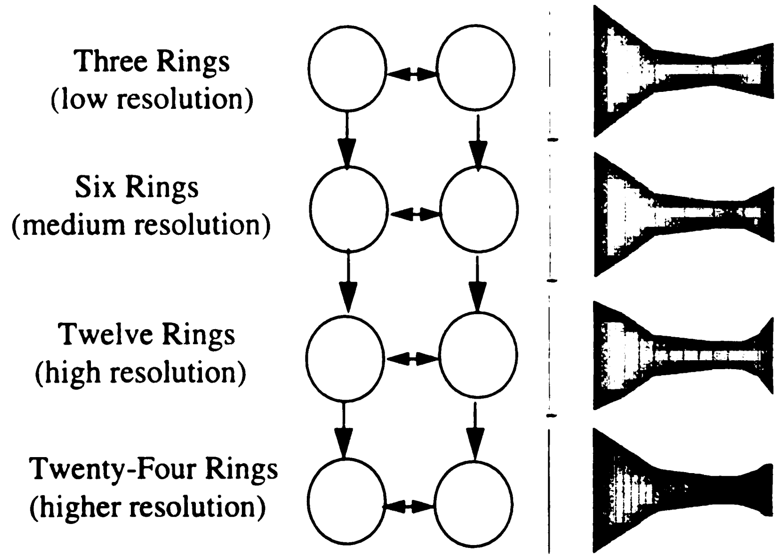

Figure 2.2. Possible iiGA topology that searches at various levels of geometric resolution.

Multi-objective optimization requires combining many performance measures to find an optimal design. Each individual fitness measure may have its own optimal or sub-optimal solutions. By using iiGAs, each individual performance could be used as a "sub-fitness" function since it represents "good" designs within the search space. Often, only the best individual in a population is allowed to migrate, to allow "good" ideas to be combined with other "good" ideas to find "better" ideas amongst islands of different "sub-fitness" functions. Next, the individuals are injected into a final node where the evaluation of an overall fitness function is employed. This search method ensures a robust exploration of the search space for all aspects of the overall fitness. Of course, many variations on these island injection architectures can be custom tailored for specific problems.

iiGAs have the following advantages over other PGAs. Building blocks of lower resolution can be directly found by search at that resolution. After receiving lower resolution solutions from its parent node(s), a node of higher resolution can "fine-tune" these solutions. The search space in nodes with lower resolution is proportionally smaller. This typically results in finding "fit" solutions more quickly, which are injected into higher resolution nodes for refinement. Nodes connected in the hierarchy (nodes with a parent-child relationship) share portions of the same search space, since the search space of parent is contained in the search space of child. Fast search at low resolution by the parent can potentially help the child find fitter individuals. iiGAs embody a divide-and-conquer and partitioning strategy which has been successfully applied to many problems. Homogeneous PGAs cannot guarantee such a division since crossover and mutation may produce individuals that belong to many subspaces, i.e., the divisions cannot be maintained. In iiGAs, the search space is fundamentally divided into hierarchical levels with well defined overlap (the search space of the parent is contained in the search space of the child).

2.3 Simulated Annealing and Threshold Accepting

Simulated Annealing (SA) is a combinatorial optimization technique that is based on the statistical mechanics of annealing of solids [45]. To understand how such an approach can be used as an optimization tool, one must consider how to coerce a solid into a low energy state. Annealing is a process typically applied to solid materials to force the atomic structure of the material into a highly ordered state. Atomic structures that maintain a highly ordered state are also at a low energy state. In an annealing process, a material is heated to a temperature that allows many atomic arrangements, then cooled slowly, minimizing energy, while statistically allowing an occasional increase in atomic energy. When the material is extremely hot, the probability of an increase in atomic energy is very high. As the cooling continues, the probability of an increase in atomic energy decreases. Similarly, SA methods use analogous set of parameters that simulate controlled cooling effects found in the annealing of materials.

SA methods begin with an initial solution that is often generated randomly, and try to perturb the solution to improve it. If the perturbation improves the solution then it is accepted and the process of perturbing continues. In this manner, SA methods are like iterative methods that climb hills. As with hill climbing methods, this process of searching just for a better solution tends to force the process to a local optimum. However, SA methods are different in this manner: annealing occasionally allows perturbations that are harmful to the solution to be accepted. This allows SA methods to climb out of local optima to search for the global optima. In actual physical systems, jumps to a higher (harmful) state of energy actually do occur. These jumps are monitored by the current temperature. As the annealing process (cooling) continues, the probability that only better solutions will be accepted increases. At the beginning of the annealing process (associated with a high temperature), the chance that a harmful solution is accepted is higher while later in the annealing process (at a lower temperature) that chance that a harmful solution is accepted is small. This probability of accepting harmful solutions is based on a Boltzmann distribution:

$$Pr[accept] = e^{\frac{-\Delta E}{T}} \qquad 2.1)$$

By successively lowering the temperature T, the simulation of material coming into equilibrium at each newly reduced temperature can effectively simulate physical annealing.

Threshold Accepting (TA) is a simplified version of Simulated Annealing. The probability of accepting a harmful solution is governed by the Boltzmann distribution for SA applications and TA algorithm, but the TA algorithm is not dependent upon a specified temperature. Instead the TA algorithm "cooling" is based on a specified percentage of the current solution's fitness. This percentage decreases over the set of generations. This causes the TA in lower generations to have a higher probability of accepting a worse individual, while later generations in the optimization are less likely to accept a worse solution.

Chapter 3

Finite Element Models of Flywheels

3.1 Introduction

Two axi-symmetric finite element models were developed to predict planar and three-dimensional stresses that occur in flywheels composed of orthotropic materials undergoing a constant angular velocity. Both finite element models can be developed by applying the principal of minimum potential energy. An alternate but equivalent approach to formulating the finite element model is based on the weak statement of the governing differential equation.

To insure realistic results in an optimization problem the evaluation tool should be verified for accuracy. The axi-symmetric plane stress finite element model is verified by comparing results with the closed form solution [46] for constant thickness solid flywheel. Results from the axi-symmetric three-dimensional finite element model are compared to the commercial finite element code MARC [47] for a flywheel of variable thickness.

3.2 Finite Element Model Formulations

In this section, two axi-symmetric finite element models that predict the response of an orthotropic flywheel undergoing a constant angular velocity will be developed. First, the plane stress finite element model will be developed. Next, the plane stress approximation will be ignored to formulate the three-dimensional finite element model.

3.2.1 Plane Stress Finite Element Model Formulation

The finite element model that assumes a planar state of stress assumes no variation of stress will occur through the transverse normal (thickness) direction of the flywheel. Also, the model assumes that the transverse normal and in plane shearing stresses are small when compared to the tangential and radial stresses. The plane stress finite element model is accurate when the radial gradient of flywheel ring thickness is small.

The equilibrium equation in polar coordinates for a flywheel in a plane stress state is:

$$\frac{dtr\sigma_r}{dr} - \sigma_\theta t + trB_r = 0 \qquad (3.1)$$

where the thickness t is a function of the radius. Figure 3.1 displays how the geometry of the flywheel was modeled with concentric rings that varied in thickness linearly as a function of the radius. The body forces induced from rotations in the radial direction, B_r can be defined as:

$$B_r = r\rho\omega^2 \qquad (3.2)$$

where ω is the angular velocity and ρ is density.

Next, strains in cylindrical coordinates for plane stress axi-symmetric problems are defined as:

$$\varepsilon_r = u,_r \qquad (3.3)$$

$$\varepsilon_\theta = \frac{u}{r} \qquad (3.4)$$

Hooke's law for orthotropic material in the condition of plane stress:

$$\begin{bmatrix} \sigma_r \\ \sigma_\theta \end{bmatrix} = \begin{bmatrix} C_{11} & C_{12} \\ C_{12} & C_{22} \end{bmatrix} \begin{bmatrix} \varepsilon_r \\ \varepsilon_\theta \end{bmatrix} \qquad (3.5)$$

The governing differential equations for plane stress axi-symmetric problems with orthotropic materials is defined by substituting equations 3.3-3.5 into equation 3.1 yielding:

$$\frac{\partial}{\partial r}\left(tr\left(C_{11}\frac{\partial u}{\partial r}+C_{12}\frac{u}{r}\right)\right)-t\left(C_{12}\frac{\partial u}{\partial r}+C_{22}\frac{u}{r}\right)+trB_r = 0 \tag{3.6}$$

The plane stress weak statement:

$$\int_V L\left(\frac{\partial}{\partial r}\left(tr\left(C_{11}\frac{\partial u}{\partial r}+C_{12}\frac{u}{r}\right)\right)-t\left(C_{12}\frac{\partial u}{\partial r}+C_{22}\frac{u}{r}\right)+trB_r\right)rdrd\theta dz = 0 \tag{3.7}$$

Introducing finite element approximations:

$$L = \Psi_i \tag{3.8}$$

$$u = \sum_{j=1}^{n} u_j\Psi_j \tag{3.9}$$

and integrating by parts the plane stress stiffness matrix becomes:

$$K_{ij} = \int_V\left(\frac{\partial\Psi_i}{\partial r}\left[tr\left(C_{11}\frac{\partial\Psi_j}{\partial r}+C_{12}\frac{\Psi_j}{r}\right)\right]+\Psi_i\left(t\left[C_{12}\frac{\partial\Psi_j}{\partial r}+C_{22}\frac{\Psi_j}{r}\right]\right)\right)rdrd\theta dz \tag{3.10}$$

The plane stress forcing vector is:

$$\{f^1\} = \int_V\{B_r r\}rdrd\theta dz \tag{3.11}$$

The plane stress boundary conditions are:

EBC'S	NBC's	
u	$tr(\sigma_r n_r)$	(3.12)

A three-noded element with one degree of freedom per node using Lagrangian quadratic shape functions in the plane stress finite element model is shown in Figure 3.2a. A four point Guassian quadrature rule was used to numerically integrate the stiffness matrix. A two point Guassian quadrature rule was used to evaluate stresses.

3.2.2 Three-dimensional Finite Element Model Formulation

The finite element model that yields a three-dimensional stress state is truly a two-dimensional finite element model and is accurate for all shapes. It captures the variation of stress through the transverse normal direction, and makes no assumptions about the transverse normal and in-plane shearing stresses.

Assuming that the displacement field does not change as a function of angle, the problem can be modeled with a planar mesh. Figure 3.3 displays a planar symmetric cross section of a flywheel to be analyzed. Only half the cross section of a flywheel needs to be modeled due to symmetry. Symmetry boundary conditions (no displacement in the transverse normal direction) were applied along the horizontal symmetry plane of the flywheel. Forces induced from angular rotation were included as body forces. The essential boundary condition at the center of the flywheel was not directly applied due to the coupling of the stiffness matrix, enforcing displacements according to the physics of the problem.

The formulation of the three-dimensional axi-symmetric finite element model begins by defining the equilibrium equations in cylindrical coordinates:

$$\sigma_{r,r} + \tau_{zr,r} + \frac{1}{r}(\sigma_r - \sigma_\theta) + B_r = 0 \tag{3.13}$$

$$\tau_{rz,r} + \sigma_{z,z} + \frac{1}{r}\tau_{rz} = 0 \tag{3.14}$$

Next, strains in cylindrical coordinates for three-dimensional axi-symmetric problems are defined as:

$$\varepsilon_r = u,_r \tag{3.15}$$

$$\varepsilon_\theta = \frac{u}{r} \tag{3.16}$$

$$\varepsilon_z = w,_z \tag{3.17}$$

$$\gamma_{rz} = u,_z + w,_r \tag{3.18}$$

Hooke's law for three-dimensional axi-symmetric orthotropic material:

$$\begin{bmatrix} \sigma_r \\ \sigma_\theta \\ \sigma_z \\ \tau_{rz} \end{bmatrix} = \begin{bmatrix} C_{11} & C_{12} & C_{13} & 0 \\ C_{12} & C_{22} & C_{23} & 0 \\ C_{13} & C_{23} & C_{33} & 0 \\ 0 & 0 & 0 & C_{44} \end{bmatrix} \begin{bmatrix} \varepsilon_r \\ \varepsilon_\theta \\ \varepsilon_z \\ \gamma_{rz} \end{bmatrix} \tag{3.19}$$

The governing differential equations for three-dimensional axi-symmetric problems with orthotropic materials are defined by substituting equations 3.15-3.19 into equations 3.13 and 3.14 yielding:

$$\begin{gathered} \frac{1}{r}\left(C_{11}\frac{\partial u}{\partial r} + C_{12}\frac{u}{r} + C_{13}\frac{\partial w}{\partial r} - C_{12}\frac{\partial u}{\partial r} - C_{22}\frac{u}{r} - C_{23}\frac{\partial u}{\partial z}\right) + \\ \frac{\partial}{\partial r}\left(C_{11}\frac{\partial u}{\partial r} + C_{12}\frac{u}{r}\right) + \frac{\partial}{\partial z}C_{55}\left(\frac{\partial u}{\partial z} + \frac{\partial w}{\partial r}\right) + B_r = 0 \end{gathered} \tag{3.20}$$

$$\begin{gathered} \frac{\partial}{\partial r}\left(rC_{55}\left(\frac{\partial u}{\partial z} + \frac{\partial w}{\partial r}\right)\right) + \frac{\partial}{\partial z}\left(C_{13}\frac{\partial u}{\partial r} + C_{23}\frac{u}{r} + C_{33}\frac{\partial w}{\partial z}\right) + \\ \frac{\partial}{\partial r}\left(rC_{55}\left(\frac{\partial u}{\partial z} + \frac{\partial w}{\partial r}\right)\right) + \frac{\partial}{\partial z}\left(C_{13}\frac{\partial u}{\partial r} + C_{23}\frac{u}{r} + C_{33}\frac{\partial w}{\partial z}\right) + B_z = 0 \end{gathered} \tag{3.21}$$

The weak statement can be written as:

$$\begin{gathered} \int_V L\left(\frac{1}{r}\left(C_{11}\frac{\partial u}{\partial r} + C_{12}\frac{u}{r} + C_{13}\frac{\partial w}{\partial r} - C_{12}\frac{\partial u}{\partial r} - C_{22}\frac{u}{r} - C_{23}\frac{\partial u}{\partial z}\right) + \right. \\ \left. \frac{\partial}{\partial r}\left(C_{11}\frac{\partial u}{\partial r} + C_{12}\frac{u}{r}\right) + \frac{\partial}{\partial z}C_{55}\left(\frac{\partial u}{\partial z} + \frac{\partial w}{\partial r}\right) + B_r\right) r dr d\theta dz = 0 \end{gathered} \tag{3.22}$$

$$\int_V L\left(B_z + \frac{\partial}{\partial r}\left(rC_{55}\left(\frac{\partial u}{\partial z} + \frac{\partial w}{\partial r}\right)\right) + \frac{\partial}{\partial z}\left(C_{13}\frac{\partial u}{\partial r} + C_{23}\frac{u}{r} + C_{33}\frac{\partial w}{\partial z}\right)\right.$$

$$\frac{\partial}{\partial r}\left(rC_{55}\left(\frac{\partial u}{\partial z} + \frac{\partial w}{\partial r}\right)\right) + \frac{\partial}{\partial z}\left(C_{13}\frac{\partial u}{\partial r} + C_{23}\frac{u}{r} + C_{33}\frac{\partial w}{\partial z}\right) +$$

$$\left.\frac{1}{r}\left(C_{55}\left(\frac{\partial u}{\partial z} + \frac{\partial w}{\partial r}\right)\right) + B_z\right) r\,dr\,d\theta\,dz = 0 \tag{3.23}$$

Introducing finite element approximations:

$$u = \sum_{j=1}^{n} u_j \Psi_j \tag{3.24}$$

$$w = \sum_{j=1}^{n} w_j \Psi_j \tag{3.25}$$

and integrating by parts, the three-dimensional axi-symmetric stiffness matrices become:

$$K_{ij}^{11} = \int_V \left(\frac{\partial \Psi_i}{\partial r}\left[C_{11}\frac{\partial \Psi_j}{\partial r} + C_{12}\frac{\Psi_j}{r}\right] + \frac{\Psi_i}{r}\left[C_{12}\frac{\partial \Psi_j}{\partial r} + C_{22}\frac{\Psi_j}{r}\right] + \frac{\partial \Psi_i}{\partial z}\left[C_{55}\frac{\partial \Psi_i}{\partial z}\right]\right) r\,dr\,d\theta\,dz \tag{3.26}$$

$$K_{ij}^{12} = \int_V \left(\frac{\partial \Psi_i}{\partial r}\left[C_{13}\frac{\partial \Psi_j}{\partial z}\right] + \frac{\Psi_i}{r}\left[C_{23}\frac{\partial \Psi_j}{\partial z}\right] + \frac{\partial \Psi_i}{\partial z}\left[C_{55}\frac{\partial \Psi_j}{\partial r}\right]\right) r\,dr\,d\theta\,dz \tag{3.27}$$

$$K_{ij}^{21} = \int_V \left(\frac{\partial \Psi_i}{\partial z}\left[C_{13}\frac{\partial \Psi_j}{\partial z} + C_{23}\frac{\Psi_j}{r}\right] + \frac{\Psi_i}{r}\left[C_{55}\frac{\partial \Psi_j}{\partial z}\right]\right) r\,dr\,d\theta\,dz \tag{3.28}$$

$$K_{ij}^{22} = \int_V \left(\frac{\partial \Psi_i}{\partial z}\left[C_{33}\frac{\partial \Psi_j}{\partial z}\right] + \frac{\Psi_i}{r}\left[C_{55}\frac{\partial \Psi_j}{\partial r}\right]\right) r\,dr\,d\theta\,dz \tag{3.29}$$

The axi-symmetric three-dimensional forcing vectors are:

$$\{f^1\} = \int_V \{B_r r\} r dr d\theta dz \tag{3.30}$$

$$\{f^2\} = 0 \tag{3.31}$$

Where B_r is the body forces in the radial direction induced from rotations.

The axi-symmetric three-dimensional essential and natural boundary conditions are:

$$\begin{array}{ll} \text{EBC'S} & \text{NBC's} \\ u & r(\sigma_r n_r + \tau_{rz} n_z) \\ w & r(\sigma_z n_z + \tau_{rz} n_r) \end{array} \tag{3.32}$$

Equations 3.26-3.31 can be presented to form the complete axi-symmetric three-dimensional finite element model in following matrix form:

$$\begin{bmatrix} K^{11} & K^{12} \\ K^{21} & K^{22} \end{bmatrix} \begin{bmatrix} u \\ w \end{bmatrix} = \begin{bmatrix} f^1 \\ f^2 \end{bmatrix} \tag{3.33}$$

The three-dimensional axi-symmetric finite element model was implemented into a finite element code that used four noded elements with two degrees of freedom per node (Figure 3.2b) with linear Lagrangian interpolation functions. A two point Guassian quadrature rule was used to numerically integrate the stiffness matrix. A one point Guassian quadrature rule was used to evaluate stresses. An automated mesh generator was written to allow for element refinement through the transverse normal and the radial directions. Therefore, the finite element code that predicts three-dimensional stresses can have various levels of refinement. A coarse mesh with a small number of degrees of freedom will be less accurate but more computationally efficient compared to a refined mesh containing a larger number of degrees of freedom. The mesh was also generated in such a way as to minimize the time required to solve the set of banded linear equations created by the finite element code.

3.3 Verification of Results

Figure 3.4 displays results comparing the analytical solution to the plane stress finite element computational solution for the tangential and radial stresses in a flat solid flywheel as a function of flywheel radius. Ten quadratic elements are used in the plane stress finite element model. Stress contour plot obtained using the MARC analysis code displays an arrow which represents the cross-section where the stresses are compared. There is little difference between the plane stress FEM solution and analytical solution for the radial and tangential stresses. Figure 3.5 displays results comparing the analytical solution to the plane stress FEM computational solution for radial and tangential stresses for a flat annular flywheel composed of 20 quadratic elements as a function of flywheel radius. Again, the plane stress FEM solution agrees with the analytical solution.

To compare three-dimensional results with a solution obtained using MARC, the variation of stresses were plotted through the thickness near the inner radius, being very close to zero. The flywheel shape has moderately steep ring gradients, and was chosen to demonstrate the capabilities of capturing the variation of transverse normal and in-plane shearing stresses with the axi-symmetric three-dimensional finite element code. Figures 3.6-3.9 compare the solutions from MARC and the present FEM code as a function of flywheel thickness. Again the MARC analysis stress contour plot displays an arrow which represents the cross-section where the stresses are compared. All components of the stress agree with the solution obtained by MARC. It should be noted that the solution obtained by MARC measures the stresses at the center of each element and then interpolates to the nodes of each element. The present FEM code measures stresses (with no interpolation) at the center of each element. Interpolating the stresses from the center of the element to the nodes will cause slight variations in solutions obtained from MARC and the present FEM code. This is more evident near the surface of the flywheel, where a stress free boundary condition exists.

The three-dimensional analysis convergence was sought by refining the mesh from 30, to 120, 480 and finally 960 linear elements. The difference in maximum stress in the problem converged from 15.1% to 10.1% to 2.1% respectively. The transverse normal stress converged much more slowly. This could come from the domination of the tangential and radial stresses in the minimization of potential energy. Often, the minimization of potential energy sacrifices the accuracy of a non-dominating stress component in order to accurately capture the dominating stress components.

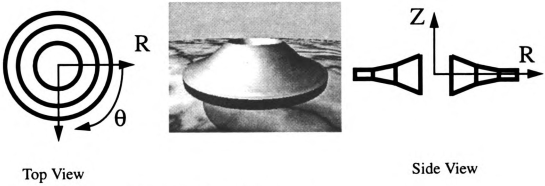

Figure 3.1. Flywheel geometry.

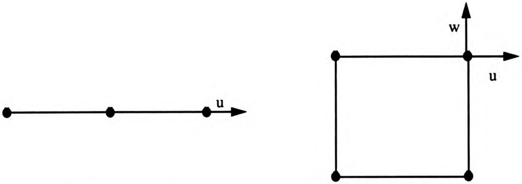

3.2a. 1 Dimensional Element
(1 DOF per node)

3.2b 2 Dimensional Element
(2 DOF per node)

Figure 3.2 Element topology.

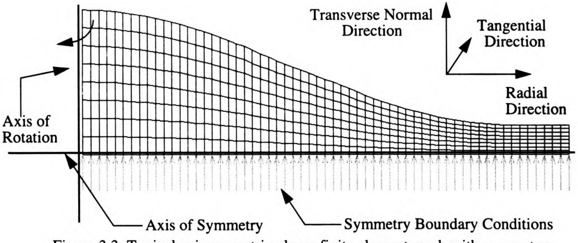

Figure 3.3. Typical axi-symmetric planar finite element mesh with symmetry boundary conditions (1,134 degrees of freedom).

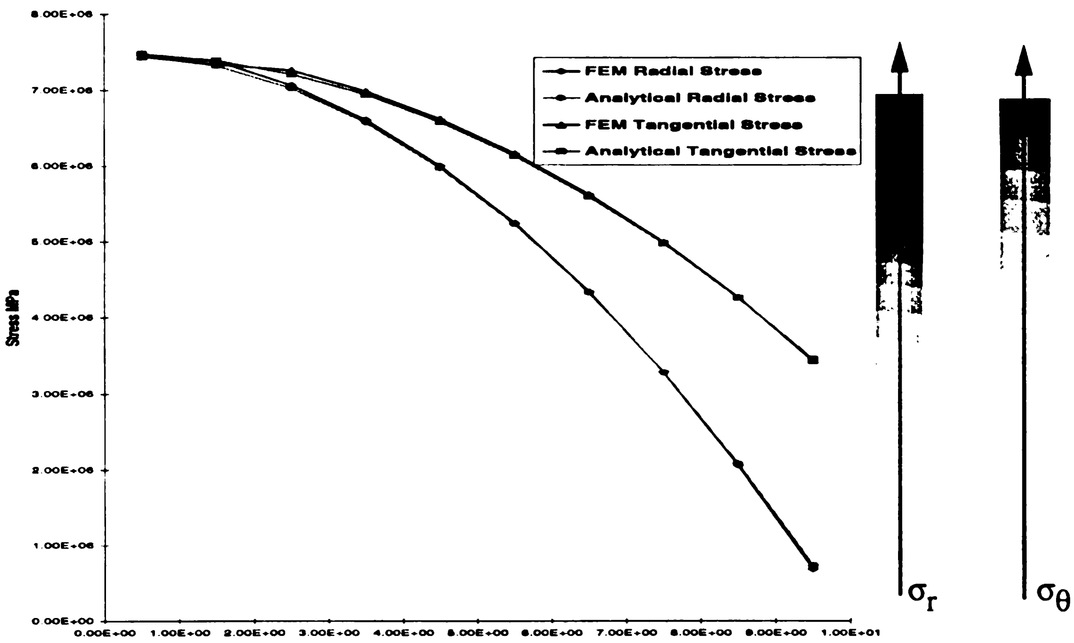

Figure 3.4. Tangential and Radial Stresses as a Function of Radius Predicted by Plane Stress Finite Element Code and Analytical Solution for a Flat Solid Flywheel. Arrow Represents Cross Section Analyzed.

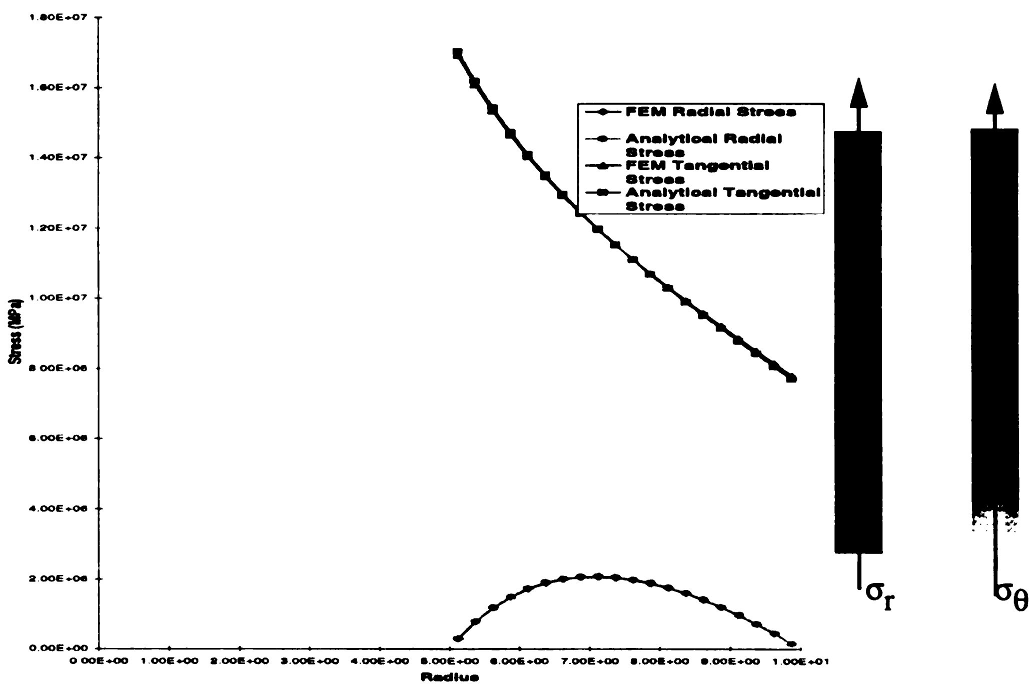

Figure 3.5. Tangential and Radial Stresses as a Function of Radius Predicted by Plane Stress Finite Element Code and Analytical Solution for a Flat Annular Flywheel. Arrow Represents Cross Section Analyzed.

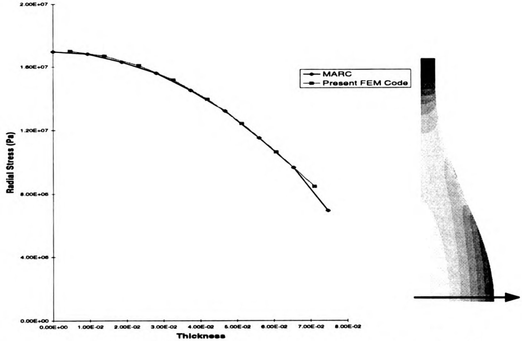

Figure 3.6. Variation of Radial Stress Through the Thickness for the MARC and Present Finite Element Code for a Solid Isotropic Flywheel that Varies in Thickness. Arrow Represents Cross Section Plotted.

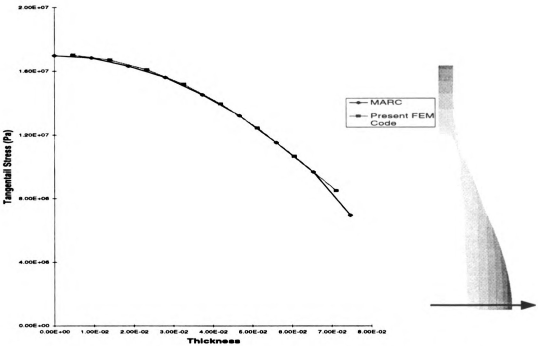

Figure 3.7. Variation of Tangential Stress Through the Thickness for the MARC and Present Finite Element Code for a Solid Isotropic Flywheel that Varies in Thickness. Arrow Represents Cross Section Plotted.

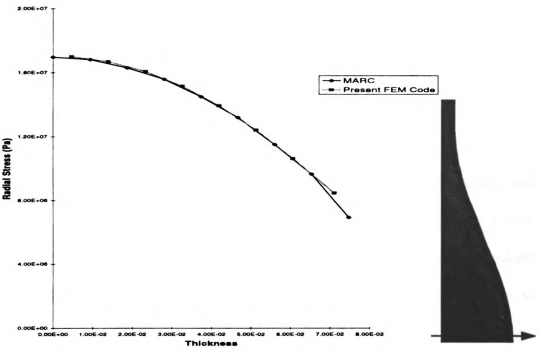

Figure 3.8. Variation of Transverse Stress Through the Thickness for the MARC and Present Finite Element Code for a Solid Isotropic Flywheel that Varies in Thickness. Arrow Represents Cross Section Plotted.

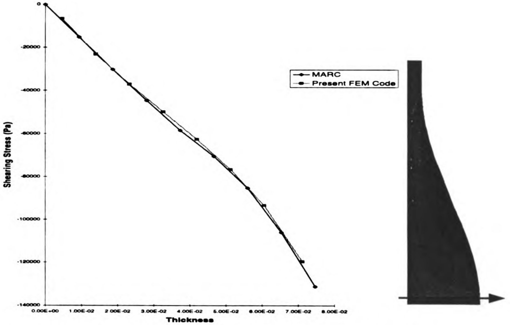

Figure 3.9. Variation of Shear Stress Through the Thickness for the MARC and Present Finite Element Code for a Solid Isotropic Flywheel that Varies in Thickness. Arrow Represents Cross Section Plotted.

Chapter 4

Optimal Design of Flywheels Using Genetic Algorithms

4.1 Introduction

Various GA approaches are presented in this thesis to search for flywheels with varying shape to maximize SED, while controlling angular velocity and "air" gap growth. A simple Genetic Algorithm (sGA) will be compared to a set of optimization techniques. This set includes parallel GAs with topological ring structures, Island Injection Genetic Algorithms (iiGAs), local improvement methods, Threshold Accepting (TA) algorithms and hybrid GAs. First, the optimization of solid isotropic flywheels will be presented. Next, comparisons of the set of optimization techniques for an enumerable search space will be presented. Optimization of annular and solid composite flywheels are presented. Finally, "safer" annular flywheels (while constraining angluar velocity) will be sought by penalizing flywheels that have a large "air gap" growth.

4.2 Description of Optimization Problem

Structural optimization problems have been around for centuries and many have been reviewed in this thesis. The formulation of this optimization problem begins with the definition of overall fitness, in this case the maximization of Specific Energy Density (SED). Conflicting interests arise when performing optimization of flywheels. The criteria considered are: maximize SED, minimize "air gap" growth while controling high angular velocities. The minimization of "air gap" growth is considered to find "safer" flywheel designs. SED can be defined as:

$$SED = \frac{1}{2}\frac{I\omega^2}{mass} \tag{4.1}$$

The definition of SED contains angular velocity squared, so as we search for flywheel shapes with a controlled angular velocity we are also limiting SED. The GA will then be able to optimize the fitness function by placing more mass near the end of the flywheel, increasing the mass moment of inertia. "Air gap" growth (which is the maximum displacement of the inner radius of an annular flywheel due to forces induced from angular rotations) will typically be higher for flywheels that have a higher SED value due to the association of higher failure angular velocities.

Constraints, such as maximum angular velocity and air gap growth, are here enforced in the GA by penalizing individuals that violate specific constraints. In this case, a constraint on maximum angular velocity was not practically known. The goal of decreasing angular velocity is to search for safer flywheels. Therefore, an initial GA run was performed without constraining angular velocity. Next, the values for the constraints on maximum angular velocity were formed based on the maximum angular velocity for the best individual found in the initial GA run. This approach was also taken with constraints on the "air gap" growth in flywheels.

The fitness was defined as:

$$Fitness(maximize) = C_1\frac{SED}{SED_{max}} - P_1\frac{\omega_{failure}}{\omega_{max}} - P_2\frac{GAP_{failure}}{GAP_{max}} \qquad 4.2)$$

subject to

$$\sigma_{r,\,min} \le \sigma_r \le \sigma_{r,\,max}\,,\ \sigma_{\theta,\,min} \le \sigma_\theta \le \sigma_{\theta,\,max}$$

$$\sigma_{z,\,min} \le \sigma_z \le \sigma_{z,\,max}\,,\ \tau_{rz,\,min} \le \tau_{rz} \le \tau_{rz,\,max}$$

where C_1 is the value used to weight the normalized fitness and P_i are penalty coefficients used if an individual violates a constraint. This definition of fitness is based on the maximum stress failure criteria for isotropic materials which can easily be transformed into terms of strain for composite analysis. If the angular velocity was lower than a prescribed amount then the coefficient P_1 was set to zero. Otherwise, the values for the coefficients in equation 4.4.1 are given in Table 4.2.1.

Table 4.2.1. Weighting Coefficient Values.

C_1	P_1	P_2
100.0	40.0	20.0

As mentioned, an initial GA run was performed to determine the maximum SED, angular velocity and "air gap" values without penalizing for constraints and normalizing equation 4.2 with unity. The constraints were determined by taking a percentage of the maximum angular velocity while penalizing based on "air gap" growth.

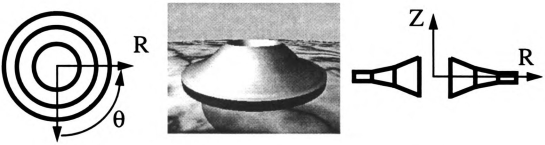

Top View

Side View

Figure 4.1. Visual Display of Flywheel.

4.3 Model Description

Figure 4.1 is a visual display of an annular flywheel that shows how the flywheel is modeled as a series of concentric rings. The thickness of each ring varies linearly in the radial direction with the possibility for a diverse set of material choices for each ring. When using the axi-symmetric plane stress analysis, a three-noded "line" element was used to represent the flywheel (see Figure 4.2). The axi-symmetric three-dimensional finite element model required a planar mesh. Figure 4.3 displays a typical planar mesh generated, using symmetry to increase computational efficiency for the axi-symmetric three-dimensional analysis.

The flywheel dimensions were chosen based on research provided by [44]. The maximum and minimum thickness, inner and outer radii were taken from [44] to ensure realistic dimensions.

An aluminum alloy material was chosen for isotropic flywheels due to its high strength low, density characteristics. Table 4.3.1 contains all isotropic material properties used in this thesis. For composite flywheels, quasi-isotropic material properties were chosen and are given in Table 4.3.2.

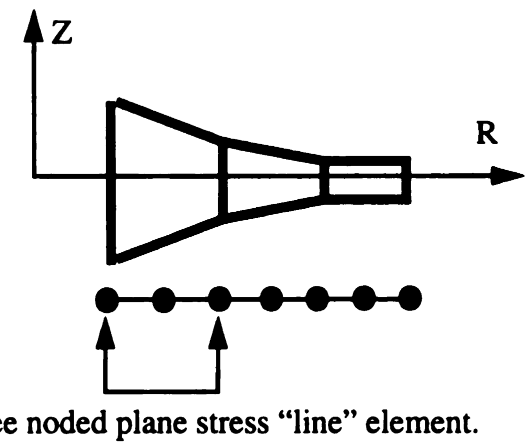

Figure 4.2. Plane stress finite element representation.

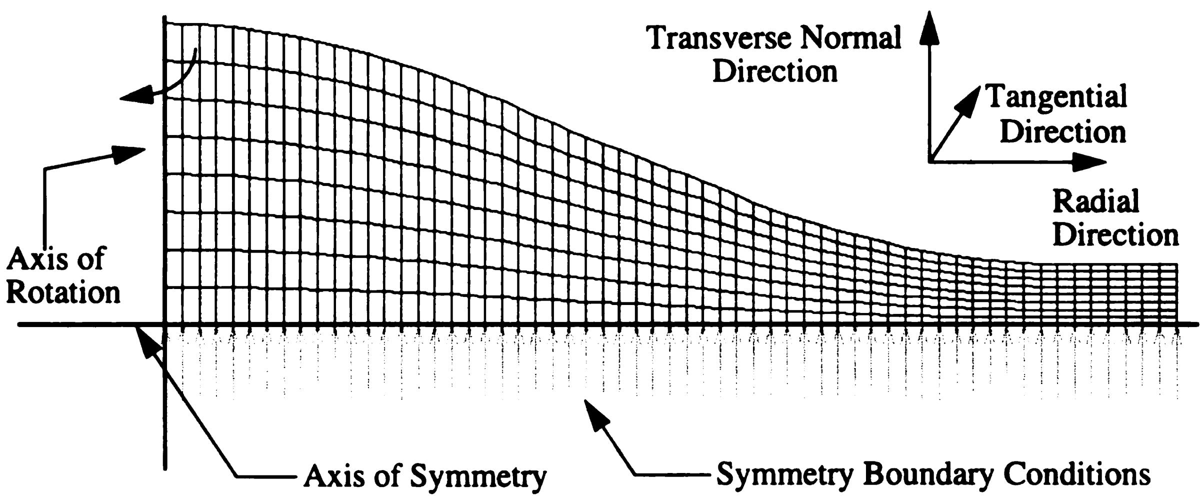

Figure 4.3. Typical planar finite element mesh with symmetry boundary conditions used in the three-dimensional fem evaluations (1,134 degrees of freedom).

Table 4.3.1. Isotropic Material Properties.

Material	E (GPa)	ν	Density (Kg/m^3)	Tensile Strength (MPa)	Compressive Strength (MPa)
Steel	200.0	0.30	8.86E3	400	400
Aluminum	72.0·	0.285	2.80E3	480	480

Table 4.3.2. Composite Material Properties.

Property	E-Glass Epoxy [0^0]	E-Glass Epoxy [90^0]
E (GPa)	18.96	18.96
Density (Kg/m^3)	1.6E3	1.6E3
ν	0.27	0.27
G(GPa)	7.47	7.47
ε_r(tensile)	8.99E-3	15.9E-3
ε_t (tensile)	15.9E-3	8.99E-3
ε_z (tensile)	8.99E-3	8.99E-3
ε_{rz}	31.37E-3	31.37E-3
ε_r (compressive)	22.47E-3	8.21E-3
ε_t (compressive)	8.21E-3	22.47E-3
ε_z (compressive)	22.47E-3	22.47E-3

The maximum stress failure criterion was used to predict the maximum failure angular velocity in the analysis of isotropic flywheels, while the maximum strain criterion was used for composite flywheels. The absolute value of the maximum stress (or strain) can be used to scale the angular velocity and "air gap" growth. By assuming an initial angular velocity, the stresses and strains were calculated by the finite element method. A failure index was defined as the largest ratio of the absolute maximum stress (or strain) to the maximum allowable stress (or strain) produced by the initialized angular velocity. The failure index was used to scale the initialized angular velocity to the maximum failure angular velocity. The failure index was also used to scale the "air gap" growth to the "air gap" growth at failure. Also, the origin of the maximum stress (or strain) predicted the flywheel failure ring.

4.4 Island Injection Genetic Algorithm Approach

This next section will describe the advantages of first exploring the search space efficiently at various levels of resolution using an efficient and simple calculation performed by a finite element code that assumes that the flywheel is in a plane stress state, basing fitness on a sub-fitness function using an Island Injection Genetic Algorithm (iiGA). The iiGA can discretize an objective function by breaking it down into separate sub-fitness functions used to evaluate fitness on various islands. Building blocks are first sought using a low level of geometric resolution with a plane stress assumption basing the fitness on a sub-fitness function. Good solutions found at a low level of geometric resolution based on a plane stress assumption with the sub-fitness function are then injected into islands that measure fitness with a refined three-dimensional finite element code at a higher level of geometric resolution, basing fitness on an overall fitness definition.

4.4.1 Island Injection GA Geometric Resolution

Figure 4.4 displays an iiGA topology that first searches at a low level of geometric resolution (three rings) for building blocks needed to inject into islands of medium geometric resolution. At the end of a prescribed number of generations per cycle a file is written containing good solutions from the existing population. The iiGA then searches at a medium level of geometric resolution (six rings) to find building blocks to inject into a high level of geometric resolution (twelve rings). One complete cycle ends by generating and evaluating the populations on the islands with the highest level of geometric resolution. The next cycle begins with the islands with the lowest geometric resolution (three rings) searching to improve the existing building blocks in the island. Now, the islands with a medium level of geometric resolution (six rings) receives migrating solutions from the file containing good building blocks from the island with the lowest level of geometric resolution. The process of migrating building blocks from a lower level of geometric resolution to a higher level of geometric resolution continues. Islands with the highest level of geometric resolution receive building blocks from the islands with a medium level of geometric resolution. This process of searching at low levels of resolution to improve building blocks is continued and is exploited to accelerate the convergence of a typical GA.

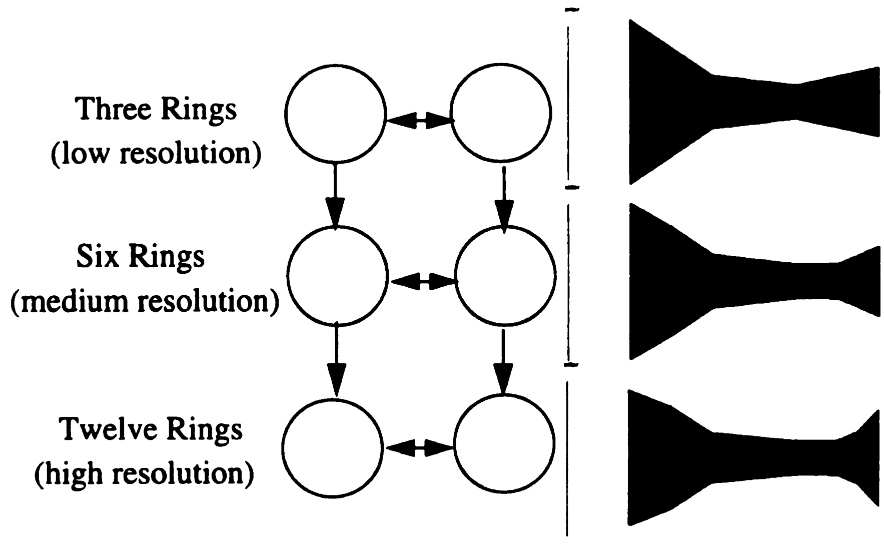

Figure 4.4. iiGA topology that performs multiple refinements in geometric resolution.

4.4.2 Efficient Evaluation Tools

The finite element codes can evaluate fitness at various levels of efficiency. The axi-symmetric plane stress finite element evaluation is extremely efficient, but less accurate for odd shapes. The axi-symmetric three-dimensional finite element code will also have various levels of efficiency. A three-dimensional finite element model with a large number of degrees of freedom will be extremely accurate, but computationally less efficient. Using these varying levels of efficiency in fitness evaluations can be used to increase the computational efficiency of the iiGA. A unique dilemma occurs when comparing the plane stress and three-dimensional finite models. The plane stress evaluation is efficient, but not entirely accurate while the three-dimensional model is computationally hindersome yet accurate. Therefore it would be satisfactory to first quickly approximate the response of a flywheel with the plane stress evaluation to discard poor individuals and then fine tune the design with a refined analysis. Figure 4.5 displays an iiGA topology that searches at various levels of geometric resolution and uses various objective evaluations governed by two factors. The first factor would be whether or not to evaluate with a plane stress assumption. If the evaluation is not based on a plane stress analysis then the level of accuracy, or the total number of degrees of freedom must be chosen for the three-dimensional evaluation. Any migration of individuals requires re-evaluation of fitness due to the different levels of accuracy in measuring fitness.

Further inspection of the iiGA topology in Figure 4.5 reveals that at each low level of geometric resolution, both plane stress and three-dimensional evaluations exist. The islands that evaluate fitness based on plane stress quickly evaluate individuals to be injected into the islands that evaluate fitness with the a more refined analysis tool. Also, the islands that evaluate fitness with the more refined three-dimensional model are allowed to evolve independently, sharing only portions of the search space with other islands at the same level of geometric resolution.

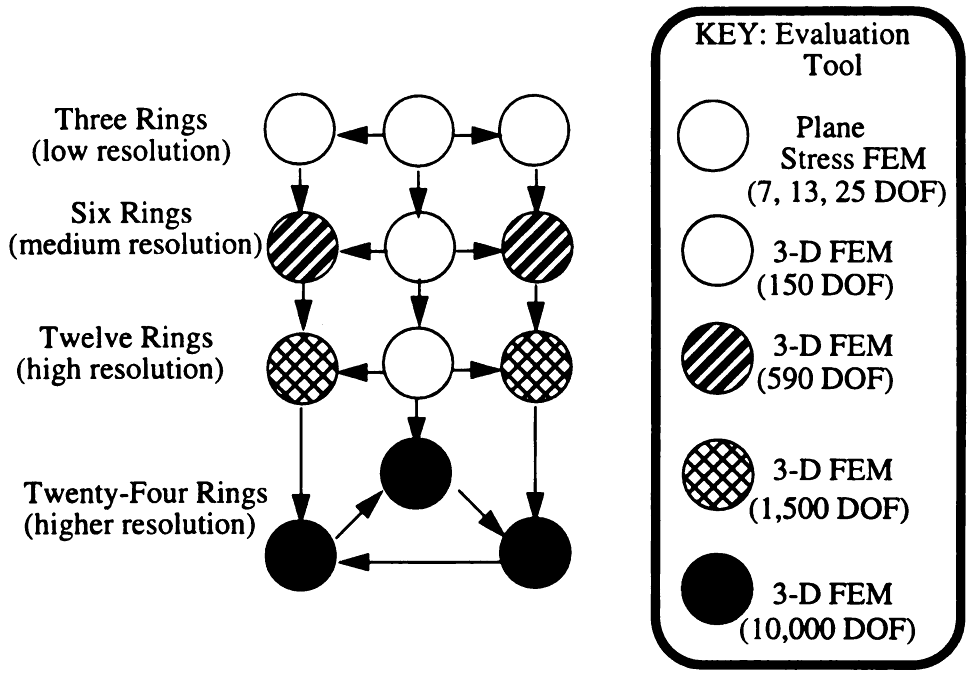

Figure 4.5. Island injection GA topology with various levels of fitness evaluation efficiency.

4.4.3 Sub-Fitness Functions

Each island could possibly evaluate fitness based on a sub-fitness function. For instance, it was found earlier by Eby [9] that angular velocity was an important factor in the optimization of Specific Energy Density (SED) of flywheels when limited to a plane stress evaluation. Figure 4.6 displays an iiGA topology that searches at various levels of geometric resolution evaluating fitness with plane stress and three-dimensional analyses basing fitness on angular velocity and SED respectively. This allows for efficient search at low levels of geometric resolution with a plane stress fitness evaluation, which bases fitness on a “sub-fitness” function, while also using a refined analysis to fine tune the flywheel at higher levels of geometric resolution.

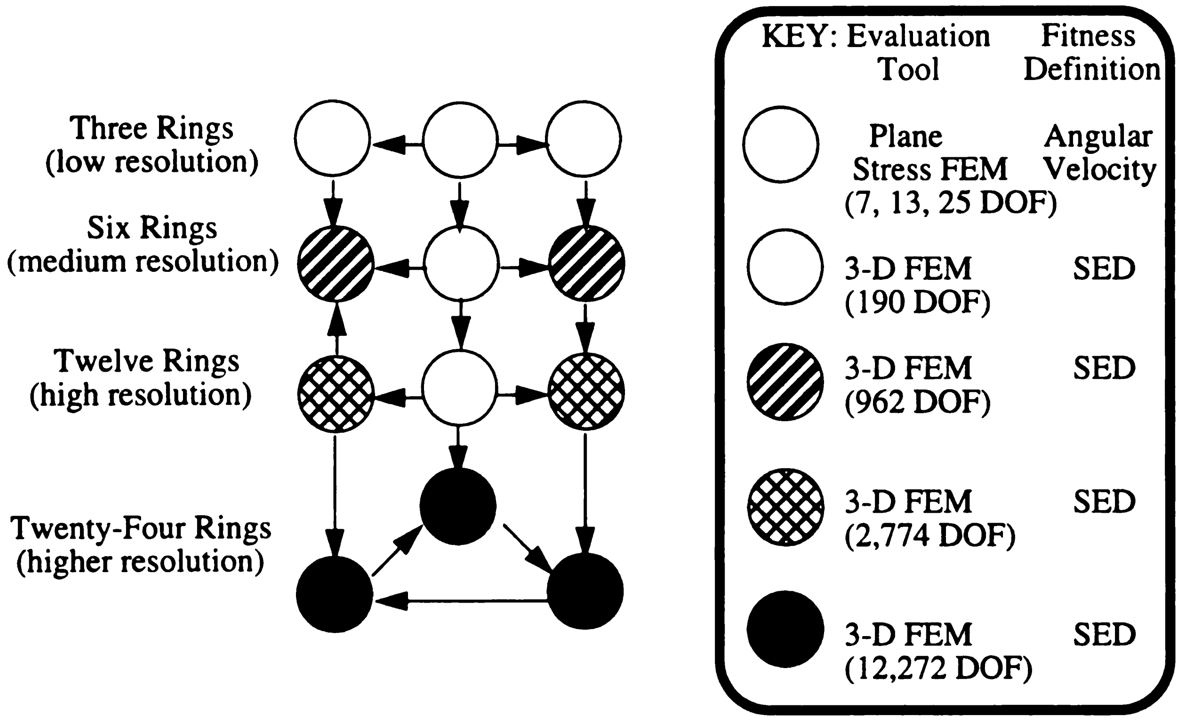

Figure 4.6. Island injection genetic algorithm topology with multiple fitness definitions.

4.4.4 Hybrid Injection Island Genetic Algorithms

GAs excel at searching on a global level to quickly find near-optimal solutions, however they lack in the abilities to quickly climb hills in a local convex search space. Threshold Accepting (TA) is an efficient hill climbing method and seems ideal to incorporate into the GA. The TA algorithm can be initiated with the best solution found by the GA, allowing the TA to quickly climb from a near-optimal solution to the optimal solution. This was done to climb hills that are close to the nearly globally optimal solutions found by the GA. The new solution found with the TA approach can be reinserted into the iiGA replacing the worst individual in the population.

A local search procedure was also developed to use with the iiGA. This local search varied the thickness of the failure ring of the flywheel. This was done with the best individual at the end of each generation to discover improvements through slight variations in the local failure ring thicknesses. Each ring has an inner and outer thickness, so the local search first held the inner thickness constant and varied the outer thickness by increasing and decreasing by small increment. Next, the outer thickness was varied in a similar fashion. If a better solution was found it replaced the worse solution in the population, and if only worse solutions were found, then no individuals were replaced. Each local search contained four evaluation calls working on a specific failure ring. Either a local or a TA technique could be applied to an island, but not coincidentally. Figure 4.7 displays a hybrid iiGA topology that benefits from local and TA methods.

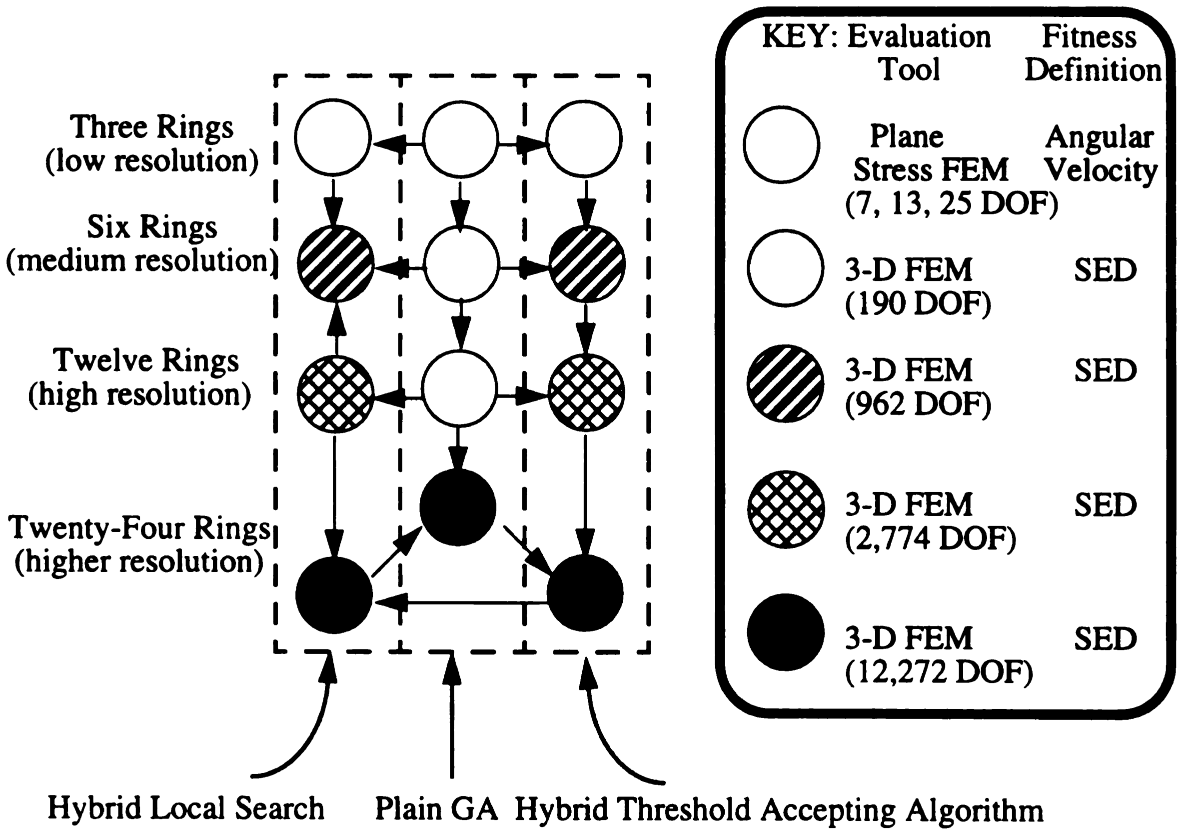

Figure 4.7 Typical hybrid island injection genetic algorithm toplogy.

4.5 Results and Discussion

First, the solid constant stress flywheel shape will be found and compared to the plane stress closed formed solution [1]. Next, the natural boundary condition at the end of the plane stress constant stress flywheel will be made homogeneous to remove the assumption that the optimal design is one with equal stresses throughout, an assumption that facilitates the analytical solution.

The global optimum solution for a relatively small design search space (2,097,152 designs) was found by enumerating (exhausting) the search space. The known global optimum solution was then used to benchmark a set of algorithms that includes: simple Genetic Algorithms (sGAs), Genetic Algorithms that compose topological "rings", island injection Genetic Algorithms (iiGAs), Threshold Accepting (TA) algorithms and hybrid Genetic Algorithms. The hybrid Genetic Algorithms incorporate TA algorithms and or a local improvement method into either a sGA or an iiGA.

Next, multi-material solid and annular composite flywheels will be optimized with no constraints on angular velocity or air gap growth. Finally, multi-material annular composite flywheels will be optimized constraining angular velocity while minimizing "air gap" growth.

4.5.1 Results of Optimized Solid Isotropic Flywheels

The first attempt to optimize the SED of solid isotropic flywheels with no constraints on angular velocity or "air gap" growth involved using a simple GA that evaluated fitness with the plane stress finite element code to search for the well known constant stress profile. First the fitness function was defined as SED with no constraints; the final result is shown in Figure 4.8. The GA is simply placing mass at the outer edge of the flywheel to increase the mass moment in the fitness function. The GA is exploiting the simplified plane stress fitness evaluation. A stress concentration will be located at the point of inflection near the end of the flywheel. This flywheel design violates the simplified plane stress assumption that stress does not vary through the thickness.

The fitness function was next defined as angular velocity due to the fact that SED is directly proportional to the square of the angular velocity of the flywheel. Figure 4.9 compares the analytical solution of a constant stress flywheel to the simple GA's constant stress flywheel. The difference in SED is less than 1%. All simple GA runs had a 75% crossover rate, 1% mutation rate and initial population size of 300. The search for the constant stress profile converged within 5 minutes on a Sun Sparc Ultra workstation. Figure 4.10 displays the evolution of the constant stress flywheel. Each fitness evaluation using the plane stress evaluation lasted less than 0.001^{th} of a second.

To solve the boundary value problem of a flywheel of constant stress a force (natural boundary condition) must be applied in the radial direction at the end of the flywheel. To search for the optimal shape of a flywheel with stress free edges the natural boundary condition at the end of the flywheel will be made homogeneous (zero). Again the fitness was evaluated on angular velocity. Figure 4.11 compares the design of a solid isotropic flywheel with stress free edges to the constant stress flywheel. The flywheel with stress free edges has a 55% increase in SED when compared to the constant stress flywheel with the axi-symmetric three-dimensional finite element code. The commonly used rotor shape of the constant stress flywheel is not optimal when a flywheel has stress free edges.

4.5.2 Comparison of Optimization Methods Through Enumeration

To prepare a problem that is computationally enumerable, a relatively small search space was designed. A six-ringed solid single isotropic material flywheel that used a coarse spatial resolution (three bits per ring height) represented a design search space of $(2^{\#bits})^{\#Rings+1} = (2^3)^7 = 2{,}097{,}152$. An algorithm was written to search exhaustively for the global solution, taking 49 hours on a Sun Sparc Ultra with the axi-symmetric three-dimensional finite element analysis containing 962 degrees of freedom in each analysis. Each evaluation lasted approximately a 0.084th of a second. Now, comparisons for a set of optimization techniques can be made with a known global solution. The optimization techniques include simple Genetic Algorithms (sGAs), island injection Genetic Algorithms (iiGAs), Threshold Accepting (TA) algorithms and hybrid iiGAs that incorporate TA and local improvement methods. Statistics that pertain to the number of evaluations needed to find the global solution are relevant measures of algorithm exploration efficiency. But after exploring a search space with an iiGA using various levels of computationally efficient evaluation tools, a better measure of algorithm performance can be conceived as the total computation time (or effort) spent before discovering the global solution. Of course, this does not measure the additional gains possible using the iiGA on multiple processors. Statistics for the total number of evaluation calls will also be given to satisfy the different ways to evaluate algorithm exploration efficiency. For each optimization approach, five randomly generated initial populations were allowed to run for a total of two hours each to compute the average time to find the global optimal solution. The fitness was based only on SED for this simple problem.

The first optimization techniques to explore the enumerable search space were the sGA and the TA methods. Figure 4.12 displays the normalized fitness as a function of time for typical runs for the sGA, TA, and a hybrid GAs. Hybrid GAs incorporated either a TA algorithm or local search method at the end of each generation. In a hybrid approach, the TA algorithm was initiated with the best solution in the population and tried to improve the solution within 10 calls, replacing the worse solution in the population. As previously described, the local search method explored a small search space associated with the failure ring. This was done by slightly varying the failure ring heights. In Figure 4.12, the sGA alone quickly converges to a sub-optimal solution, never discovering the global solution in any of the five runs. The TA algorithm starts at a lower fitness because it starts the problem with a single, randomly generated flywheel. The TA algorithm quickly climbs to a sub-optimal solution. Figure 4.12 displays a typical run in which the TA algorithm seems to be taking small steps in climbing to a local solution. Figure 4.12 also displays typical runs where the hybrid iiGAs that incorporate either the local search method or TA algorithm discover solutions that are extremely close to the global optimal solution.

The iiGA topology shown in Figure 4.13 was run on a single computational node. The iiGA parameters are shown in Table 4.5.1 demonstrate how the iiGA topology in Figure 4.15 can explore a design space with various levels of resolution and evaluation accuracy. Islands 0-2 can quickly search the design space with larger populations due to the efficient plane stress finite element code which bases fitness on angular velocity. These islands will converge quickly due to the low level of geometric resolution and the efficient plane stress finite element code. The iiGA completes a high number of generations (termed generations per cycle) before solutions migrate to neighboring islands to further increase the rate of convergence. A slightly higher crossover rate will encourage the iiGA to introduce new designs into the population. Islands 3 and 4 search at a low level of geometric resolution, evaluating individuals with an efficient axi-symmetric three-dimensional finite element code (with a low number of degrees of freedom) basing fitness on SED. Islands 5-8 have lower population sizes with a lower number of generations per cycle and are increasingly refined in geometric resolution. They measure fitness with various levels of accuracy with an axi-symmetric three-dimensional finite element code. The iiGA completes a lower numbers of generations before migrating solutions to neighboring islands. Islands 9-11 have the highest level of geometric resolution and three-dimensional finite element evaluation accuracy. They also have the lowest number of generations completed before migrating any solutions to neighboring islands. The iiGA topology and parameters were specifically chosen to reduce the total number of expensive finite element evaluations needed in the optimization of large scale engineering structures. Due to the fact the GAs often require a large number of evaluations, decreasing the number of expensive finite element evaluations will help increase the computational efficiency of a typical GA. The TA algorithm was called at most 10 times at the end of each generation. The TA algorithm was initiated with the best solution in the population and replaced the worst solution in the population.

Figure 4.14 displays the normalized fitness (recomputed with the axi-symmetric three-dimensional 962 degree of freedom analysis) of each island as a function of time. Figure 4.14 displays the iiGA slightly "jumping" to higher values in fitness due to the injection of high fitness low resolution individuals. The second and third islands (which are at a low level of resolution) quickly converge (less than 10 seconds) to near global optimal solutions. Figure 4.14 conveys the benefits of searching at various levels of resolution to quickly find building blocks to be injected into islands of higher resolution. Unfortunately, for this particular small search space, the difference in geometric resolution plays a small role in the actual fitness. A near global optimal solution (within 2% of the global optimal solution) can be found using only three rings, causing difficulties to fully realize the impact of searching at various geometric levels with the iiGA. Most of the work done by the iiGA occurs quickly in the first few islands (at a low level of resolution). This makes it difficult to realize the full benefits of an iiGA for such a simple problem. The global optimal solution is discovered first on the fourth island for this optimization run in less than 200 seconds. The average time for the iiGA in Figure 4.13 to find the global optimal solution in any island of high resolution measuring fitness with the axi-symmetric three-dimensional finite element model (containing 962 degrees of freedom) in five runs was 768 seconds. The sixth, seventh and eighth islands discover the global solution within 900 seconds in Figure 4.14. These iiGA results illustrate the efficiency of searching at various levels of resolution to quickly find building blocks to increase robustness and help decrease computational demands of a typical GA.

Table 4.5.1 Hybrid Island Injection Genetic Algorithm Parameters for the Enumerable Coarse Design Space of a Solid Isotropic Flywheel.

Island #	Pop Size	Gens per Cycle	Crossover Probability	Mutation Probability	Analysis Tool	Fitness Definition	# Migrated
0	300	12	75%	1%	Plane Stress	ω	3
1	300	12	75%	1%	Plane Stress	ω	3
2	200	6	70%	1%	3-D	SED	3
3	200	6	70%	1%	3-D	SED	3
4	200	4	65%	1%	3-D	SED	3
5	200	4	65%	1%	3-D	SED	3
6	100	2	60%	1%	3-D	SED	3
7	100	2	60%	1%	3-D	SED	3
8	100	2	60%	1%	3-D	SED	3

The iiGA topology shown in Figure 4.15 was run on a single computational node that combined a TA algorithm to create a hybrid iiGA. iiGA parameters are shown in Table 4.5.1. Figure 4.16 displays the normalized fitness (recomputed with the axi-symmetric three-dimensional 962 degree of freedom analysis) for a typical optimization run for the hybrid iiGA for each island as a function of time. The second and third islands quickly converge to near global optimum solutions. The global optimum is discovered first on the fifth island in less than 200 seconds. The average time for the iiGA in Figure 4.15 to find the global optimum in any island of high resolution measuring fitness with the axi-symmetric three-dimensional finite element model (containing 962 degrees of freedom) in five runs was 674 seconds. The sixth, seventh and eight islands converge to the global optimum within 500 seconds for this optimization run. When comparing Figure 4.14 to 4.16, it can be seen that the hybrid iiGA climbs from local optimum solutions that are near by the global optimum to the global optimum through help from the TA algorithm. Also when comparing Figure 4.14 to 4.16, a the hybrid iiGA makes noticeably smaller steps to the global optimum when compared to the iiGA. These hybrid iiGA results demonstrate how a local hill climber such as a TA algorithm can help the iiGA to find a global optimum in an efficient manner.

The iiGA topology shown in Figure 4.17 was run on a single computational node that combined a local search procedure to create a hybrid iiGA. iiGA parameters are shown in Table 4.5.1. The local search procedure was called at most 10 times at the end of each generation. The local search procedure took the best solution in the population and replaced the worst solution in the population if a better solution was discovered. Figure 4.18 displays the normalized fitness (recomputed with the axi-symmetric three-dimensional 962 degree of freedom analysis) for the hybrid iiGA for each island as a function of time. The second and third islands quickly converge to near global optimums. The global optimum is discovered first on the fifth island in less than 200 seconds. The average time for the hybrid iiGA in figure 4.17 to find the global optimum in all islands of high resolution measuring fitness with the axi-symmetric three-dimensional finite element model (containing 962 degrees of freedom) in five runs was 715 seconds. The sixth, seventh and eight islands converge to the global solution within 750 seconds for this optimization run. When comparing Figure 4.14 to 4.18, it can be seen that the hybrid iiGA that uses a local search procedure to help climb from local solutions that are near by the global solution to the global solution. These hybrid iiGA results demonstrates how a local search procedure can help the iiGA find the global optimum in an efficient manner.

The iiGA topology shown in Figure 4.19 was run on a single computational node that combined local search procedure and TA algorithms to create a hybrid iiGA. iiGA parameters are shown in Table 4.5.1. The TA algorithm and local search procedure was called at most 10 times at the end of each generation in each island. The local search procedure took the best solution in the population and replaced the worst solution in the population if a better solution was discovered. Figure 4.20 displays the normalized fitness (recomputed with the axi-symmetric three-dimensional 962 degree of freedom analysis) for the hybrid iiGA for each island as a function of time. The second and third islands quickly converge to near global optimums. The global optimum is discovered first on the fifth island in less than 200 seconds. The average time for the iiGA in Figure 4.19 to find the global optimum in any island of high resolution measuring fitness with the axi-symmetric three-dimensional finite element model (containing 962 degrees of freedom) in five runs was 417 seconds.

The GA ring topology shown in Figure 4.21 was run on a single computational node. GA parameters were as follows: 75% crossover and 1% mutation. Figure 4.22 displays the normalized fitness computed with the axi-symmetric three-dimensional 962 degree of freedom analysis for the GA ring topology for each island as a function of time. All the islands slowly converged to a near optimal solution. The algorithm was allowed to run 5 hours, never discovering the global optimum.

When comparing all the optimization techniques presented above, some general conclusions can be drawn. The best solution discovered with the TA algorithm had a lower fitness when compared to all other approaches for all optimization runs. The sGA approach was improved in terms of computational efficiency when combining with either the TA algorithm or the local search method. The iiGA approach outperformed the TA algorithm and all single island and ring topology GA approaches in terms of a lower computational effort to locate the global optimum. All hybrid iiGA approaches required less computational effort (averaged over five runs) compared to other iiGA approaches. The hybrid iiGA that used a combination of the TA algorithm and the local search procedure required less computational effort (when averaged over five runs) compared to a hybrid iiGA that used either the TA algorithm or the local search procedure independently. It appears the hybrid iiGA that incorporates both TA and the local search method is more robust in terms of efficient exploration of the search space, at least for the problem considered. Table 4.5.2 contains the statistics on the average number of calls made over the five runs. The hybrid iiGA that used the TA algorithm and local search method searched less than 5% of the entire search space, taking less than 0.5% of the time to enumerate the entire search space, measuring more than half of the evaluations with the plane stress finite element model to find the global optimum.

Table 4.5.2. Statistics on the Total Number of Evaluation Calls made for Various Optimization Approaches in Average 2-Hour Run.

Optimization Approach	Total FEM Calls	Total 3-D FEM Calls	Plane Stress FEM Calls	Total TA FEM Calls	Total Local FEM Calls
TA	12,201	0	12,201	12,201	0
sGA	26,877	0	26,877	0	0
SGA plus TA	19,902	0	19,902	980	0
SGA plus Local	23,543	0	23,543	0	3,110
iiGA	122,900	52,828	70,072	0	0
iiGA plus Local	117,102	49,051	68,051	0	12,150
iiGA plus TA	111,521	46,051	65,470	11,340	0
iiGA plus TA and Local	98,853	43,771	55,082	3,880	7,800

4.5.3 Optimization of Multi-Material Composite Flywheels

Finally, optimum multi-material composite flywheel shapes will be sought. First, solid multi-material flywheel shapes will be optimized with no constraints on maximum angular velocity with an iiGA, hybrid iiGA and topological "ring" GA. Next, annular multi-material composite flywheels will be optimized while controlling the maximum allowable angular velocity while reducing "air gap" growth. It was found that the iiGA and hybrid iiGA search was extremely efficient when compared to a "ring" topology GA. Also, it was found that the hybrid iiGA found solutions with slightly higher fitness values when compared to the iiGA or "ring" topology GA.

It was discovered in previous iiGA optimization runs that an extremely refined three-dimensional finite element mesh was needed to avoid "artifacts" in the solutions. The solutions that contained "artifacts" of the evaluation typically placed a large amount of material near the outer radius of the flywheel, creating a sharp inflection point near the ring interfaces. Figure 4.23 displays a solution that is an artifact of the analysis due a stress concentration that would be associated with the sharp inflection point. The three-dimensional finite mesh contained 2,482 degrees of freedom. This solution was re-evaluated multiple times with an increasingly refined three-dimensional finite element model until the maximum stress in the model ceased to increase by more than 5%. The three-dimensional finite element model required 12,272 degrees of freedom to converge. As expected, the origin of failure in the converged solution was located near the sharp point of inflection. Further refinements in the three-dimensional model would be fruitless due to the nature of the specific flywheel geometry. In other words, a further refinement in the analysis would only accentuate the stress concentration located near the sharp point of ring inflection. The maximum stress in the flywheel will be dominated by the stress concentration. The iiGA needs only realize that designs of this nature are not optimal. This level of refinement helped the GA realize that flywheel designs of this sort are not optimal.

The optimization of solid and annular composite multi-material flywheels will be approached with the hybrid iiGA topology shown in Figure 4.7 using 10 bits per ring height in spatial resolution while ranging the geometric resolution from a 3 to 24 rings. This type of hybrid iiGA topology performed better on average compared to other hybrid iiGA topologies in the previous study of the coarsely designed solid isotropic flywheel. Notice islands

9-11 are the most refined in geometric resolution and are evaluated with the three-dimensional finite element code with 12,272 degrees of freedom to avoid "artifacts" in the final solution.

iiGA parameters are contained in Table 4.5.3. The iiGA parameters were chosen to help decrease computational costs as previously outlined in the optimization of an enumerable search space of a solid isotropic flywheel. Table 4.3.3 contains one quasi-isotropic material, but the GA can choose the direction of "strength" in either the radial or tangential direction. Also, the GA was given the choice of two isotropic materials (Steel and Aluminum, Table 4.3.1). It is hypothesized that the GA could place materials that have a higher density at the outer radius of the flywheel to increase the mass moment of inertia term in the definition of SED. Next, a solid multi-material flywheel will be optimized with respect to SED.

Figure 4.24 shows the "raw" fitness for solid multi-material flywheels as a function of time for each island in an iiGA depicted in Figure 4.7. iiGA parameters are contained in Table 4.5.3. The "raw" fitness is the actual fitness measured by each island's specific finite element evaluation. Islands 0-2 measure "raw" fitness with an approximate but efficient evaluation based on angular velocity. The axi-symmetric plane stress finite element code predicts fitness accurately for flywheel shapes that have small ring gradients, producing results in Figure 4.24 that are excessively optimistic. The axi-symmetric three-dimensional finite element code evaluated islands 3-8 with a reduced number of degrees of freedom when compared to islands 9-11. Therefore we can expect some discrepancy in fitness values for islands 3-8 when re-evaluating fitness with the most refined axi-symmetric three-dimensional finite element model. From this point forward, all plots that display fitness as a function of time will be recomputed with the most accurate evaluation used in the run.

Figure 4.25 displays the fitness of solid multi-material flywheels as a function of time (re-evaluated fitness measured at the highest level accuracy with the three-dimensional axi-symmetric finite element model containing 12,272 degrees of freedom). Hybrid iiGA topological structure is shown in Figure 4.7 while all parameters are contained in Table 4.5.3. In Figure 4.7, islands 0-8 evaluated individuals with either an axi-symmetric plane stress or three-dimensional finite element code that is less accurate when compared to the axi-symmetric three-dimensional finite element code that evaluated fitness with 12,272 degrees of freedom in islands 9-11. The inaccuracies of the evaluation in islands 0-8 are shown in Figure 4.25. Figure 4.25 displays an expected response; islands 0-8 initially find good solutions but begin to find worse solutions as time progresses. These solutions contain building blocks that are used to help evolve islands at higher levels of resolution through injection and therefore cannot be discarded even though they have a low fitness when evaluated with the most accurate finite element model. We can expect, but cannot discard what appears to be "noise" in Figure 4.25 for islands of lower resolution. This expectation would be a snafu for islands that were initially evaluated using the finite element model with the highest degree of accuracy. An explanation of the origin of noise and noise effects are given next.

The iiGA explores the search space defined by the fitnesses of the individuals in a population through successive generations. Noise occurs when the iiGA cannot decipher the differences between a solution that does or does not violate an assumption of a fitness evaluation (for example a plane stress finite element evaluation). If a high fitness is associated with solutions that violate a fitness evaluation then the iiGA will sooner or later exploit this to improve the existing solutions in the population. Initially, the *intended* fitness definition dominates the iiGA search procedure for islands that evaluate fitness with an efficient, less accurate finite element evaluation. After a certain amount of time this dominating effect lessens, allowing the iiGA to explore areas of the search space that have high *actual* fitness values, but violate evaluation assumptions. The *intended* fitness can be conceived as the fitness the engineer or user ideally defines, assuming that the fitness can be evaluated absolutely in closed form. The *actual* fitness can be thought of as the fitness that can also be a function of violations in the fitness evaluation. The iiGA searches the *actual* fitness definition, often finding artifacts in the final solution. This can force an engineer or the user to use analyses that are more refined and computationally demanding. Any increase in computational time will amplify the total time required to effectively explore the search space. An analysis refinement can severely limit the practical application of a typical GA. This is truly one area where the iiGA can shine by searching at various levels of computational efficiency to quickly explore the search space to find potentially fruitful areas. These fruitful areas can be re-evaluated at a higher level of accuracy to double check the solution.

Figure 4.26 is Figure 4.25 "zoomed" in to help accent the effects of searching at various levels of resolution while exploiting less accurate, computationally cheap finite element evaluations with the hybrid iiGA shown in Figure 4.7. All islands that did not evaluate fitness with the most refined three-dimensional finite element evaluation contain noise as previously discussed. Islands 0, 3 and 4 begin with high fitness values, initially finding fit building blocks due to a low flywheel geometric resolution (three rings) and an extremely efficient finite element evaluation. Island 0, 1 and 2 were evaluating fitness with a plane stress finite element evaluation basing fitness on angular velocity. Figure 4.26 shows that basing fitness on a "sub-fitness" function was fruitful. Islands 5 and 6 begin with a high initial fitness and initially converge slower to a higher fitness when compared to islands 0 through 4. Islands 7 and 8 initially converge slower but converge to a higher fitness when compared to islands 5 and 6. After a period of time the iiGA begins to find worse solutions due to inaccuracies in the finite evaluation in islands 0-8. Islands 9, 10 and 11 begin with the lowest inital fitness, converging the slowest when compared to all other islands while evolving to the most fit individuals. This was due to the fashion that the hybrid iiGA searched.

The technique begins by first quickly finding building blocks at a low (three rings) then medium-low (six rings) then medium (twelve rings) and high (24 rings) levels of resolutions with various evaluation tools. Islands that do not search at the highest level of resolution use two different evaluation tools and fitness definitions. The fitness definitions for these islands were measured with an axi-symmetric plane stress finite element code based on angular velocity or an axi-symmetric three-dimensional finite element code basing fitness on SED. Next, the iiGA migrates solutions containing good building blocks in an hierarchical order (from lower to higher level of resolution). Each island receives the solutions that contain building blocks in the next cycle of the algorithm. Figure 4.26 shows that islands 9, 10 and 11 evolve individuals with a higher level of fitness (compared to all other islands) due to the increase in geometric resolution.

Figure 4.27 shows the best solid multi-material composite flywheel found at each level of geometric refinement for the axi-symmetric plane stress (basing fitness as a function of angular velocity) and the three-dimensional finite element evaluation (basing fitness on SED). The plane stress evaluations allow the iiGA to efficiently explore the search space to discover fruitful solutions by sacrificing evaluation accuracy. Often, many optimization approaches use a similar level of accuracy to approximate expensive evaluations, giving rise to solutions that are artifacts of the simplified analysis. Comparing the best flywheel found by the axi-symmetric plane stress finite element code to the three-dimensional finite element code in Figure 4.27 (at each level of resolution) displays solutions that are vividly artifacts of a simplified analysis tool (plane stress approximation). Completely dismissing the solutions found by the plane stress evaluation is a mistake because they are just exaggerated shapes that have helped evolve the shapes found with the refined axi-symmetric three-dimensional finite element analysis. The latter statement can be better understood by re-examining Figure 4.25, where the best flywheel found at each level of resolution and accuracy is displayed as a function of time. Figure 4.27 also conveys how the iiGA "fine tunes" the solutions in islands of higher resolution and higher accuracy. The iiGA places only the E-Glass material throughout out the flywheel at various orientations, never using the more dense isotropic material. Evidently, the iiGA did not find that exploiting the mass moment of inertia (with either aluminum or steel) of an unconstrained solid composite flywheel to increase the SED when compared to the associated sacrifices that would have been made in the failure angular velocity.

Figures 4.28 and 4.29 display the fitness of an annular multi-material flywheel as a function of time (re-evaluated fitness measured at the highest level accuracy with the three-dimensional axi-symmetric finite element model containing 12,272 degrees of freedom) for the iiGA and hybrid iiGA displayed in Figures 4.6 and 4.7, respectively. All iiGA parameters are contained in Table 4.5.3. Figure 4.30 and Figure 4.31 are Figures 4.28 and 4.29

that are "zoomed" in to help emphasize the effects of searching at various levels of resolution while exploiting less accurate, computationally cheap finite element evaluations.

As previously stated regarding the iiGA results for a solid multi-material composite flywheel, islands with a coarse geometric resolution initially find solutions containing building blocks extremely fast. This is due to the combination of a small search space and computationally efficient finite element evaluations. Islands with a refined geometric resolution converge slower due to a larger search space and a computationally demanding three-dimensional finite element model. Islands at a lower resolution quickly find solutions that contain good building blocks that were injected in islands in an hierarchical fashion (from lower to higher level of resolution). Islands with higher levels of geometric resolution converge slower to solutions that have an increase in fitness (when compared to islands of lower geometric resolution) due to the increase in search space.

Table 4.5.3 Island Injection Genetic Algorithm Parameters.

Island #	Pop Size	Gens per Cycle	Prob. Xover	Prob. Mutation	Analysis Tool	Fitness Def.	# Migrated	# Rings
0	300	12	75%	1%	Plane Stress	ω	Best	3
1	300	12	75%	1%	Plane Stress	ω	Best	6
2	300	12	70%	1%	Plane Stress	ω	Best	12
3	200	8	70%	1%	3-D	SED	Best	3
4	200	8	65%	1%	3-D	SED	Best	3
5	200	6	65%	1%	3-D	SED	Best	6
6	100	6	60%	1%	3-D	SED	Best	6
7	100	4	60%	1%	3-D	SED	Best	12
8	100	4	60%	1%	3-D	SED	Best	12
9	100	2	60%	1%	3-D	SED	Best	24
10	100	2	60%	1%	3-D	SED	Best	24
11	100	2	60%	1%	3-D	SED	Best	24

Table 4.5.4 Genetic Algorithm Topological "Ring" Parameters.

Island	Pop Size	Gens per Cycle	Prob. Xover	Prob. Mutation	Analysis Tool	Fitness Def.	# Migrated	# Rings
All	105	3	65%	1%	3-D	SED	Best	24

Figure 4.32 depicts 20 islands that form a topological "ring" GA used to obtain the fitness as a function of time presented in Figure 4.33 for an annular multi-material composite flywheel. All islands operated on the identical GA parameters given in Table 4.5.4 measuring fitness with the axi-symmetric three-dimensional finite element model containing 12,272 degrees of freedom. The topological "ring" GA contained the same total number of individuals found in the hybrid iiGA, equally divided amongst the islands. Figure 4.33 shows that each island slowly finds better solutions in the "ring" topology GA, taking nearly six days to converge.

Figure 4.34 compares the results obtained from the iiGA, hybrid iiGA and topological "ring" GA. For the iiGA approach, Figure 4.25 displays that the best solution found in each island (that evaluated fitness with the highest level of finite element accuracy) is nearly identical as a function of time. This is also true for the hybrid iiGA and topological "ring" GA. For these reasons, the results shown in Figure 4.34 are drawn from typical islands that evaluated fitness with the most refined three-dimensional finite element model for both the iiGA, hybrid iiGA and topological "ring" GA. Both the iiGA and the hybrid iiGA converge over five times faster when compared to the topological "ring" GA. The hybrid iiGA also converges to a higher fitness compared to both the iiGA and topological "ring" GA. Table 4.5.5 contains statistics for the total number of evaluation calls made during each GA optimization approach. Since each topological "ring" GA run takes nearly six days, no attempt was made to compute averages over a set of independent runs for this optimization approach. However, a second set of independent runs for both the iiGA and hybrid iiGA were done for two reasons: they took just over one day to converge and to display the fact that these results were not biased by the initial population. The second runs produced nearly identical results in terms of final fitness values and total time until convergence for both the iiGA and hybrid iiGA.

Figure 4.35 compares the best solution found the iiGA, hybrid iiGA and the topological "ring" GA. They are all similar in shape, with some slight variations. The best solution found by the "ring" topology GA is not completely smooth in shape, placing more material at the end of the flywheel to increase the mass moment of inertia. All solutions contain similar material placement near inner radius of the flywheel. This can be expected since the maximum stress found typically in an annular flywheel is located at the inner radius in the tangential direction. All the optimization approaches placed the strongest direction of E-Glass epoxy in the tangential direction. The hybrid iiGA and iiGA found solutions that are very similar in shape, but vary slightly in material placement away from the inner radius of the flywheel. The hybrid iiGA found a solution that has the least amount of mass placed near the end of the flywheel.

Table 4.5.5. Statistics on the Total Number of Evaluation Calls for iiGA, Hybrid iiGA and Topological "Ring" GA Optimization Approaches.

Optimization Approach	Total FEM Calls	Total 3-D FEM Calls	Plane Stress FEM Calls	Total TA FEM Calls	Total Local FEM Calls
Topological "Ring" GA	12,201	12,201	0	0	0
iiGA	1,244,717	383,074	861,643	0	0
Hybrid iiGA (local and TA)	861,889	306,544	555,345	43,750	34,980

To use the iiGA to design flywheels that have a reasonable angular velocity, a "target" angular velocity of a flywheel must be specified. The iiGA should also penalize flywheels that have a large amount of "air gap" growth to discover "safer" designs. A lower "target" angular velocity can be specified by the designer to help control the high angular velocities associated with the solutions found in an unconstrained optimization approach of a flywheel (as just previously presented). A new "target" angular velocity was determined by reducing the angular velocity that was found in best solution in the previous unconstrained optimization problem. A reduction of 25% in angular velocity was chosen so the iiGA could place materials and form flywheel shapes while still maintaining a reasonable SED. For the constrained problem, the fitness was based on equation 4.2. In equation 4.2, the SED term was normalized with SED results ascertained previously in the unconstrained optimization approach. This was done similarly to normalize the "air gap" growth at failure. The angular velocity was normalized with the "target" velocity. Flywheels were penalized only if the angular velocity surpassed the "target" angular velocity. This means the iiGA can avoid all penalties associated with high angular velocities by maintaining flywheels that have angular velocities below the "target" value.

For the constrained optimization of multi-material annular composite flywheels a a slight variation in the hybrid iiGA topology is shown in Figure 4.36. The only difference from the previous hybrid iiGA topology is the elimination of the plane stress evaluations. Substituted instead of a plane stress evaluation was the three-dimensional evaluation. This change in approach was made due to the fact that the optimization of an annular multi-material composite flywheel requires control of the maximum angular velocity of a flywheel, not simply maximizing the "sub-fitness" function (angular velocity). The islands that previously evaluated with the efficient plane stress evaluation were replaced with three-dimensional evaluations that were reduced in the total number of degrees of freedom in the analysis.

Figure 4.37 displays the fitness of the constrained optimization of an annular multi-material flywheel as a function of time (re-evaluated fitness measured at the highest level of accuracy with the three-dimensional axi-symmetric finite element model containing 12,272 degrees of freedom). Hybrid iiGA parameters are contained in Table 4.5.3. Figure 4.38 shows the hybrid iiGA quickly finding solutions that contain building blocks at various levels of geometric resolution. Some "noise" is present due to the multiple levels in the three-dimensional finite element fitness evaluation.

Figure 4.39 shows the best solution found a various levels of geometric resolution for the constrained optimization of multi-material annular flywheels. All show interesting patterns in shape an material placement. The next few lines include reasonings for specific material placement throughout the flywheel, starting at the inner radius and ending at the outer radius. To overcome penalties due to large "air gap" growth the iiGA placed the stiffer material (aluminum) near the inner portion of the flywheel. To maintain a relatively high SED the hybrid iiGA next placed composite material in the flywheel with an orientation of strength in the tangential direction. Next, the hybrid iiGA placed composite material in the flywheel with an orientation of strength in the radial direction. The angular velocity constraint forced the iiGA to design a flywheel that placed a higher density material (aluminum) at the outer radius to increase the mass moment of inertia of the flywheel.

The angular velocity in the best solution found at the highest level of geometric resolution was extremely close to the "target" angular velocity. The "air gap" growth found in the best solution found at the highest level of geometric resolution in the constrained optimization problem was cut in half when compared to the unconstrained single criteria optimization approach. The SED for the best solution found at the highest level of geometric resolution in the constrained optimization problem was 21.6% lower than the unconstrained single criteria optimization approach. This was due to the constraint on angular velocity, which is squared in the fitness definition.

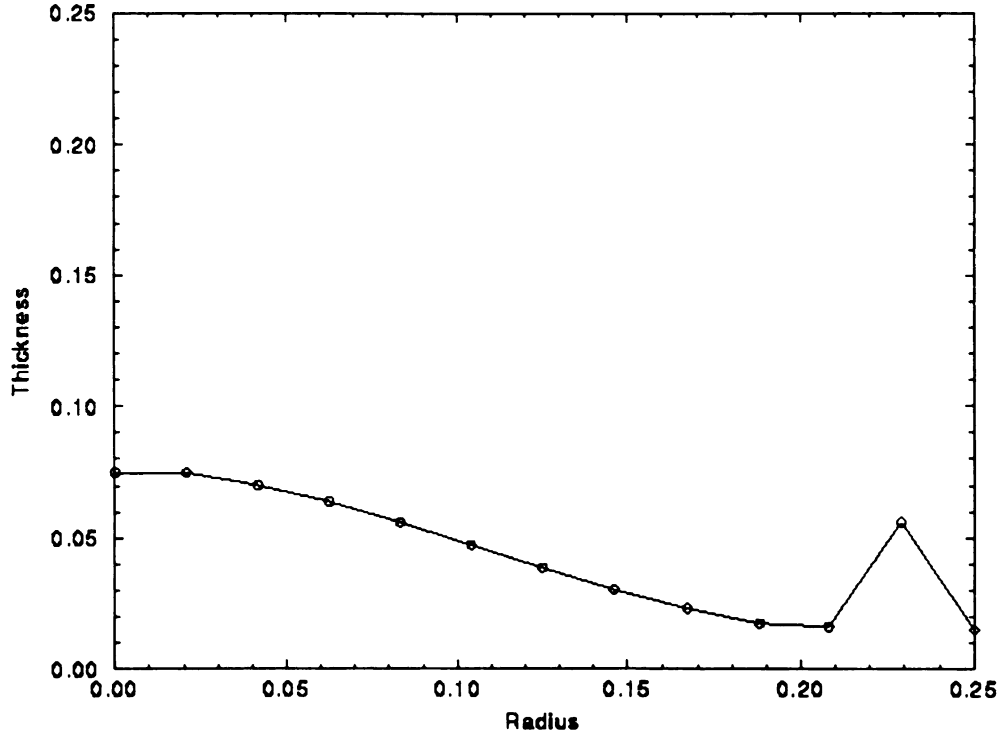

Figure 4.8. Simple genetic algorithm exploitation of plane stress evaluation.

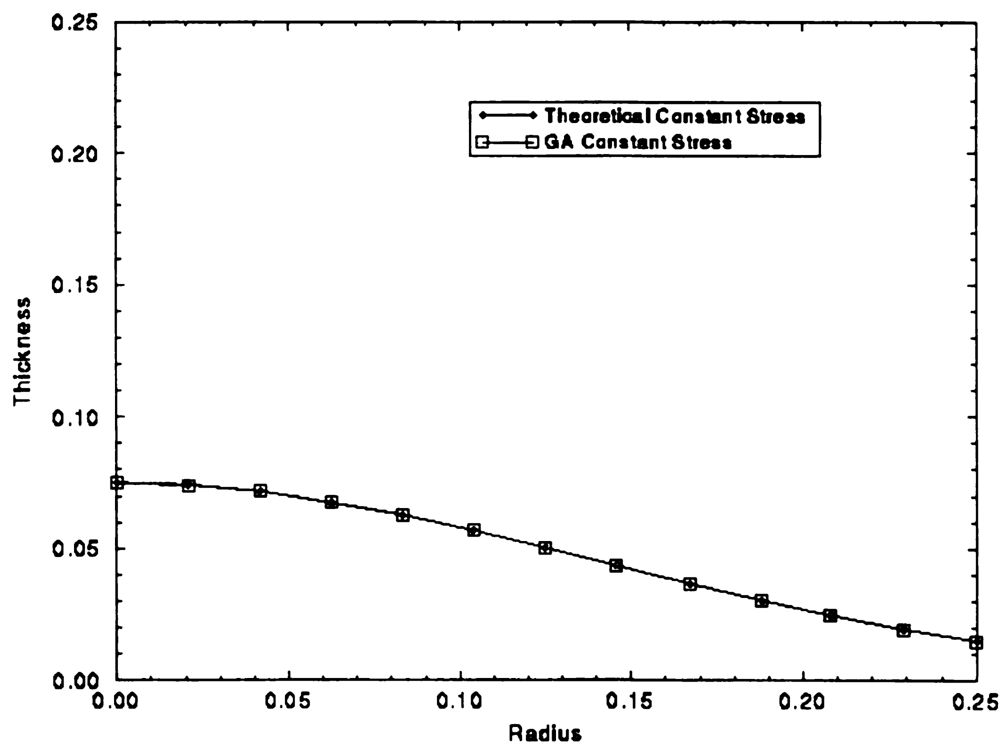

Figure 4.9. Theoretical constant stress profile compared to simple genetic algorithm constant stress profile.

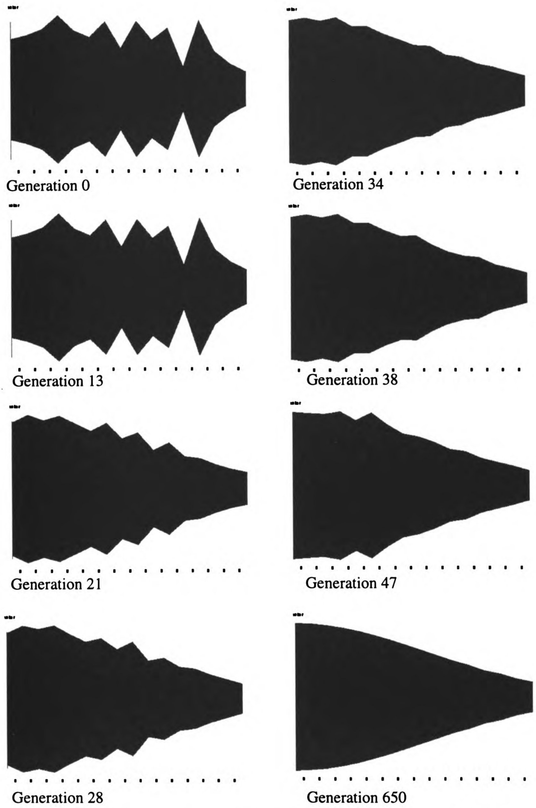

Figure 4.10. The simple genetic algorithm evolution of a constant stress flywheel.

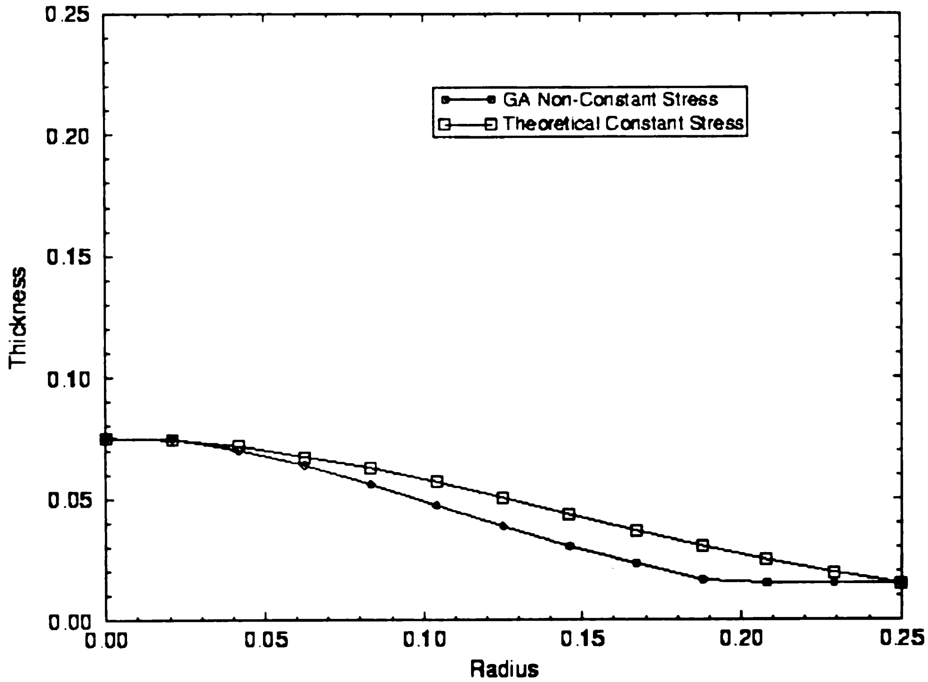

Figure 4.11. Simple genetic algorithm non-constant stress profile compared to the theoretical constant stress profile.

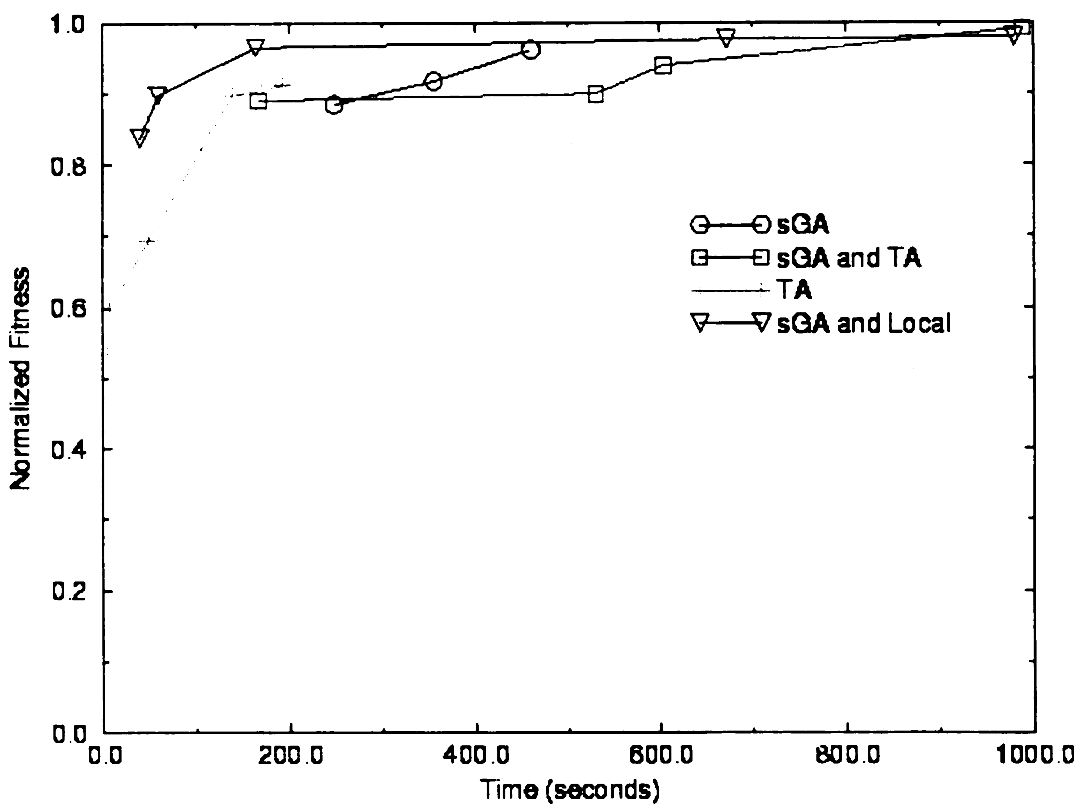

Figure 4.12. Simple genetic algorithm compared to TA algorithm and hybrid genetic algorithms for a solid isotropic flywheel in an enumerable search space.

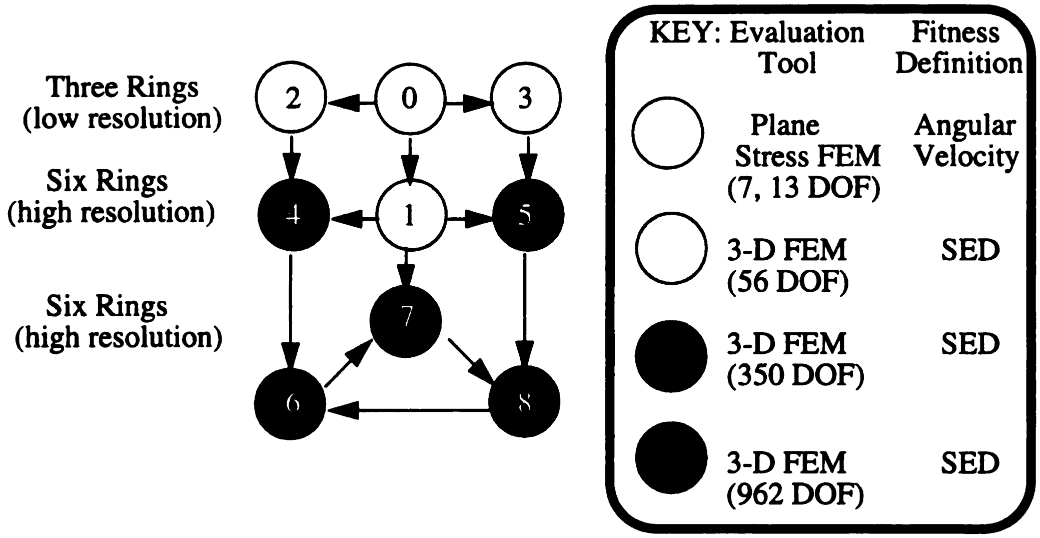

Figure 4.13. Island injection GA topology.

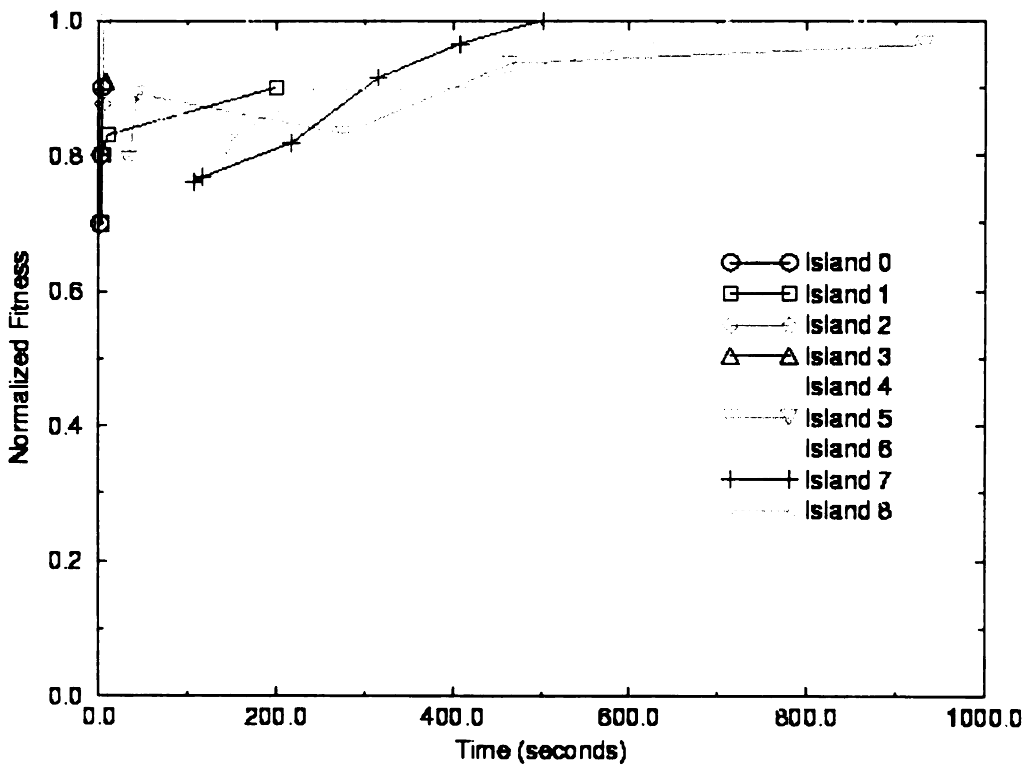

Figure 4.14. Single computational node island injection genetic algorithm results for a solid isotropic flywheel in an enumerable search space.

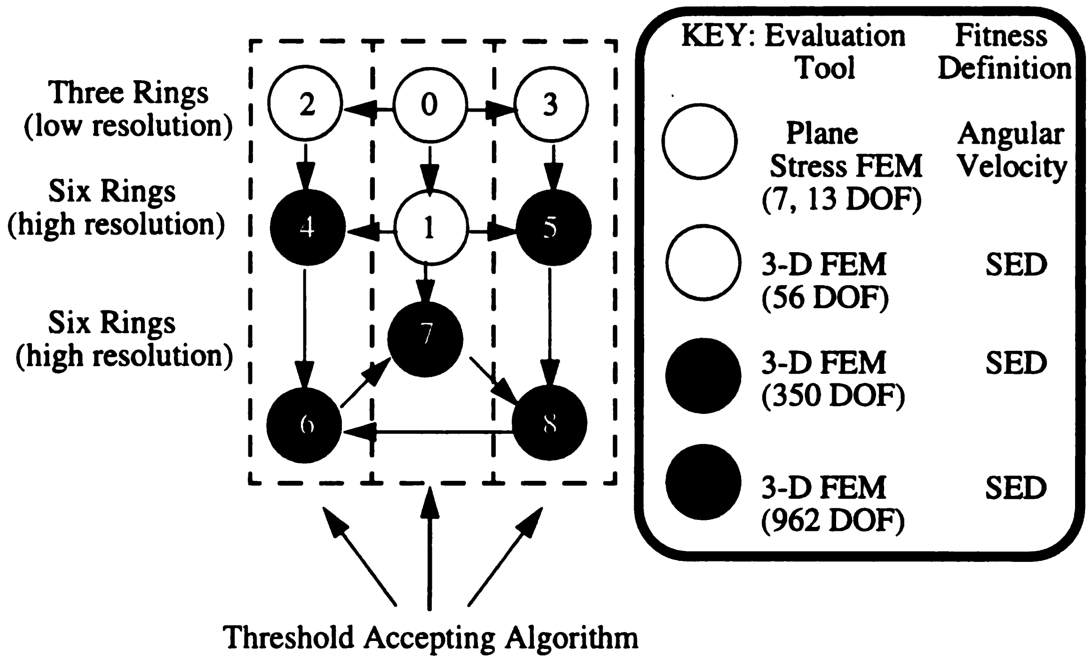

Figure 4.15. Hybrid island injection GA topology (TA algorithm).

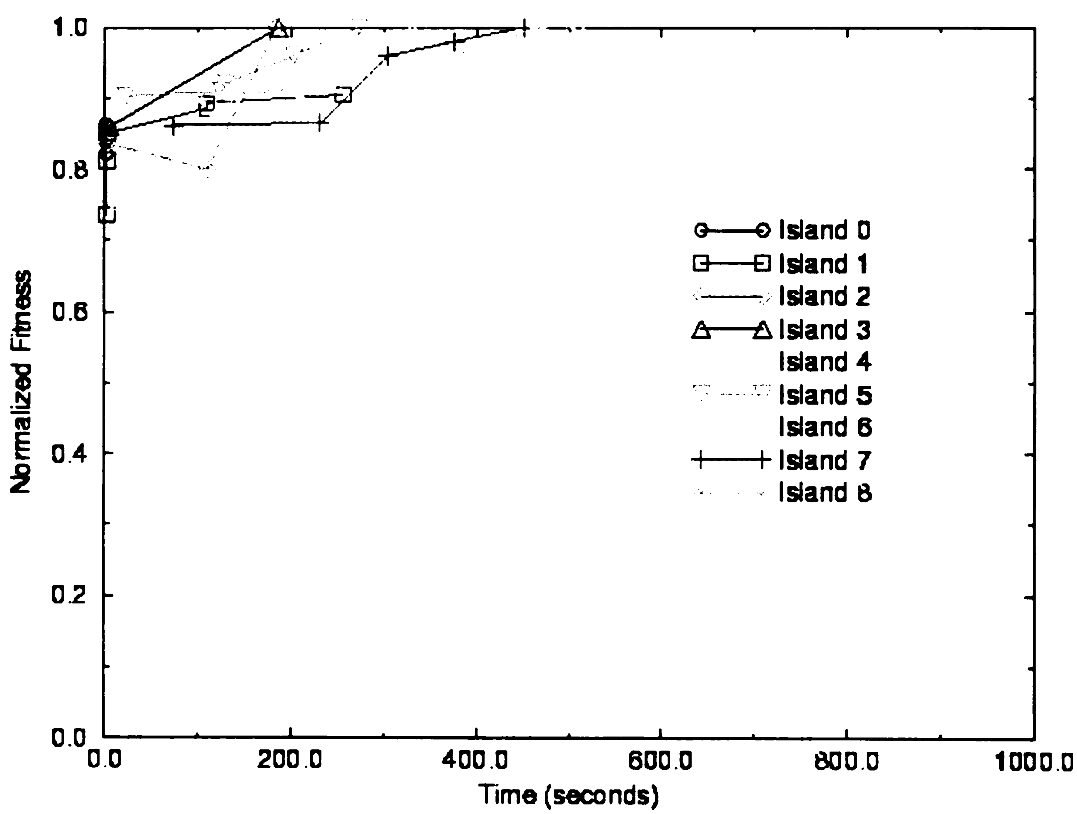

Figure 4.16. Single computational node hybrid island injection GA (TA algorithm) results for a solid isotropic flywheel in an enumerable search space.

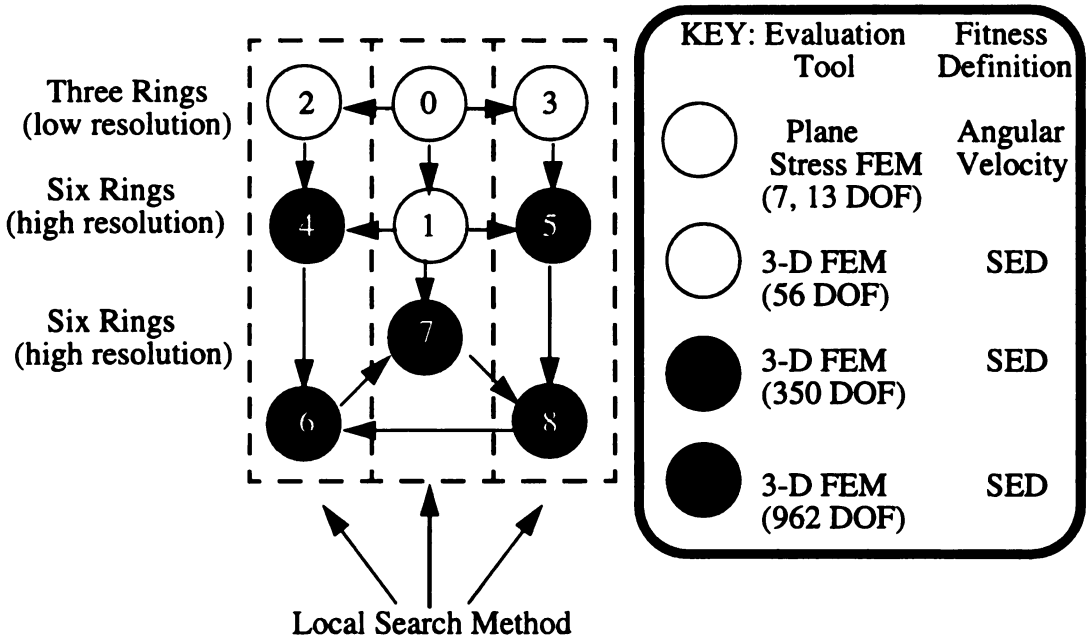

Figure 4.17. Hybrid island injection GA topology (local search method).

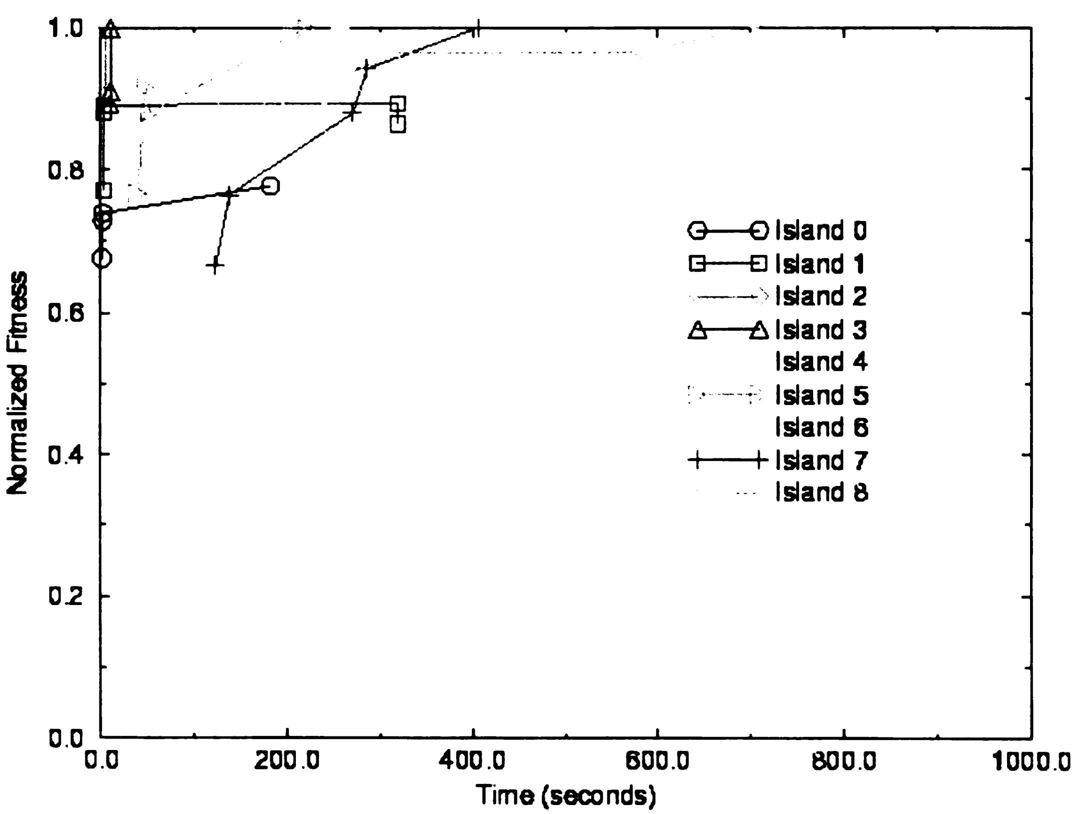

Figure 4.18. Single computational node hybrid island injection GA (local search method) results for a solid isotropic flywheel in an enumerable search space.

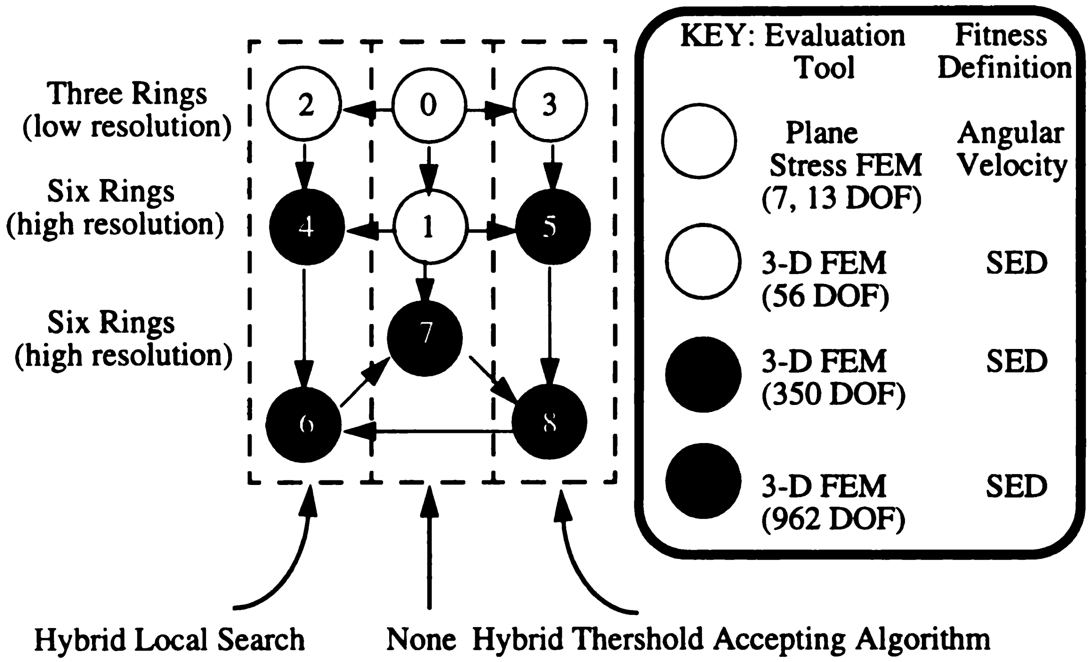

Figure 4.19 Hybrid island injection GA topology (local search and TA).

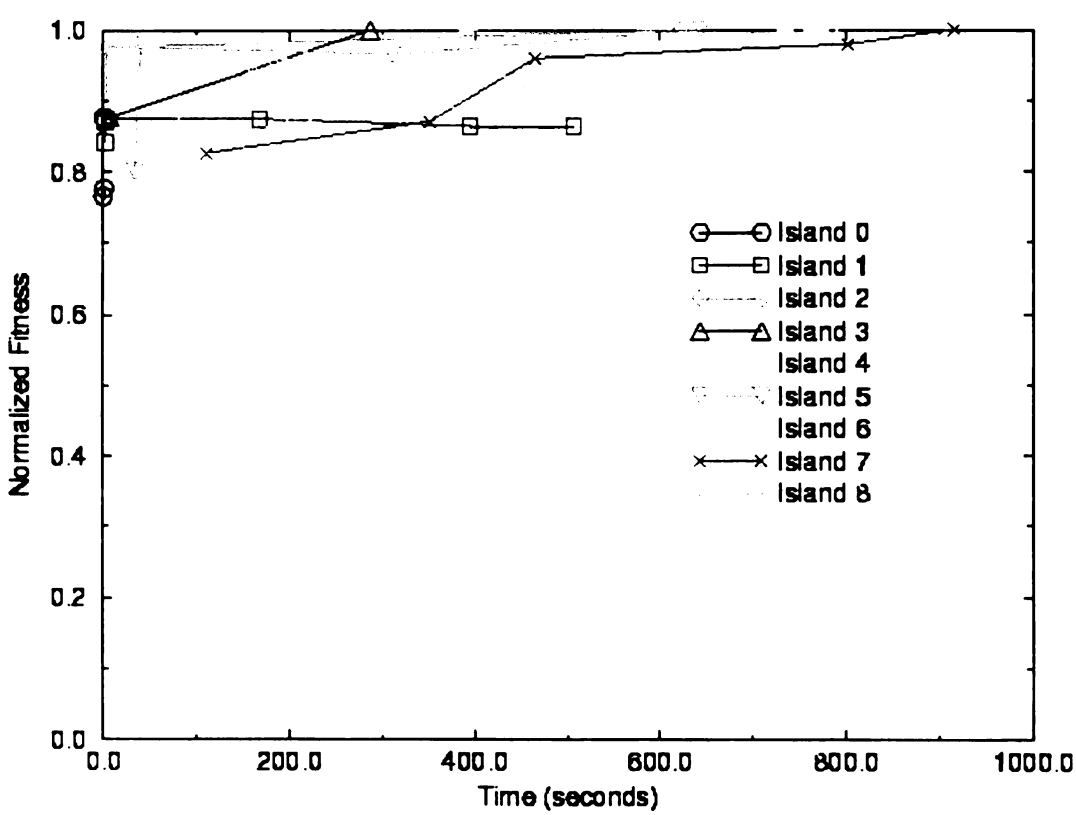

Figure 4.20. Single computational node hybrid island injection. GA (local search and TA) results for a solid isotropic flywheel in an enumerable search space.

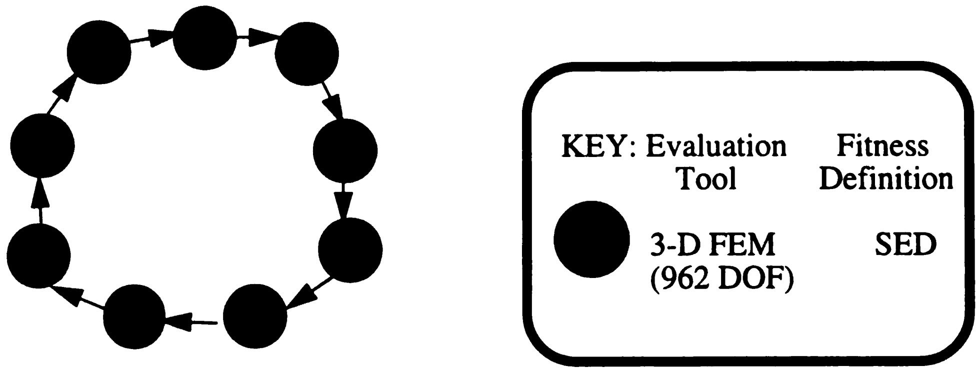

Figure 4.21. Twelve “ring” GA topology.

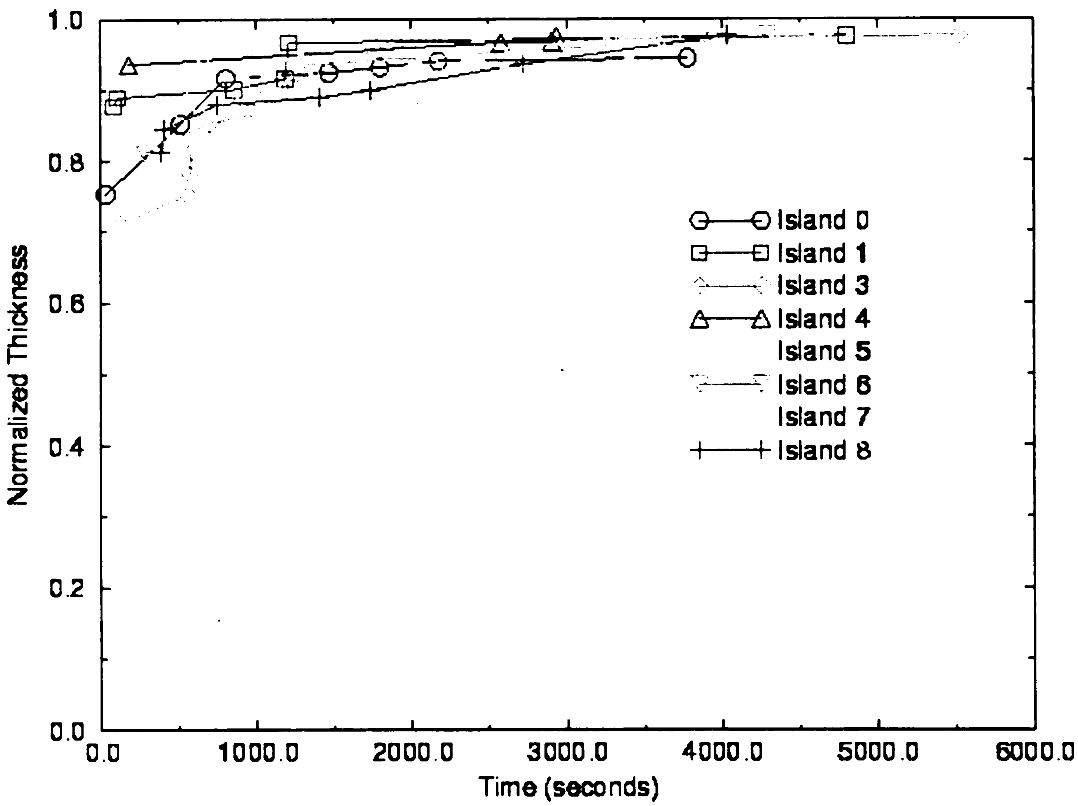

Figure 4.22. Single computational node topological “ring” GA results for a solid isotropic flywheel in an enumerable search space.

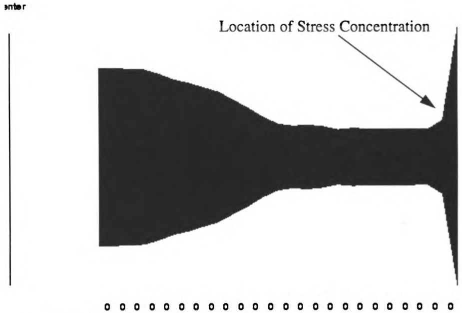

Figure 4.23. Demonstration of a flywheel that is an "artifact" for a three-dimensional finite element model (containing 2,482 degrees of freedom).

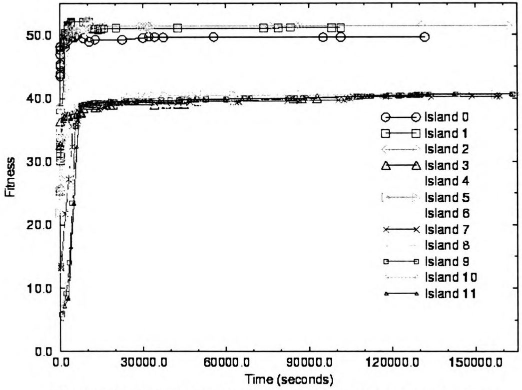

Figure 4.24. Hybrid iiGA "raw" fitness for each island as a function of time for a solid multi-material composite flywheel. Islands 0-2: plane stress fem evaluation. Islands 3-11: 3-D FEM evaluation.

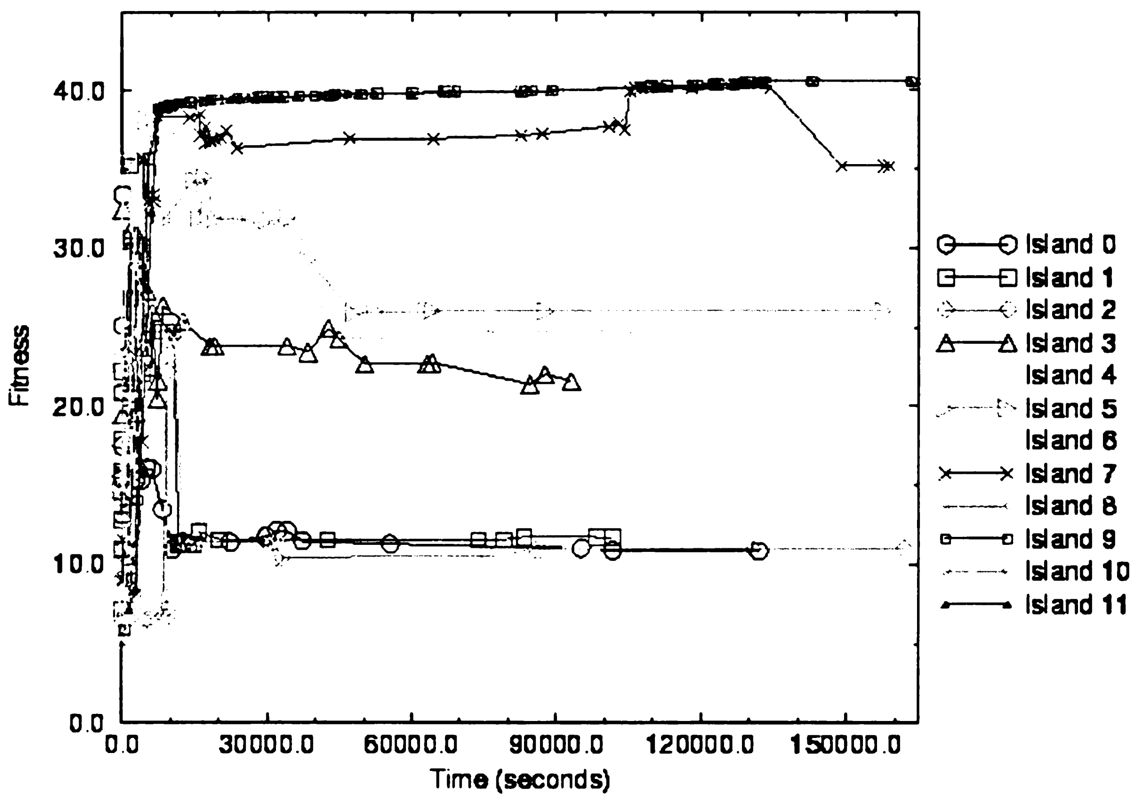

Figure 4.25. Hybrid iiGA fitness re-evaluated for each island as a function of time. All re-evaluations performed with 3-D FEM containing 12,272 degrees of freedom.

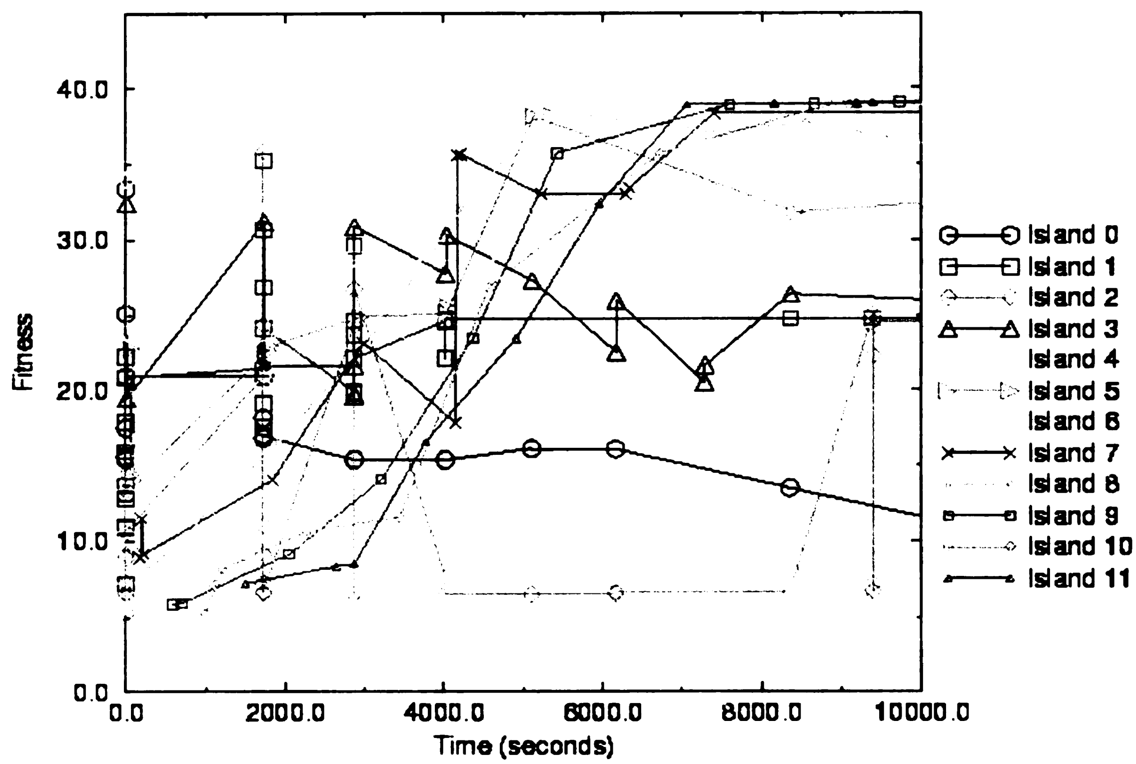

Figure 4.26. Hybrid iiGA quickly finding building blocks at low levels of geometric resolution to inject into islands of higher resolution.

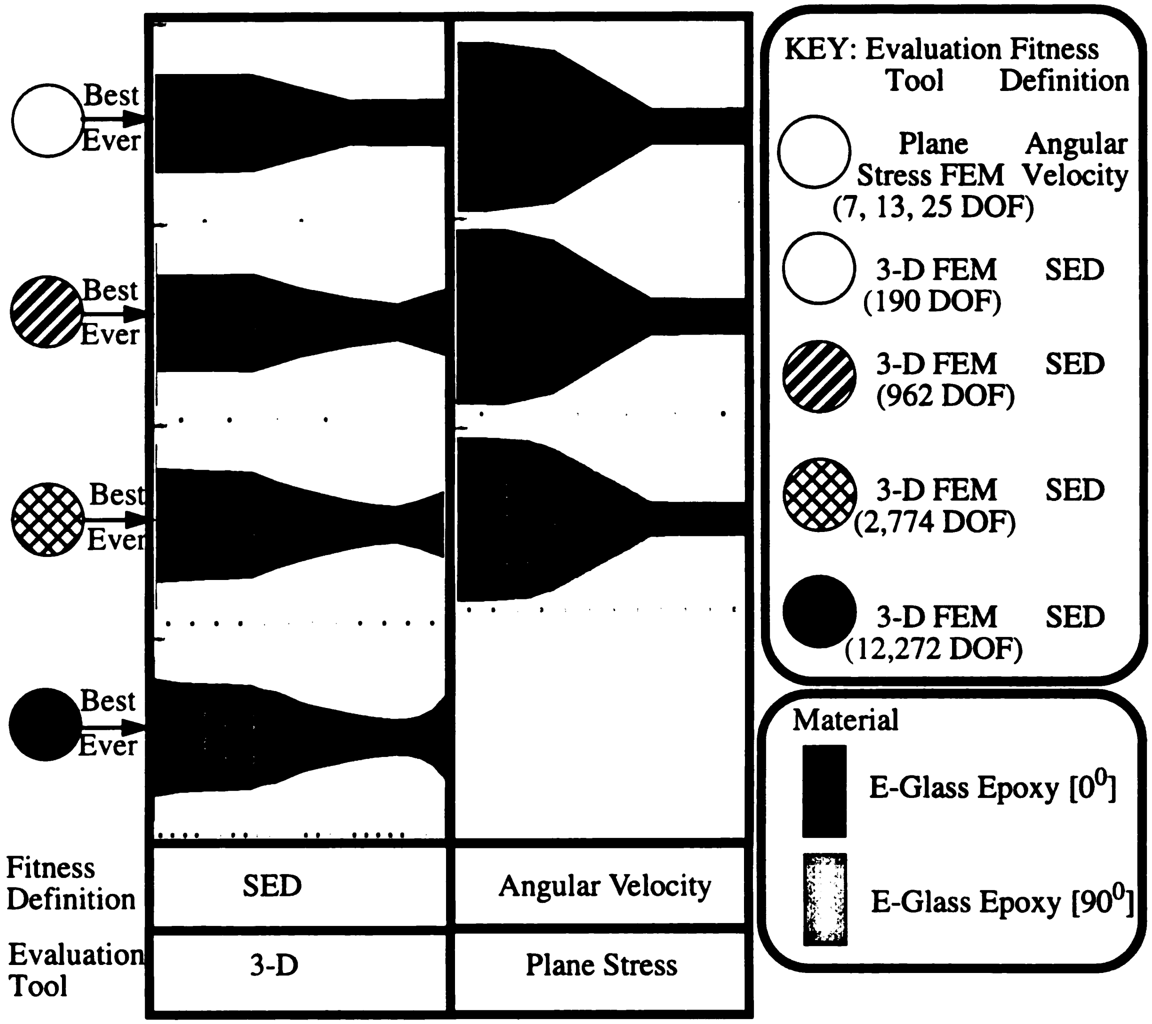

Figure 4.27. Best flywheel found at each level of resolution and fitness definition.

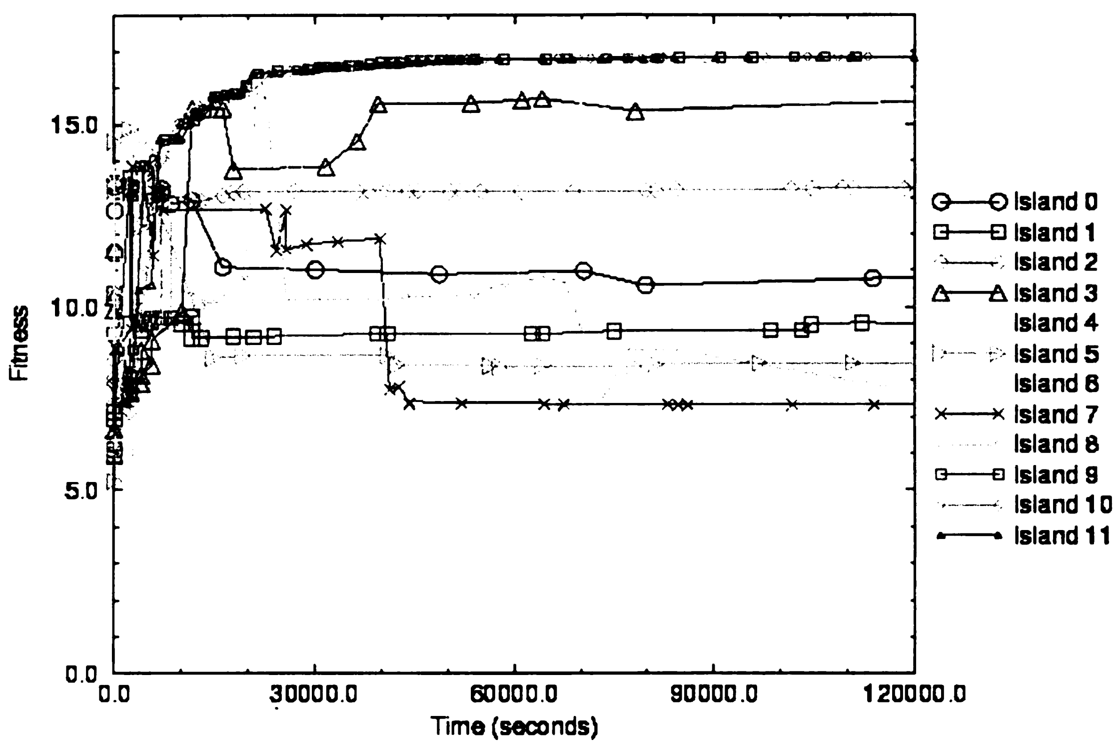

Figure 4.28. iiGA Fitness re-evaluated for each island as a function of time. All re-evaluations performed with 3-D FEM containing 12,272 degrees of freedom for an annular multi-material composite flywheel.

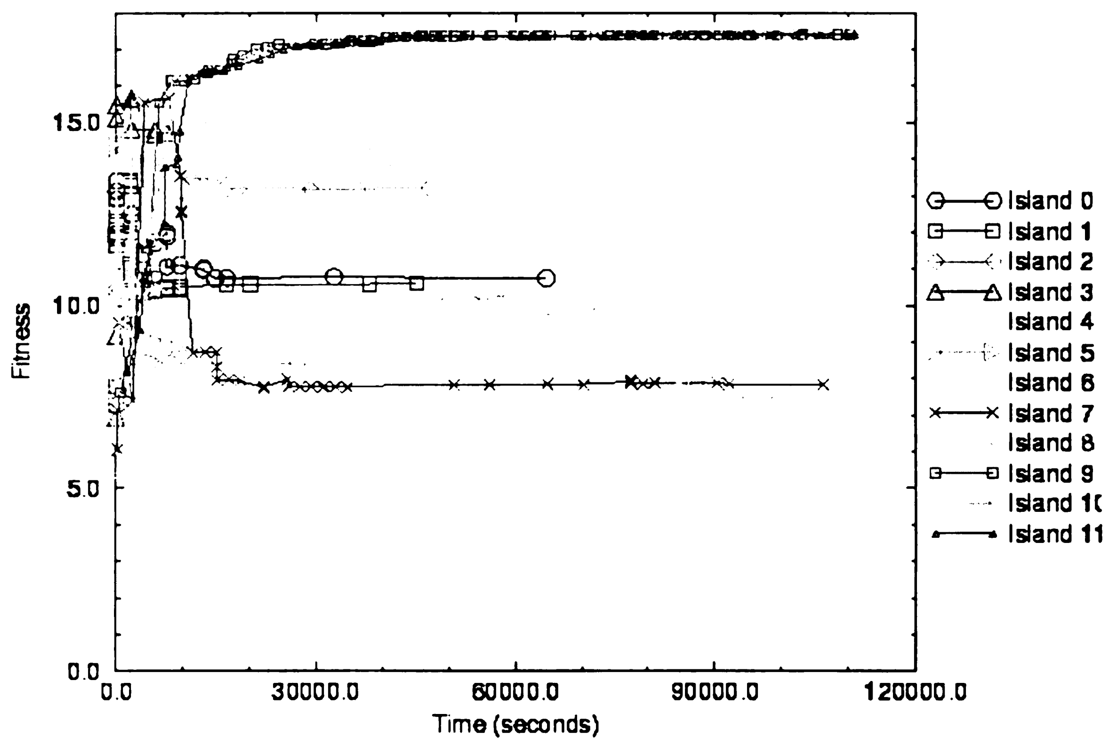

Figure 4.29. Hybrid iiGA fitness re-evaluated for each island as a function of time. All re-evaluations performed with 3-D FEM containing 12,272 degrees of freedom for an annular multi-material composite flywheel.

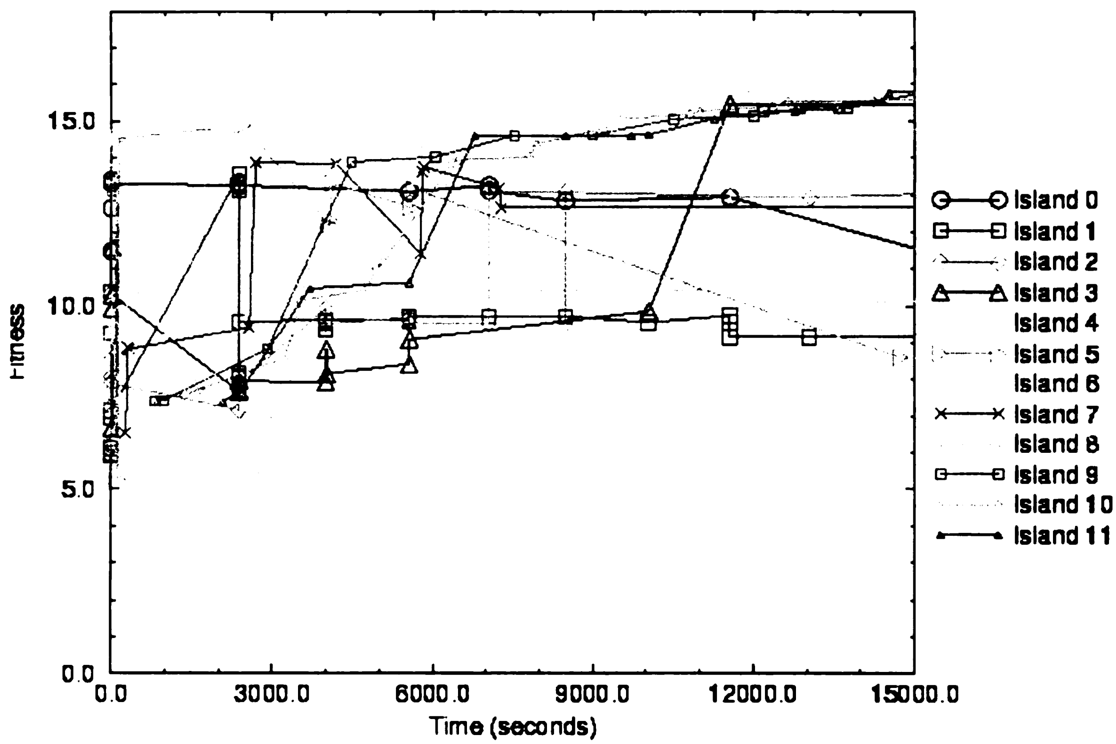

Figure 4.30. iiGA quickly finding building blocks at a low level of resolution to inject into islands of higher resolution for an annular multi-material composite flywheel.

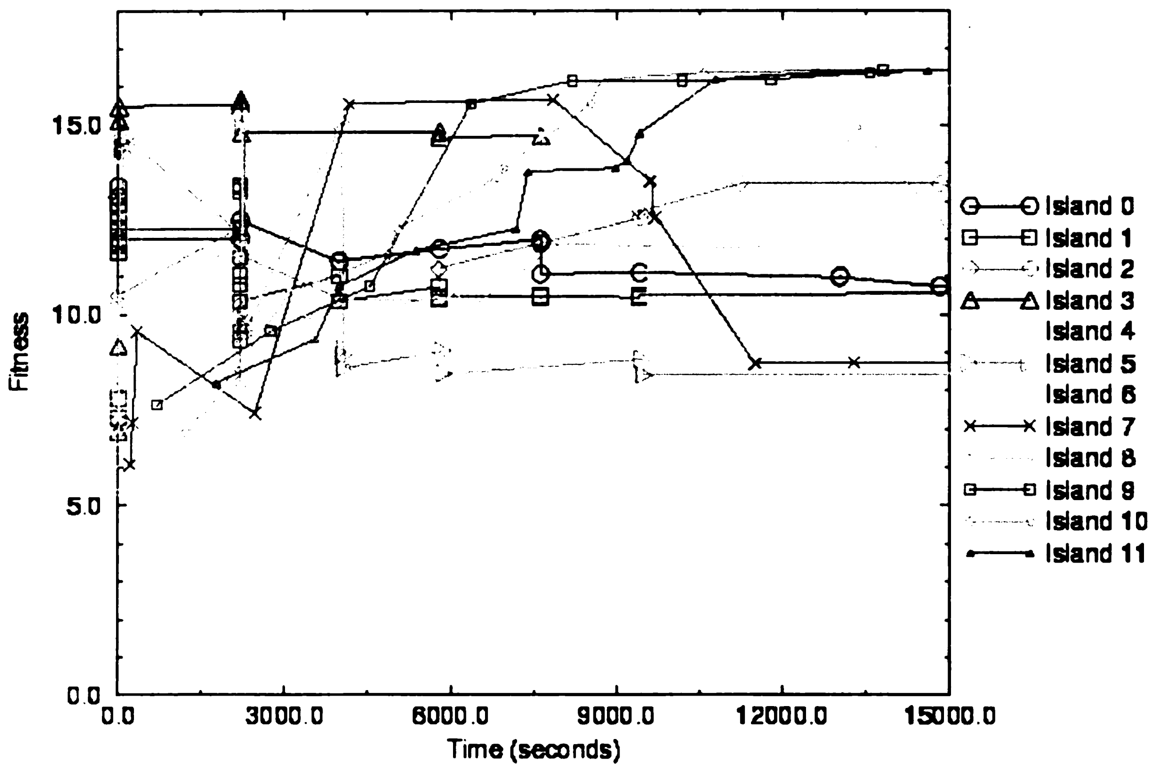

Figure 4.31. Hybrid iiGA quickly finding building blocks at a low level of resolution to inject into islands of higher resolution for an annular multi-material composite flywheel.

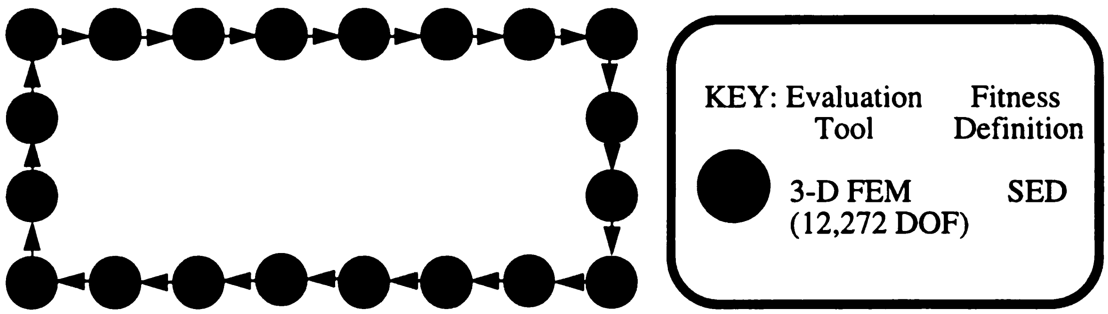

Figure 4.32. Twenty island "ring" GA topology.

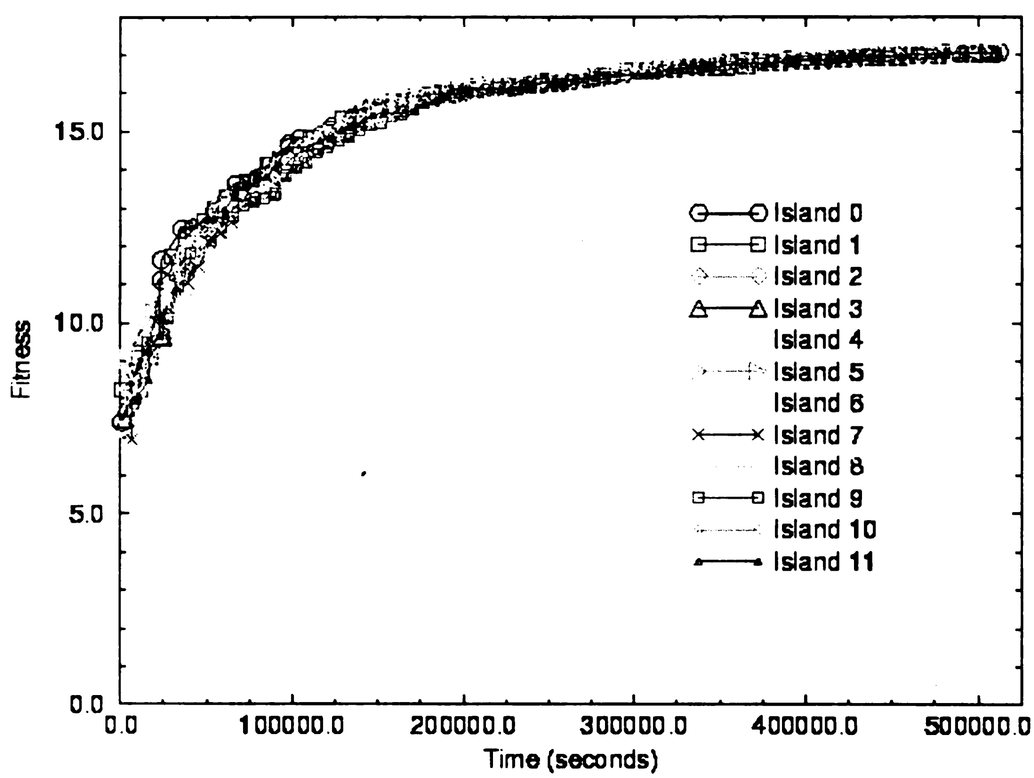

Figure 4.33. "Ring" topology GA results for an annular multi-material composite flywheel.

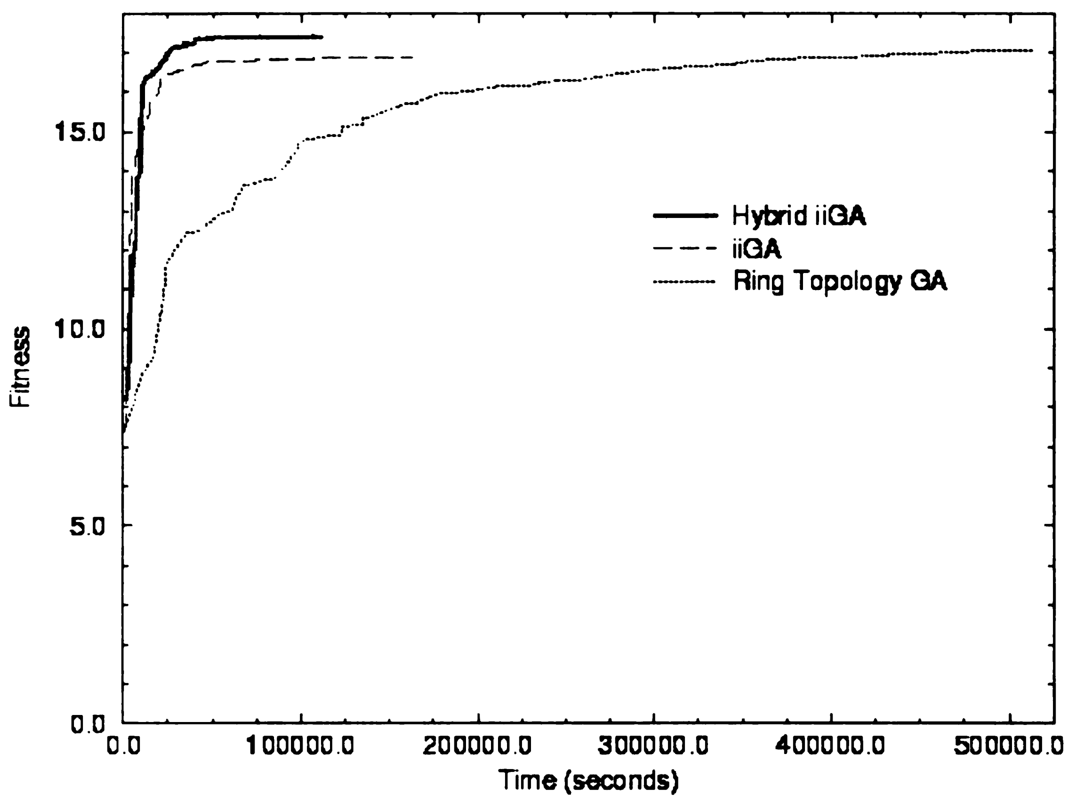

Figure 4.34. Comparison of iiGA to hybrid iiGA to "ring" topology GA. For this problem, both the iiGA and hybrid iiGA search extremely efficiently when compared to a "ring" topology GA. The hybrid iiGA discovers solutions with higher fitness values when compared to the "ring" topology GA and the iiGA alone.

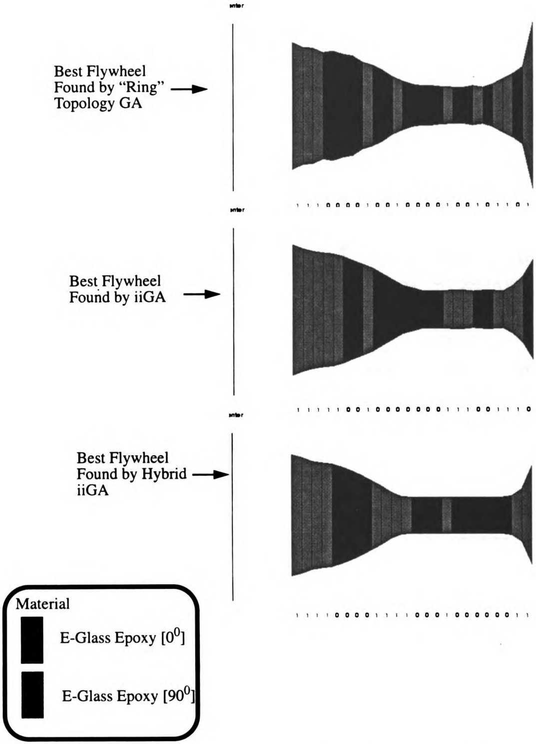

Figure 4.35. Best flywheel found by "ring" topology GA, iiGA and hybrid iiGA for an annular multi-material composite flywheel.

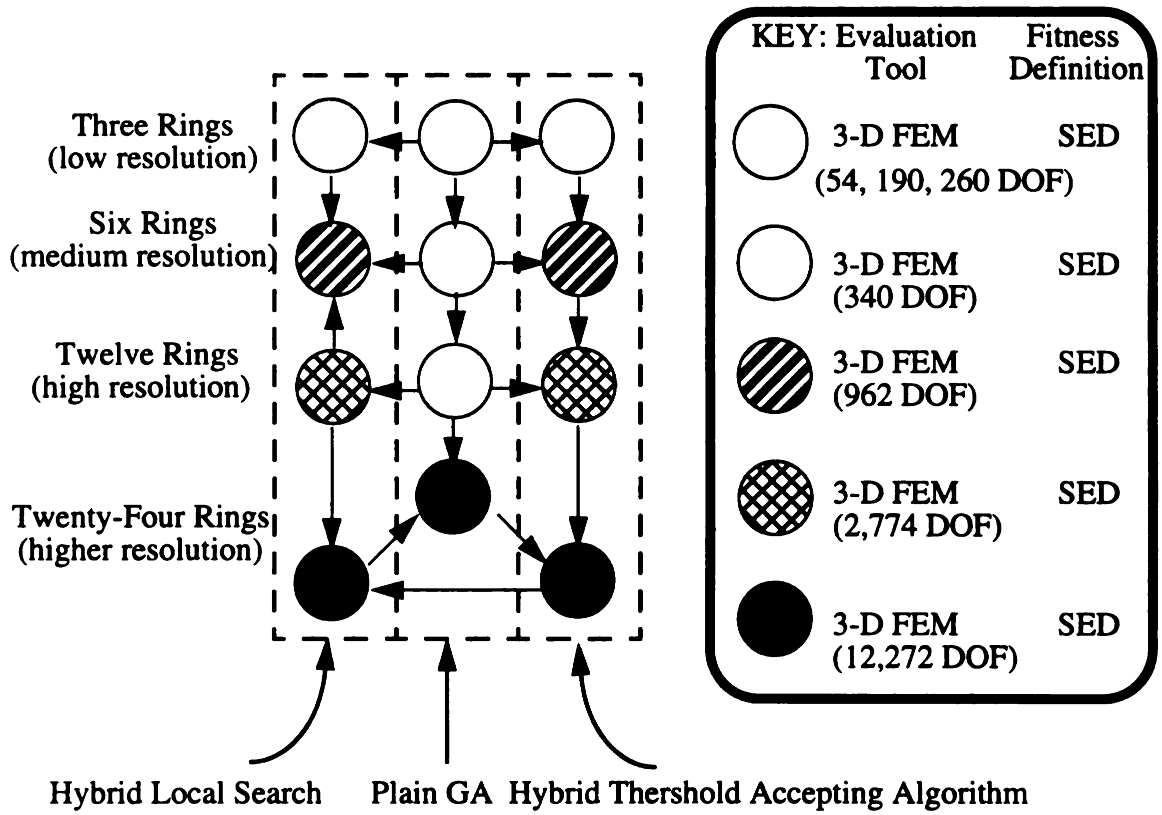

Figure 4.36. Hybrid island injection GA toplogy used in the constrained optimization of a multi-material annular flywheel.

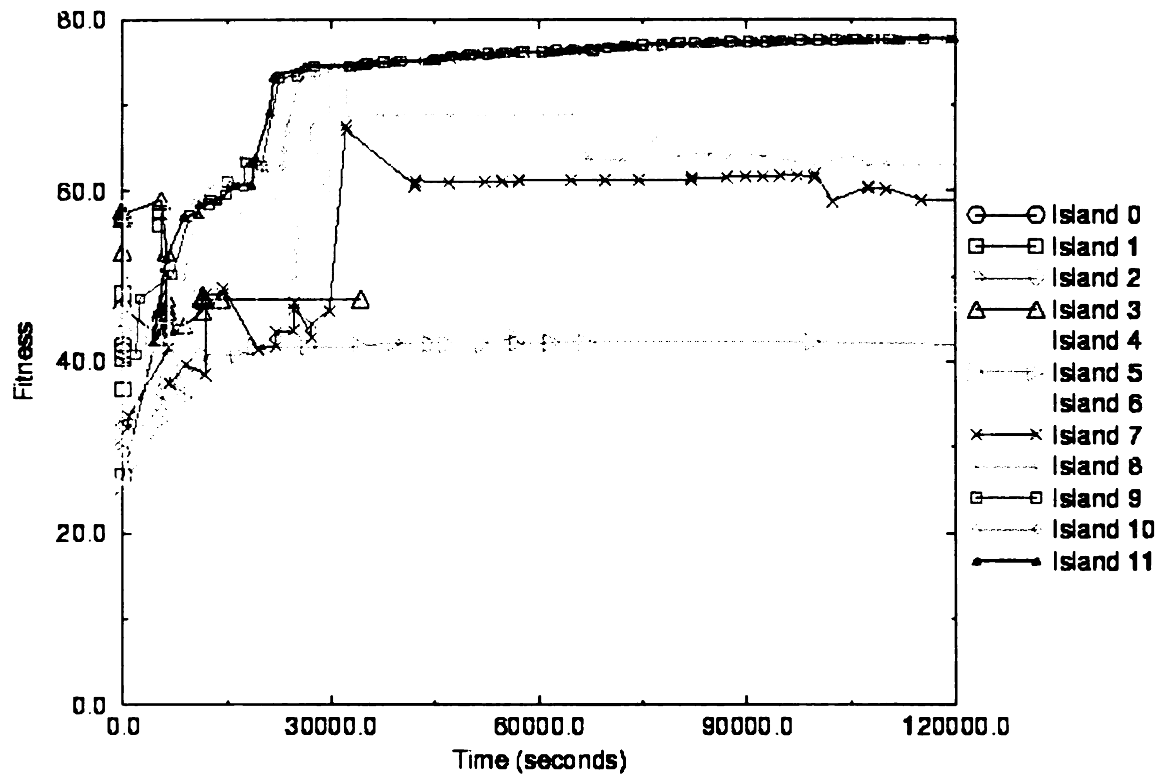

Figure 4.37. Hybrid iiGA fitness re-evaluated for each island as a function of time. All re-evaluations performed with 3-D FEM containing 12,272 degrees of freedom for the constrained optimization of an annular composite multi-material flywheel.

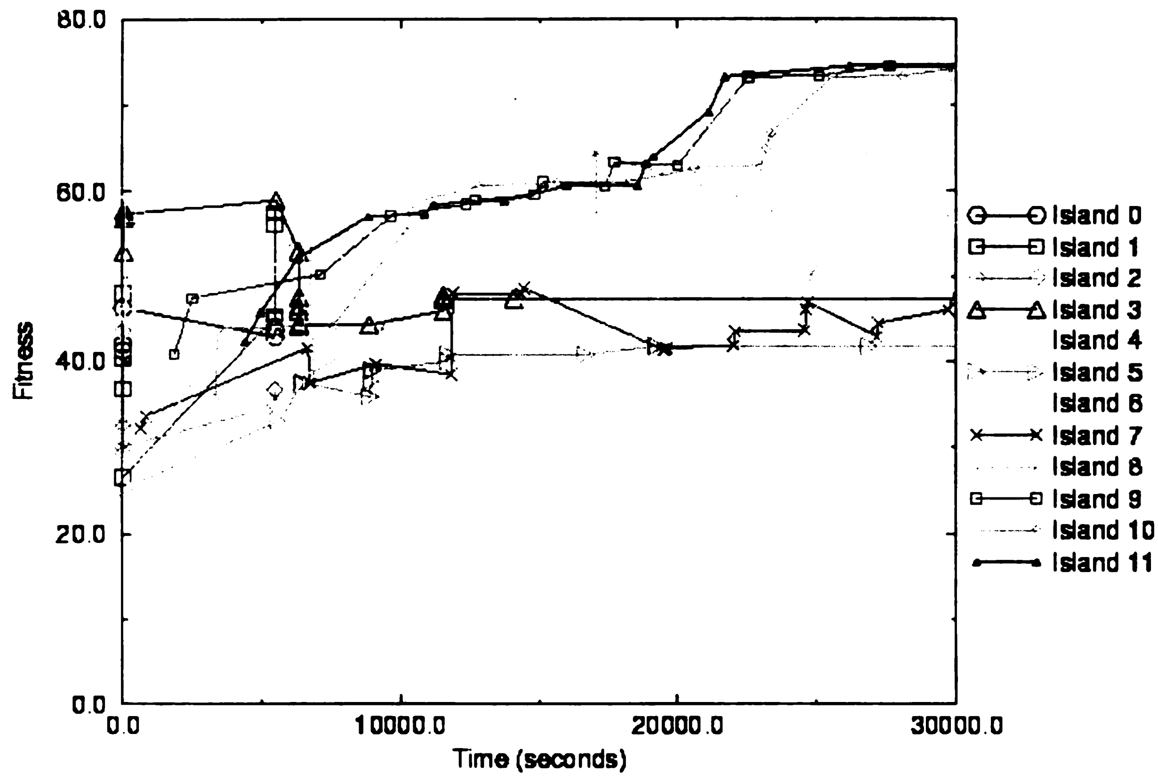

Figure 4.38. Hybrid iiGA quickly finding building blocks at a low level of resolution to inject into islands of higher resolution for the constrained optimization of an annular multi-material composite flywheel.

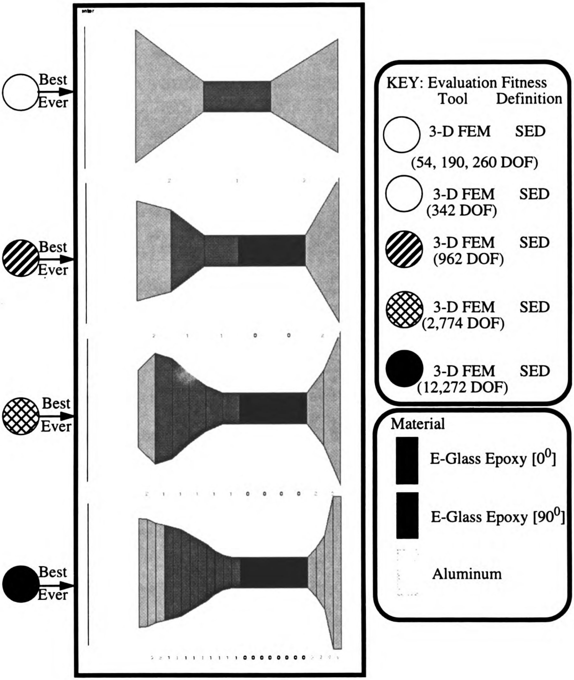

Figure 4.39. Best flywheel found at each level of resolution and fitness definition for the constained optimization of a multi-material composite flywheel.

Chapter 5

Summary and Conclusions

This thesis presents an approach to the optimization of composite flywheels and was broken down into four major segments. To familiarize the reader, a broad range of optimization topics were first reviewed. These topics included past research involving a broad class in the optimization of engineering systems. The second segment presented the mechanics of GAs. The third segment contained the development and accuracy confirmation of the finite element models used to model flywheels. The fourth segment contained the optimization of flywheels using GAs.

The simple GA found the optimal shape of a flywheel with stress free edges that has a 55% increase in SED when compared to a constant stress flywheel. The commonly used rotor shape of the constant stress flywheel is not optimal when a flywheel has stress free edges.

The iiGA can approach optimization problems in a unique way. For many problems, the iiGA can be used to break down a complex fitness function into "sub-fitness" functions, which represent "good" aspects of the overall fitness. Also, the iiGA can use differing evaluation tools. A simplified analysis tool can be used to quickly search for good building blocks. This, in combination with searching at various levels of resolution, makes the iiGA efficient and robust. Mimicking a smart engineer, the iiGA can first quickly evaluate the overall response of a structure with a coarse representation of the design and finish the job off by slowly increasing the levels of refinement until a "finely tuned" structure has been evolved. This approach allows the iiGA to decrease computational time and increase the robustness of a typical GA. The iiGA seems to have a bright future in the optimization of large scale three-dimensional composite structures.

The hybrid iiGA and iiGA were found to search more efficiently than the "ring" topology GA for the case of the enumerable search space of a solid isotropic flywheel. In fact, the iiGA found the global solution in all five independent runs while the "ring" topology GA never found the global solution for any run. The hybrid iiGA that used the combination of a TA algorithm and a local search method found the global optimum in less time than all other optimization techniques, searching less than 5% of the total search space. The hybrid iiGA found the global solution on average in less than 0.5% of the time used in the enumeration of the search space, by measuring more than half of the fitness evaluations with the plane stress finite element model.

The hybrid iiGA and iiGA were also found to search more efficiently when compared to the "ring" topology GA for the case of the annular multi-material composite flywheel. Both the hybrid iiGA and iiGA converged five times faster when compared to the "ring" topology GA. The hybrid iiGA converged to a slightly higher fitness when compared to both the iiGA and "ring" topology GA.

A hybrid iiGA designed a "safer" composite flywheel by penalizing flywheels with large "air gap" growths. The angular velocity was constrained to a lower "target" angular velocity while maximizing SED and penalizing flywheels that have a large "air gap" growth. The angular velocity in the best solution found at the highest level of geometric resolution was extremely close to the "target" angular velocity. The "air gap" growth in the best solution found at the highest level of geometric resolution in the constrained optimization problem was cut in half when compared to the unconstrained optimization approach. The SED for the best solution found at the highest level of geometric resolution in the constrained optimization problem was 21.6% lower than the unconstrained single criterion optimization approach.

REFERENCES

1. Belegundu A. D., and Zhang S., 1992, "Robustness of Design Through Minimum Sensitivity" *Journal of Mechanical Design*, Vol 114, pp213-217.

2. Bendsoe M. P., Olholf N., Taylor J. E., 1984, "A Variational Formulation of Multicriterion Structural Optimization", *Journal of Structural Mechanics*, Vol. 11, No. 4, pp. 523-544.

3. Bhavikatti K., Ramakrishnan C., 1980, "Optimum Shape Design of Rotating Disks", *Computers and Structures*, Vol. 11, pp. 397-401.

4. Carlson S.E., Shonkwiler R., and Ingrim M.E., 1994, "Comparison of Three Non-derivative Optimization Methods with a Genetic Algorithm For Component Selection", *Journal of Engineering Design*, Vol. 5, No. 4, pp 367-378.

5. Chen G., Bruno R., Salama M., 1991, "Optimal Placement of Active/Passive Members in Truss Structures Using Simulated Annealing", *AIAA Journal*, Vol. 29, No. 8, pp. 1327-1334.

6. Christensen R., Wu E., 1977, "Optimal Design of Anisotropic (Fiber-Reinforced) Flywheels", *Journal of Composite Materials*, Vol. 11, pp395-404.

7. Chu D. N., Xie Y. M., Hira A., Steven G. P., "Evolutionary Structural Optimization for Problems with Stiffness Constraints," *Finite Elements in Analysis and Design*, Vol. 22, 1996, pp. 239-251.

8. Crosseley W. A., and Lannanen D. H., 1996, "Conceptual Design of Helicopters via Genetic Algorithms", *Journal of Aircraft*, Vol. 33, No. 6, pp. 1062-1069.

9. Eby D., 1996, "Optimization of Anisotropic Flywheels Via Genetic Algorithms", Senior Research Project, Michigan State University, E. Lansing, MI, 48823.

10. Fabbri G., 1997, "A Genetic Algorithm for Fin Profile Optimization", *International Journal of Heat and Mass Transfer*, Vol. 40, No. 9, pp2165-2172.

11. Foster N., and Dulikravich G., 1997, "Three-Dimensional Aerodynamic Shape optimization Using Genetic And Gradient Search Algorithms", *Journal of Spacecraft and Rockets*, Vol. 34, No. 1, pp. 36-42.

12. Flynn R., and Sherman P., 1995, "Multicriterion Optimization of Aircraft Panels: Determining Viable Genetic Algorithm Configurations", *International Journal of Journal of Intelligent Systems*, Vol. 10, pp. 987-999.

13. Furura H., and Haftka R. T., 1993, "Locating Actuators for Vibration Suppression on Space Trusses by Genetic Algorithms", *Structures and Controls Optimization,*

ASME, AD Col. 38, pp.1-11.

14. Furuya H., and Haftka R., 1995, "Placing Actuators in Space Structures by Genetic Algorithms and Effectiveness Indicies", *Structural Optimization*, Vol. 9, pp. 69-75.

15. Genta G., 1989, "Some Considerations on the Constant Stress Disc Profile", *Meccanica,* Vol. 24, pp. 235-248.

16. Genta G., Domenico D., 1995, "Use of Genetic Algorithms for the design of Rotors", *Meccanica,* Vol. 30, pp. 707-717.

17. Georgian J., 1989, "Optimum Design of Variable Composite Flywheel", *Journal of Composite Materials*, Vol. 23, pp.2-10.

18. Goldberg D., Genetic Algorithms in Search and Machine Learning, 1989, Addison-Wesley Pub. Co. Inc.

19. Goodman E. D., 1994, GALOPPS, The Genetic Algorithm Optimized for Portability and Parallelism System, Tech. Rept. #94-5, MSU GARAGe, Michigan State University, 100pp.

20. Goodman E. D., Averill R. C., Punch III W. F., and Eby D. J., 1997, "Parallel Genetic Algorithms in the Optimization of Composite Structures", *Second World Conference on Soft Computing (WSC2),* www.egr.msu.edu/~ebydavid/ver5.html.

21. Grandi R., 1993, "Structural Optimization with Frequency Constraints-A Review", *AIAA Journal,* Vol. 31, No. 12, pp. 2296-2301.

22. Haslinger J.,and Jedelsky D., 1996, "Genetic Algorithms and Fictitious Based Approaches in Shape Optimization", *Structural Optimization,* Vol. 12, pp 257-264.

23. Homaifar A., Lai H. Y., and McCormick E., 1994, "System Optimization of Turbofan Engines Using Genetic Algorithms", *Applications in Mathematical Modeling*, Vol. 18, pp. 72-83.

24. Horn J., 1997, "Overview: Evolutionary computation for Multipleobjective Optimization", *Proceedings of the Seventh International Conference on Genetic Algorithms*, Michigan State University.

25. Jenkins W. M., 1991, "Towards Structural Optimization Via the Genetic Algorithm", *Computers & Structures*, Vol. 40, No. 5, pp 1321-1327.

26. Khot N., and Veley D., 1991, "Use of Robustness Constraints in the Optimum Design of Space Structures", *Journal of Intelligent Material System and Structures*, Vol. 2, pp. 161-176.

27. Kogiso N., Watson L. T., Gurdal Z., and Haftka R. T., 1994, "Genetic Algorithms with Local Improvement for Composite Laminate Design", *Structural Optimization*, Vol. 7, pp. 207-218.

28. Mallot B., Averill R., Goodman E., Ding Y., and Punch III W., 1996, "Use of Genetic Algorithms for Optimal Design of Laminated Composite Cantilever Sandwich Panels with Bending-Twisting Coupling", presented at AIAA SDM (Structures, Dynamics and Materials).

29. Mares C., and Surace C., 1996, "An application of Genetic Algorithms to Identify Damage in Elastic Structures", *Journal of Sound and Vibration*, Vol. 195, No. 2, pp. 195-215.

30. MARC Users Manual, Volume E, Part 1, MARC Analysis Research Corporation.

31. Miller B., and Goldberg D., 1995, "Genetic Algorithms, Tournament Selection, and the Effect of Noise", IlliGAL Report No. 95006, University of Illinois at Urbana-Champaign, Department of General Engineering.

32. Nakanishi Y., and Nakagiri S., 1996, "Optimization of Frame Topology using Boundary Cycle and Genetic Algorithm", *Japanese Society of Mechanical Engineering International Journal*, Series A, Vol. 39, No. 2, pp. 279-285.

33. Obayahi S., and Takanashi S., 1996, "Genetic Optimization of Target Pressure Distributions for Inverse Design Methods", *AIAA Journal*, Vol. 34, No. 5, pp. 881-886.

34. Olhoff N., and Taylor J. E., 1983,"On Structural Optimization", *Journal of Applied Mechanics*, Vol 50, pp. 1139-1151.

35. Osyczka A., Kuchta W., and Czula R., 1994, "Computer Aided Multicriterion System for Computationally Expensive Functions", *Structural Optimization*, Vol. 8, pp. 37-41.

36. Parmee I., and Vekeria H., 1997, "Co-Operative Evolutionary Strategies for Single Component Design", *Proceedings of the Seventh International Conference on Genetic Algorithms*, Michigan State University.

37. Punch III W. F., Averill R. C., Goodman E. D., Lin S. C., and Ding Y., February 1995,"Design Using Genetic Algorithms - Some Results for Laminated Composite Structures", *IEEE Expert*, Vol. 10 (1), pp. 42-49.

38. Punch III W. F., Averill R.C., Goodman E.D., Lin S. C., Ding Y., and Yip Y.C., 1994, "Optimal Design of Laminated Composite Structures using Coarse-Grain Parallel Genetic Algorithms," *Computing Systems in Engineering*, Vol. 5, No. 4-6, pp. 414-423.

39. Punch III W., Averill R., Goodman E., Lin S., and Yip Y., 1994, "Optimal Design of Laminated Composite Structures using Coarse-Grain Parallel Genetic Algorithms", *Computing Systems in Engineering*, Vol. 5, pp. 415-423.

40. Quagliarella D., and Cioppa A., 1994, "Genetic Algorithms applied to the Aerodynamic Design of Transonic Airfoils", *Journal of Aircraft*, Vol. 32, No. 4, pp. 889-891.

41. Queipo N., Devarakonda R., and Humphrey J., 1994, "Genetic Algorithms for the Thermosciences Research: Application to the Optimized Cooling of Electronic Components", *International Journal of Heat and Mass Transfer*, Vol 37, No. 6, pp. 893-908.

42. Rajan S. D., 1995, "Sizing, Shape and Topology Design Optimization of Trusses using Genetic Algorithm", *Journal of Structural Engineering*, Vol. 121, No. 10, pp. 1480-1487.

43. Richef R., and Haftka R., 1993, "Optimization of Laminate Stacking Sequence for Buckling Load Maximization by Genetic Algorithm", *AIAA Journal*, Vol. 31, No. 5, pp. 951-955.

44. Ries D., Kirk J., 1992, "Design and Manufacturing for a Composite Multi-Ring Flywheel", *Proceedings of the 27th Intersociety Energy Conversion Engineering Conference*, Vol. 2, pp 4.43-4.48.

45. Ruthenbar R., 1989, "Simulated Annealing Algorithms: An Overview", *IEEE Circuits and Devices Magazine*, Vol. 5, No. 1, pp. 19-26.

46. Sangren E., Ragsdell K. M., 1983, "Optimal Flywheel Design with a General thickness Form Representation", *Journal of Mechanisms, Transmissions, and Automation in Design*, Vol. 105, pp. 425-433.

47. Schraudolph N., and Grefenstette J., 1992, A User's Guide to GAucsd 1.4, July.

48. Seireg A., Surana K., 1970, "Optimum Design of Rotating Disks", *Journal of Engineering for Industry*, Vol. 92, pp. 1-10.

49. Stadler W., and Dauer J., 1992, "Multicriterion Optimization in Engineering: A Tutorial and Survey", Structural Optimization: Status and promise, Progress in Astronautics and Aeronautics, Vol. 150, AIAA Inc., pp 209-249.

50. Sundaresan S., Ishii K., and Houser D., 1992, "Design Optimization For Robustness Using Performance Simulation Programs", *Engineering Optimization*, Vol. 20, pp.163-178.

51. Todoroki A., and Watanabe K., 1995, "Applications of Genetic Algorithms to Stiff-

ness Optimization of Laminated Composite Plates with Stress-Concentrated Open Holes, *Japanese Society of Mechanical Engineering International Journal*, Series A, Vol. 38, No. 4, pp. 458-404.

52. Ugural A., Fenster S., 1995, Advanced Strength and Applied Elasticity, pp. 339-344.